

## INFORMATION TO USERS

The most advanced technology has been used to photograph and reproduce this manuscript from the microfilm master. UMI films the original text directly from the copy submitted. Thus, some dissertation copies are in typewriter face, while others may be from a computer printer.

In the unlikely event that the author did not send UMI a complete manuscript and there are missing pages, these will be noted. Also, if unauthorized copyrighted material had to be removed, a note will indicate the deletion.

Oversize materials (e.g., maps, drawings, charts) are reproduced by sectioning the original, beginning at the upper left-hand corner and continuing from left to right in equal sections with small overlaps. Each oversize page is available as one exposure on a standard 35 mm slide or as a 17" × 23" black and white photographic print for an additional charge.

Photographs included in the original manuscript have been reproduced xerographically in this copy. 35 mm slides or 6" × 9" black and white photographic prints are available for any photographs or illustrations appearing in this copy for an additional charge. Contact UMI directly to order.



300 North Zeeb Road, Ann Arbor, MI 48106-1346 USA



Order Number 8801779

**Transport phenomena and optical properties of a layered  
electron gas**

Zhang, Chao, Ph.D.

City University of New York, 1987

**U·M·I**  
300 N. Zeeb Rd.  
Ann Arbor, MI 48106



**PLEASE NOTE:**

In all cases this material has been filmed in the best possible way from the available copy. Problems encountered with this document have been identified here with a check mark .

1. Glossy photographs or pages \_\_\_\_\_
2. Colored illustrations, paper or print \_\_\_\_\_
3. Photographs with dark background \_\_\_\_\_
4. Illustrations are poor copy \_\_\_\_\_
5. Pages with black marks, not original copy
6. Print shows through as there is text on both sides of page \_\_\_\_\_
7. Indistinct, broken or small print on several pages
8. Print exceeds margin requirements \_\_\_\_\_
9. Tightly bound copy with print lost in spine \_\_\_\_\_
10. Computer printout pages with indistinct print \_\_\_\_\_
11. Page(s) \_\_\_\_\_ lacking when material received, and not available from school or author.
12. Page(s) \_\_\_\_\_ seem to be missing in numbering only as text follows.
13. Two pages numbered \_\_\_\_\_. Text follows.
14. Curling and wrinkled pages \_\_\_\_\_
15. Dissertation contains pages with print at a slant, filmed as received
16. Other \_\_\_\_\_  
\_\_\_\_\_  
\_\_\_\_\_

**U·M·I**



**TRANSPORT PHENOMENA  
AND OPTICAL PROPERTIES  
OF A LAYERED ELECTRON GAS**

by

Chao Zhang

A dissertation submitted to the Graduate Faculty in Physics  
in partial fulfillment of the requirements for the degree of  
Doctor of Philosophy, The City University of New York.

1987

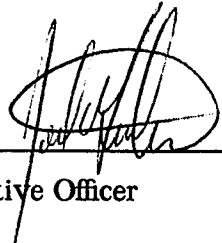
---

This manuscript has been read and accepted for the Graduate Faculty in Physics in satisfaction of the dissertation requirement for the degree of Doctor of Philosophy.

May 7 1987  
Date

Nanlis Tzoan  
Chairman of Examining  
Committee

May 7 1987  
Date

  
Executive Officer

Melvin Lax  
Robert Balfanz  
Joseph A. Jones  
Lui Lam  
Supervisory Committee

## ABSTRACT

### TRANSPORT PHENOMENA AND OPTICAL PROPERTIES OF A LAYERED ELECTRON GAS

by

Chao Zhang

Advisor: Professor Narkis Tzoar

The high-frequency conductivity of superlattices was investigated. Here, the systems are under the influence of electromagnetic waves whose frequencies are high compared to the collision frequencies, and whose wavelengths are long compared to the Bohr (Debye) radius. The treatment rests on the kinetic description for electron-ion system and on the Kubo's formula for the conductivity and the temperature dependent Green's function technique. An exact expression for conductivity, to the lowest order in plasma parameter, is obtained, which depends on frequency, electron-hole mass ratio, electron-LO phonon coupling, spacing between adjacent layers and density per unit area. We calculate the resistivity numerically for some typical value of the above four parameters. To examine the effect of finite

width of the electron distribution, we consider a model function in our calculation for type-I superlattice and find an increase in the absorption constant.

The Raman scattering cross-section from a two-component layered electron gas (such as InAs-GaSb, GaAs-AlGaAs superlattices, etc.) has been calculated within the random-phase-approximation. It is found that for a separation between two components larger than a critical value, the scattered spectra have two resonant peaks in the high-frequency regime. For small separation and small mass ratio, there is a resonant peak due to an ion acoustic mode at the low frequency regime and to a plasma mode at the high frequency regime. The finite width of the wave function of the charged particles will reduce the resonant frequencies and enhance the Raman intensities.

## Acknowledgment

It is a great pleasure to acknowledge my deep indebtedness to Professor Narkis Tzoar for his continued support, encouragement, instruction, and patient guidance during the course of this research.

I wish to express my sincere thanks to Dr. C. L. Wang for his significant help relating to the computer programming in this research.

It is my pleasure to thank the faculty of the Physics Department for its instruction and help, especially Profs. M. Lax, R. Alfano, J. Johnson, L. Lam, J. I. Gersten, T. Boyer, J. Aschner, B. Sakita, J. Birman, C. Yuan, H. Z. Cummins and M. Sarachik. I would like to thank all my fellow graduate students for providing laughter and sunshine during my stay at City College. Special thanks also to my former advisor, Prof. Z. H. Qian at East China Normal University in Shanghai.

I heartily thank Profs. T. D. Lee and N. P. Chang for their tremendous efforts to establish and promote the China-United States Physics Examination and Application (CUSPEA), which enabled me to come to City College of New York to participate in the Ph. D. program in Physics.

## Table of Contents

Abstract	
Acknowledgment	
List of Figures	
I Introduction	1
1. Optical Properties of Electron Gas	2
2. Layered Electron Gas-First Approximation to Superlattice	5
3. Optical Properties of a Layered Electron Gas	8
II Electron-Ion Scattering	13
1. Introduction	13
2. General Formalism of Total Current	15
3. The Evaluation of Conductivity	22
4. Scattering Time and Effective Mass	31
5. Discussion	37
6. Appendix 2A	39
III Two-Component Layered Electron Gas	44
1. Introduction	44
2. General Formalism for the Problem	45
3. Relation Between Electrical Conductivity and Finite Temperature Green's Function	49

4. Many Body Perturbation Theory in Layered System	51
5. Basic Rules For Evaluation of Diagrams	52
6. Effective Interaction	53
7. Evaluation of the Conductivity	57
8. Relaxation Time and Resistivity	63
9. Discussion	68
10. Appendix 3A	73
IV Electron-LO Phonon System	76
1. Introduction	76
2. Hamiltonian of the System	78
3. Evaluation of the Conductivity	80
4. Relaxation Time and Resistivity	85
5. Mass Shift	89
6. Discussion	90
V Light Scattering From a Two-Component Layered Structure	93
1. Introduction	93
2. Formalism for the Scattering Cross-Section	95
3. Dispersion Relation and Resonant Frequencies	100
4. Effect of Finite Spreading of the Electronic Wave Function	104
5. Discussion	107
6. Appendix 5A	112
7. Appendix 5B	113
Captions	115
Figures	120
References	146

---

## List of Figures

1.1	Schematic diagram for type-I superlattice and its energy diagram	118
1.2	Energy diagram for type-II superlattice	119
2.1	Collision frequency for type-I superlattice with $d=0$	120
2.2	Collision frequency for type-I superlattice with $d=0$ and $9\text{\AA}$	121
2.3	Collision frequency for type-I superlattice with $d=0,30\text{\AA}$ and $60\text{\AA}$	122
2.4	Collision frequency for type-I superlattice with $d=0,15\text{\AA}$ and $30\text{\AA}$	123
2.5	Dispersion relation for type-I superlattice	124
3.1	Class of diagram which contribute to high frequency conductivity for multi-component system	125
3.2	Effective interaction	126
3.3	Resistivity of type-II superlattice for different temperatures	127
3.4	Resistivity of type-II superlattice for different mass ratios	128
3.5	Resistivity of type-II superlattice for different spacing	129
3.6	Contour for path integral	130
4.1	Feymann diagram for electron-LO phonon system	131
4.2	Relaxation time and real part of the conductivity of electron-LO phonon system for GaAs-GaAlAs	132
4.3	Relaxation time and real part of the conductivity of electron-LO phonon system for PbTe-PbEuTeSe	133

---

4.4	Relaxation time and real part of the conductivity of electron-LO phonon system for PbTe-PbEuTeSe with different densities	134
4.5	Temperature effect on optical properties	135
5.1	Dispersion curves for Type-II superlattice	136
5.2	Dispersion curves for Type-II superlattice	137
5.3	Raman intensities at high frequencies	138
5.4	Raman intensities at low frequencies	139
5.5	Effect of width on Raman intensities	140
5.6	Effect of width on Raman intensities	141
5.7	Effect of width on Raman intensities	142
5.8	Effect of width on Raman intensities	143

---

# Chapter I

## INTRODUCTION

In the past several years there has been much interest in the rather unusual properties of layered structures.<sup>[1-3]</sup> The static dielectric response of a layered electron gas has been calculated by Visscher and Falicov<sup>[1]</sup>. The model consists of parallel equally spaced planes of electrons or holes. This model was first employed to approximate Graphite and now finds a good physical realization of semiconductor superlattices. For the discussion of intrasubband electronic collective modes of a layered electron gas, in the simplest model one assumes that the electrons (holes) remain in the lowest subband; they are allowed to move freely in each plane but tunneling between planes is completely prohibited.

The research reported in this thesis is the investigation of the optical properties a layered electron gas and the study of the light scattering from such a system. In this work, we have applied kinetic theorem, many-body perturbation theory, finite temperature Green's function technique and the theory of density-density correlation to our layered structure. We treat our system as a many-body system in which charged particles interact via the Coulomb potential. The response of this structure to an external electromagnetic radiation is studied in terms of a generalized dielectric tensor and a dynamical conductivity. It is found the optical properties of a layered electron gas are qualitatively different from that of bulk

---

material and two-dimensional system. Some new phenomena in light scattering concerning the resonant modes and line shape are also explored in this work. The main results of this thesis have been published in Physical Review B.<sup>[4-7]</sup>

In the current chapter, we first review the optical properties of a bulk material as well as two-dimensional system which are well understood. Then we will briefly describe the structure of a superlattice, although we are not dealing with the multi-quantum well system, our model can represent the superlattice structure in lowest approximation ( i.e., no tunneling and only the lowest subband being occupied ). Finally, we present the basic principles and approximations involved in this research.

### 1.1. Optical Properties of Electron Gas

The optical properties of a bulk electron gas serves as a valuable guide to the behavior of such diverse physical system as classical plasmas and degenerate conduction electrons in metal<sup>[8]</sup>. For example, the ground state energy of the electron gas yields a first approximation to that of a metal<sup>[9]</sup> and electromagnetic effect of plasma oscillation<sup>[10-11]</sup> and screening<sup>[12-13]</sup> illuminate similar phenomena found in actual physical system<sup>[8,9]</sup>. Similarly, the optical properties of a two-dimensional(2D) electron gas provides a model for that of inversion layers in semiconductors<sup>[14]</sup> and surface electrons on liquid He<sup>[15]</sup> or Ne. This later situation is quite different from the bulk configuration, for a single charged layer can not screen a test charge effectively, owing to the extended electromagnetic fields in the surrounding vacuum.

The absorption of electromagnetic radiation in bulk electron gas were extensively studied by many authors for both classical and quantum plasmas. The absorption in classical plasma has been treated with an elementary model by Dawson and Oberman<sup>[15]</sup> and by Oberman, Ron and Dawson<sup>[16]</sup> via the Liouville hierarchy. The latter work gave a complete classical derivation of the high-frequency conductivity of a plasma taking into account properly the collective effect. Another approach to the classical problem has been given by Perel and Eliashberg<sup>[17]</sup> who begin with a quantum mechanical diagram technique, but pass to classical limit, before obtaining any result. A systematic study of absorption of electromagnetic wave in quantum and classical plasmas was given by Ron and Tzoar<sup>[18]</sup>. Their treatment rests on the introduction of the temperature dependent Green's function and Kubo's formula for conductivity. Dong<sup>[19]</sup> had generalized the result of Ref.[20] to the case of finite wave number and deduced some results for a classical plasma concerning the relative importance of Landau<sup>[21]</sup> and correlation damping. Wolff<sup>[22]</sup> studied the high-frequency conductivity of a single component plasma in which carriers have a nonquadratic energy-momentum relation. In such a medium, current is not conserved in the electron-electron collision and he found an important correction to the conductivity. Gotze and Wolfe<sup>[23]</sup> expressed the frequency dependent conductivity in terms of the regular memory function. This memory function is calculated in lowest order in the impurity concentration and electron-phonon coupling. In the presence of a uniform magnetic field, Li et al<sup>[24]</sup> investigated the A.C. magnetoresistance, Hall effect and cyclotron resonance phenomena in a electron-phonon system. Lee and Tzoar<sup>[25]</sup> discussed the absorption in a simple metal consisting of electrons and phonons by using the equation of motion for

---

Wigner distribution function. For narrow gap semiconductor, Foo and Tzoar<sup>[26]</sup> calculated the optical absorption by two-band approximation.

There has been a great deal of interest in the dielectric response and transport properties of two-dimensional system<sup>[27]</sup>. Electrons at the interface of a metal-oxide-semiconductor junction<sup>[28]</sup> and those trapped at the interface of a semiconductor heterostructure<sup>[29]</sup> are examples of such systems. Plasmon collective mode in a two-dimensional electron gas (2DEG) were first discussed by Stern<sup>[30]</sup>, who calculated the dynamical polarizability of a 2D electron layer as a model for the ground state of an electron gas in a surface inversion layer. He found that, in the non-retarded limit, the frequency of a 2D plasmon  $\omega \approx \sqrt{q}$ , where  $q$  is the wave-vector in the plane. The 2D plasmon, associated with the ground subband as it is, is essentially an intraband collective mode. Oscillation of two-dimensional classical plasma was discussed by Platzman and Tzoar<sup>[31]</sup>. Fetter<sup>[32]</sup> use a hydrodynamic description to study the electrodynamics of a single layer. The absorption of electromagnetic radiation in 2D electron gas were also widely studied<sup>[33]</sup>. On the basis of the  $\omega$ -dependent current-current correlation function, Tzoar, Platzman and Simons<sup>[34]</sup> have calculated the dynamic conductivity in the two-dimensional inversion layer. The complex memory function<sup>[35]</sup> depends on electron-impurity interaction screened through a temperature- and frequency-dependent density-density correlation function. They obtained a mass shift and the collision frequency as a function of temperature and frequency which is in agreement with experimental results<sup>[36]</sup>.

An intermediate case between the two- and three-dimensional configuration is a layered electron gas<sup>[1-2]</sup>. Here the charges are confined to a regular array of

parallel planes. This system serves as a first approximation to the superlattice system. More generally the model exemplifies the transition behavior between regions of different dimensionality. For large separation between layers, the optical and physical properties reduce to that of a single layer, whereas for small separation it becomes qualitatively similar to that of a bulk continuum. In this project we shall investigate the transport phenomena and optical properties of such a layered structure.

## 1.2. Layered Electron Gas—First Approximation to Superlattices

Superlattices are a novel class of material composed of alternating layers of two (or more) different constituents. [37-40] The development of molecular beam epitaxy (MBE) has made it possible to produce high quality superlattices made from two different semiconducting materials (e.g., InAs-GaSb, GaAs-AlAs, Ge-GaAs, etc.) with similar lattice structure and matching lattice parameters. In the direction of superlattice growth (called the superlattice axis, and taken to be the z-direction), a number of atomic monolayers of semiconductor A are deposited in an atomically sharp way on atomic monolayers of semiconductor B to form new superlattice unit cells. A microscopic sample of such an A-B superlattice is a new bulk material with properties intermediate between those of materials A and B.

There are two types of superlattices whose properties have been studied in some detail. These are known as type-I and type-II superlattices. Type-I superlattices are typified by  $GaAs - Al_x Ga_{1-x} As$  system, in which the band gap of GaAs is smaller than, and contained within, that of  $Al_x Ga_{1-x} As$  (Fig.1.1), giving rise to band gap discontinuities in both conduction and valence bands of the resultant

superlattice system. If we dope the  $Al_x Ga_{1-x} As$  layers with donor impurities (which is done by "modulation doping" methods), electrons will be released from the donors to drop into GaAs sides of the band gap discontinuities. The resulting one-dimensional potential well quantizes the motion of the electron in the z-direction, and so the conduction band of GaAs will be split up into a series of subbands (if the electron wave functions in adjacent potential wells do not overlap) or miniband (if they do), each of which represents a continuum of free-electron-like states in the x-y plane. Thus, as far as electronic properties are concerned, type-I superlattices consist of a periodic array of quasi-two-dimensional electron gases.

In the type-II superlattices, as typified by InAs-GaSb system, the band discontinuities at the interfaces are so large that the conduction band edge in InAs even lies below the upper valence band edge of the GaSb (Fig.1.2). In this case, there is a transfer of electrons from one layer (GaSb) to the other (InAs), resulting in a spatial separation of electrons and holes into adjacent potential well, with the formation of electron and hole subbands. Unlike type-I superlattice where both electron or hole states are primarily in the GaAs regions, here electrons mainly exist in InAs layers while the holes are in GaSb layers.

Many aspects of the physics of superlattices have been studied in recent years [36-39]. The electronic collective excitation in semiconductor superlattices structure were examined in detail by Das Sarma and Quinn [3] and by Tselis and Quinn [41]. They have shown explicitly the existence of quasi-2D plasmons and magnetoplasmons for type-I superlattices, and coupled quasi-2D electron and hole plasmons and magnetoplasmons for type-II superlattices; these modes reduced to

correct behavior in the appropriate limits. They obtained an expression for dielectric tensor the zero of which gives the dispersion relation of collective modes. The structure of subband and cyclotron resonance have been investigated by far-infrared absorption spectroscopy <sup>[42-43]</sup> and resonant inversion scattering techniques <sup>[44-46]</sup>. (These experiment were first done on surface inversion layers, subsequent measurements have also been made on semiconductor superlattices.) considerable work has been performed on transport process in these system. Raman intensities for bulk and surface plasmons were calculated recently <sup>[47]</sup>. The implications of type-II superlattice were first studied by Sai-Halasz, Tsu and Esaki <sup>[48-49]</sup>. Calculations of the band structure were performed by Sai-halasz, Esaki and Harrison <sup>[50]</sup> and by Madhakar and Nucho <sup>[51]</sup> and by Dohler <sup>[52]</sup>. Experimental studies were also actively performed in this field <sup>[53-55]</sup>.

Interband collective modes, associated with the transitions between subbands (the quantized motions of the electrons in the z-direction), were discussed by Chen, Chen and Burstein<sup>[56]</sup> in a simplified model. More complete treatments of the inter-subband modes were given by Dahl and Sham<sup>[57]</sup> and by Eguiluz and Maradudin<sup>[58]</sup>, who considered different polarizations and effects of retardation. They showed that the effect of resonant screening is to shift the resonance energy above the subband separation; this is the depolarization shift. In a discussion of many body effect, Vinter<sup>[59]</sup> stressed the importance of vertex correction. Ando<sup>[60]</sup> showed that, in a static local approximation, the vertex correction introduced another shift in the resonance energy which almost exactly cancelled the effects of depolarization shift for typical inversion layer electron densities. This another shift is known as the "final state interaction" or "excitonic shift", and is associated with

the hole left in the lower subband. Tselis and Quinn<sup>[61]</sup> gave a unified model of collective modes in surface inversion layers, in which the effects of dispersion in xy plane on interband modes were given to second order in  $q$ , along with the effects of resonant screening and the vertex correction (the latter evaluated in a static local approximation). They also included the effects of magnetic fields and obtained the 2D analogue of hybrid magnetoplasmon mode in three dimensions, with  $\omega^2 = \omega_c^2 + \omega_p^2(q)$ , where  $\omega_c$  is the cyclotron frequency and  $\omega_p(q)$  is the 2D plasmon.

The plasmon modes of a two layer system were discussed by Chui, Quinn, Lee and Eguluz<sup>[62]</sup> and by Das Sarma and Madhukar<sup>[63]</sup> who found, in addition to the usual 2D plasmon, an acoustical plasmon mode with  $\omega \approx q$ , the latter found to be undamped under appropriate circumstances.

Considerations of multiple layer system have usually been restricted to one-dimensional array of purely 2D electron gas.<sup>[1-3]</sup> Fetter<sup>[2]</sup> has given an extensive discussion of the plasmon modes of such system in a hydrodynamic approximation. Apostol<sup>[64]</sup> has done a similar calculation using the equation of motion method, obtaining results in RPA. Caille<sup>[65]</sup> et al considered the effects of LO phonons on interface plasmons in multi-layer system. Mizuno<sup>[66]</sup> et al calculated the effects of magnetic fields and obtained magnetoplasmon modes in these systems.

### 1.3. Optical Properties of a Layered Electron Gas

The spatial separation between carriers and scatterers in the layered structure has obvious consequences in the optical properties such as absorption. The mobility of this structure is higher than that of bulk material because of a

reduction in the carrier-scatterer scattering. Thus, we are particularly interested in studying the problem of electrical conductivity and the optical absorption process. Our task is to investigate the dynamical response of such layered electron gas under the influence of electromagnetic waves whose frequencies are high compared to the collision frequencies and whose wave-lengths are long compared to the Bohr radius. Once we find the expression of conductivity, we compare it with Drude formula for conductivity, we can immediately recognize the the effective mass of the carriers and its relaxation time. The absorption constant can be obtained from relaxation time or the collision frequency.

The collective behavior in electron or electron-hole plasmas of a lower dimensionality is quite different from that in three-dimensional system. The difference occurs because the electric fields remains three dimensional while the induced charge density have reduced dimensionality. As a part of this research we will give a determination of plasma frequency dispersions in a two component layered system. For the first time we show that in such a system there exists two high frequency acoustic plasma modes. We will discuss the condition for these modes to exist and how the finite width of the electronic wave function will affect these modes.

A powerful method for studying the properties of superlattice structure and space charge layers is Ramam scattering<sup>[68-81]</sup>. For type-II superlattice, there is no translational invariance between electron layers and hole layers and effective Coulomb interaction become a tensor. We expect that some new phenomena could be observed in light scattering. To the best of our knowledge no theory of Ramam scattering from a two-component layered electron gas exist. In this work, we will

also present such a theory. We calculate exactly (in RPA) the density-density correlation function for a periodic electron-hole system. From this correlation function we calculate the plasma dispersion relation. A full theory of Ramam scattering cross-section will be given including the line shape and the intensities of various collective modes.

We calculate our response function to the lowest order of plasma parameter  $r_s \approx \frac{\langle V \rangle}{\langle K \rangle}$  where  $V$  and  $K$  are respectively the potential and kinetic energy per particle. Therefore our results are valid under the condition that the average potential energy per particle should be less than the average kinetic energy per particle. For nondegenerate plasmas,  $\langle K \rangle \approx k_B T$  and  $\langle V \rangle$  is roughly  $\frac{e^2}{\epsilon_0 r_0}$ , where  $\epsilon_0$  is the dielectric constant of the medium through which the particles move and  $r_0$  is the mean interparticle spacing. The quantity  $r_0$  is about equal to  $n^{1/3}$  ( or  $n^{1/2}$  for two-dimensional system) where  $n$  is the particle density ( volume or surface). Thus our requirement for weakly coupled system is:

$$\frac{\langle V \rangle}{\langle K \rangle} \approx \frac{e^2 n^{1/3} \beta}{\epsilon_0} \ll 1 \quad (1.1)$$

or for two-dimensional system

$$\frac{\langle V \rangle}{\langle K \rangle} \approx \frac{e^2 n^{1/2} \beta}{\epsilon_0} \ll 1 \quad (1.1a)$$

where  $\beta$  is the inverse temperature in energy unit. Eq.(1.1) can be rewritten in another way

$$\frac{\langle V \rangle}{\langle K \rangle} \approx \frac{1}{4\pi r_D^2 n^{2/3}} \sim \frac{1}{N_D^{2/3}} \quad (3D) \quad (1.2)$$

$$\frac{\langle V \rangle}{\langle K \rangle} \approx \frac{1}{2\pi r_D n^{1/2}} \sim \frac{1}{N_D^{1/2}} \quad (2D) \quad (1.2a)$$

where  $r_D$  is the Debye radius:

$$r_D^2 = \frac{\epsilon_0}{4\pi\beta n e^2} \quad (3D) \quad (1.3)$$

$$r_D = \frac{\epsilon_0}{2\pi\beta n e^2} \quad (2D) \quad (1.3a)$$

and  $N_D$  is the number of particles in the Debye sphere (circle).

For degenerate plasmas,  $\langle K \rangle \sim E_F$ , therefore

$$\frac{\langle V \rangle}{\langle K \rangle} \approx \frac{e^2 n^{1/3} \beta}{\epsilon_0 E_F} \ll 1. \quad (1.4)$$

In Eq.(1.4)  $E_F$  is the Fermi energy of particles  $E_F = \frac{(3\pi^2 n)^{2/3}}{2m^*}$ ,  $n$  is set to unity through this work. Or for 2D system we have

$$\frac{\langle V \rangle}{\langle K \rangle} \approx \frac{e^2 n^{1/2} \beta}{\epsilon_0 E_F} \ll 1. \quad \text{with} \quad E_F = \frac{2\pi n}{2m^*} \quad (1.5)$$

It is convenient to rewrite Eq.(1.4-1.5) in terms of effective Bohr radius,

$r_B = \frac{\epsilon_0}{m^* e^2}$ , then for degenerate plasmas:

$$\frac{\langle V \rangle}{\langle K \rangle} \sim \frac{1}{r_B n^{1/3}} \sim \frac{1}{N_B^{1/3}} \quad (3D) \quad (1.6)$$

and

$$\frac{\langle V \rangle}{\langle K \rangle} \sim \frac{1}{r_B n^{1/2}} \sim \frac{1}{N_B^{1/2}} \quad (2D) \quad (1.6)$$

Therefore the number of particles in Bohr (Debye) sphere ( Bohr(Debye) circle for

2D system) is required to be large for our model. In our numerical calculation  $\tau_s$  is taken to be around 1. This case can be achieved for surface density around  $10^{11}$  to  $10^{12}$  per  $cm^2$ .

Our work will be divided into five chapters: An general introduction is given in Chapter I. Conductivity due to electron-ion scattering will be discussed in Chapter II. In Chapter III, we will investigate the absorption properties of electron-hole system. The effect of electron-LO phonon coupling on the conductivity will be considered in Chapter IV. The Raman intensity for a two-component layered system will be studied in Chapter V. We point out again that our model is only the first approximation to the real superlattice structure. This is a good model in the sense that both electronic temperature and their Fermi energy is small compared to the subband splitting. Also, the photon energy is taken to be small in comparison with the subband splitting. It is expected that our result should reduce to that of single layer for large separation between layers and it should become qualitatively similar to that of a bulk continuum for small separation. Finally, for the conductivity in type-I superlattice system, we have carried a model calculation beyond the layered approximation. Here we allowed the electron to spread in the  $z$ -direction around their  $z=la$  position. Corrections due to the spreading are only significant when the spreading is larger compared to the inter-particle distance.

## Chapter II

### ELECTRON-ION SCATTERING

#### 2.1. Introduction

In this chapter, we shall consider electron-ion layered system and discuss the absorption properties of such a system. We give a schematic diagram in Fig.(1.1) to illustrate the system. We would like to start our work without the pure 2D restriction. Let the electrons have density per unit area  $n$  and mass  $m$ , occupying wells which are positioned at  $z=la$  with well width  $d$  and the fixed ions randomly distributed in planes which are positioned at  $z=na+b$  ( $l, n$  being any integer and  $b$  is the small distance from the well center where the impurities to be doped  $b > \frac{d}{2}$ ). Thus, our system is formed by infinite electron-ion layers. Here  $a$  is the period of the superlattice, i.e., distance between adjacent electron layers. To the lowest order approximation, we may assume that the electrons are all in the ground state and a one band approximation is applicable. We apply a homogeneous, oscillating electric field to our system and use linear-response theory to calculate the current response of the system to such an external field. Since here the motion of electrons in the  $z$ -direction is quantized by the potential well, our model is simplified to a one dimensional array of quasi-two dimensional electron gases. We calculated, for this model, the general expression of conductivity. By comparison of the expression with the Drude formula, we have identified the

---

change in the reactive part of the conductivity with a frequency-dependent effective mass and the expression for scattering time was also obtained by this comparison.

The simplest microscopic approach to the problem of electromagnetic waves and plasma interaction is based on a kinetic description of the plasma in a self-consistent-field approximation<sup>[82]</sup>. We will follow such a description in this Chapter. We start with the equation of motion which is a simplified version of Martin-Schwinger<sup>[83]</sup> Green's function formalism. This method, though not a completely general one, is entirely adequate for the present purpose and has the advantage of closely paralleling the technique that is used in the classical plasma problem<sup>[16,17]</sup>. As in the classical case, the basic approximation is the factorization of a high order correlation function into products of lower order ones. Such a procedure is valid when the average interaction energy of particle in the plasma is small compared to their kinetic energy.

It can easily be shown that in the absence of the ions the long-wavelength frequency-dependent conductivity is independent of electron-electron scattering<sup>[84]</sup>. However, here impurities or scatterers play a crucial role in our interpretation of such a high-frequency uniform-field-transport effect. These scatterers break the translational symmetry and reintroduce Coulombic effects into the conductivity<sup>[36]</sup>.

Tzoar et al <sup>[34]</sup> had calculated the high-frequency conductivity of electrons in 2D inversion layers. We have added to these results expressions for the conductivity at very small and large frequencies and extended their work to superlattices. We will discuss following effects on the absorption such as interference between

layers and finite spreading of the electron wave function.

## 2.2. General Formalism of Total Current

Let us assume that the ions are fixed and that the electrons can move freely on the layers but are quantized by the wells at  $z=la$ . The wave function of single electron will be given as

$$\phi_l(\vec{p}, \vec{r}, z) = e^{i\vec{p}\cdot\vec{r}} \xi(z-la) \quad (2.1)$$

For the infinite height of well,  $\xi(z-la)$  is given as the wave function of single quantum well:

$$\xi(z-la) = \sqrt{\frac{2}{d}} \cos \frac{\pi(z-la)}{d} \theta(z-la + \frac{d}{2}) \theta(la + \frac{d}{2} - z) \quad (2.2)$$

where one-band approximation has been used, i.e., all higher energy bands are neglected because the frequency is smaller compared to the subband gap.  $\vec{p}$  and  $\vec{r}$  are, respectively 2D momentum and position vectors. In Eq.(2.2)  $\theta(x)$  is the step function which is unity for  $x$  larger than zero and vanishes for  $x$  less than zero.

The wave function of the superlattice is given as

$$\Psi(\vec{r}, z, t) = \sum_{\vec{p}, l} a_{\vec{p}, l} e^{i\vec{p}\cdot\vec{r}} \xi(z-la) \quad (2.3)$$

The Hamiltonian of the system is

$$H = T + V^{e-e} + V^{e-I} \quad (2.4)$$

where

$$T = -\frac{(-i\nabla + \frac{e}{c}\vec{A})^2}{2m} \quad (2.5)$$

and the electron-electron interaction is written as:

$$V^{e-e} = \frac{1}{2} \sum_{i,j} \frac{e^2}{[(\vec{r}_i - \vec{r}_j)^2 + (z_i - z_j)^2]^{\frac{1}{2}}} \quad (2.6)$$

The electron-ion interaction is given as:

$$V^{e-I} = - \sum_{i,j} \frac{Ze^2}{[(\vec{r}_i - \vec{R}_j)^2 + (z_i - R_{jz})^2]^{\frac{1}{2}}} \quad (2.7)$$

In second quantized notation, our Hamiltonian can be written as:

$$H = H_1 + H^{e-e} + H^{e-I} \quad (2.8)$$

and

$$\begin{aligned} H_1 &= \frac{1}{2m} \int d\vec{r} dz \Psi^*(\vec{r}, z) \left( -i \hbar \nabla + \frac{e}{c} \vec{A} \right)^2 \Psi(\vec{r}, z) \\ &= \frac{1}{2m} \sum_{\vec{p}, l} \left[ \left( \vec{p} + \frac{e}{c} \vec{A} \right)^2 + \frac{\hbar \pi^2}{d^2} \right] a_{\vec{p}, l}^\dagger a_{\vec{p}, l} \end{aligned} \quad (2.9)$$

Here  $a_{\vec{p}, l}^\dagger$  and  $a_{\vec{p}, l}$  represent, respectively, the electron creation and destruction operators with momentum  $\vec{p}$  on  $l$ th layer. The second term in Eq.(2.9)  $\frac{\hbar \pi^2}{2md^2}$  is the energy of ground state for infinite quantum well. This constant energy does not contribute to the current as we will see shortly. Actually one can drop this term by including it into background.

$$\begin{aligned} H^{e-e} &= \int d\vec{r} dz \int d\vec{r}' dz' \Psi^*(\vec{r}, z) \Psi^*(\vec{r}', z') \times \\ &\quad V^{e-e}(\vec{r} - \vec{r}', z - z') \Psi(\vec{r}', z') \Psi(\vec{r}, z) \end{aligned}$$

$$= \frac{1}{2} \sum_{\vec{q}, \vec{p}, \vec{p}'} \sum_{l'} \frac{2\pi e^2}{q} e^{-q |l-l'|a} f(qd |l-l') a_{\vec{p}+\vec{q}, l} a_{\vec{p}-\vec{q}, l} a_{\vec{p}, l} a_{\vec{p}, l} \quad (2.10)$$

where  $f(qd |l-l')$  is structure factor arising from the integration in the wells because of the finite spatial spreading of the wave function.

$$\begin{aligned} f(qd |l-l') &= \\ & e^{q |l-l'|a} \int dz \int dz' \xi^*(z-la) \xi^*(z'-l'a) e^{-q |z-z'|} \xi(z'-l'a) \xi(z-la) \\ &= \left(\frac{2}{qd}\right)^2 \sinh^2\left(\frac{qd}{2}\right) \left[1 + \left(\frac{qd}{2\pi}\right)^2\right]^{-2} (1 - \delta_{l,l'}) \\ &+ \left[ \frac{2}{qd} \left(1 + \frac{\left(\frac{qd}{2\pi}\right)^2}{2\left(1 + \left(\frac{qd}{2\pi}\right)^2\right)}\right) - \frac{2}{(qd)^2} \frac{(1 - e^{-qd})}{\left[1 + \left(\frac{qd}{2\pi}\right)^2\right]^2} \right] \delta_{l,l'} \end{aligned} \quad (2.11)$$

and

$$\begin{aligned} H^{e-I} &= \int d\vec{r} dz \Psi^*(\vec{r}, z) V^{e-I}(\vec{r} - \vec{R}_i, z - R_{zi}) \Psi(\vec{r}, z) \\ &= - \sum_{\vec{p}, \vec{q}, l, n} \frac{2\pi Z e^2}{q} e^{-q |(l-n)a-b|} g(qd) a_{\vec{p}+\vec{q}, l} a_{\vec{p}, l} \sum_i e^{i\vec{q} \cdot \vec{R}_{ni}} \end{aligned} \quad (2.12)$$

Where  $R_{ni}$  is the position of the  $i$ th ion on the  $n$ th layer.  $g(qd)$  is the following integration:

$$\begin{aligned} g(qd) &= e^{q |(l-n)a-b|} \int dz e^{-q |z-na-b|} \xi^*(z-la) \xi(z-la) \\ &= \frac{2}{qd} \sinh\left(\frac{qd}{2}\right) \left[1 + \left(\frac{qd}{2\pi}\right)^2\right]^{-1} \end{aligned} \quad (2.13)$$

Now the total average 2D current of the system is defined as

$$\vec{j} = c \frac{\delta H}{\delta \vec{A}} \quad (2.14)$$

With the help of Eq. (2.9), we get

$$\vec{j} = \frac{e}{m} \sum_{\vec{p}, l} (\vec{p} + \frac{e}{c} \vec{A}) a_{\vec{p}, l}^\dagger a_{\vec{p}, l} \quad (2.15)$$

where

$$\vec{A} = \vec{A}_0 e^{-i \omega t}$$

and

$$\vec{E} = -\frac{1}{c} \frac{\partial \vec{A}}{\partial t}$$

The total average 2D current is given by

$$\vec{j}(\omega) = \vec{j}_1(\omega) + \vec{j}_2(\omega) \quad (2.16)$$

where

$$\vec{j}_2(\omega) = \sum_l \vec{j}_{2l}(\omega) = \frac{ie^2}{m \omega} \vec{E} \sum_{\vec{p}, l} \langle a_{\vec{p}, l}^\dagger a_{\vec{p}, l} \rangle = \frac{ine^2}{m \omega} \vec{E} \quad (2.17)$$

i.e.

$$\vec{j}_2(\omega) = \sigma_0(\omega) \vec{E} \quad ( \sigma_0(\omega) = \frac{ine^2}{m \omega} ) \quad (2.18)$$

and

$$\vec{j}_1(\omega) = \sum_l \vec{j}_{1l}(\omega) = \frac{e}{m} \sum_{\vec{p}, l} \vec{p} \langle a_{\vec{p}, l}^\dagger a_{\vec{p}, l} \rangle. \quad (2.19)$$

In order to obtain the value of average of the product of two operators we define the single-electron density matrix element between states  $\langle \vec{p}, l |$  and  $| \vec{p} + \vec{k}, l \rangle$  as:

$$F_l(\vec{p} + \vec{k}, \vec{p}, t) = \langle a \dagger_{\vec{p}, l}(t) a_{\vec{p} + \vec{k}, l}(t) \rangle. \quad (2.20)$$

In Heisenberg representation, the equation of motion for the single electron density matrix element is

$$i \frac{\partial}{\partial t} F_l(\vec{p} + \vec{k}, \vec{p}, t) = \langle [a \dagger_{\vec{p}, l} a_{\vec{p} + \vec{k}}, H] \rangle \quad (2.21)$$

This equation can be easily worked out with the help of the commutation rules, we obtain

$$\begin{aligned} & i \frac{\partial}{\partial t} F_l(\vec{p} + \vec{k}, \vec{p}, t) \\ &= (K_{\vec{p} + \vec{k}} - K_{\vec{p}}) F_l(\vec{p} + \vec{k}, \vec{p}, t) + \frac{ie}{m \omega} \vec{k} \cdot \vec{E} e^{-i \omega t} F_l(\vec{p} + \vec{k}, \vec{p}, t) \\ &+ \sum_{\vec{q}} \frac{2\pi e^2}{q} \sum_{l_1} e^{-q |l - l_1| a} f(qd, l - l_1) \times \\ &\langle a \dagger_{\vec{p}, l_1} a_{\vec{p} + \vec{q}, l_1} (a \dagger_{\vec{p}, l} a_{\vec{p} + \vec{k} - \vec{q}, l} - a \dagger_{\vec{p} + \vec{q}, l} a_{\vec{p} + \vec{k}, l}) \rangle \\ &- \sum_{\vec{q}} \frac{2\pi e^2}{q} Z \sum_n e^{-q |(l - n)a - b|} g(qd) \times \\ &\sum_i e^{i \vec{q} \cdot \vec{R}_i} [F_l(\vec{p} + \vec{k} - \vec{q}, \vec{p}, t) - F_l(\vec{p} + \vec{k}, \vec{p} + \vec{q}, t)] \end{aligned} \quad (2.22)$$

where we have neglected terms that are not linear in the external field. Here the kinetic energy of an electron having momentum  $\vec{p}$  is

$$K_{\vec{p}} = \frac{\vec{p}^2}{2m},$$

This is a complicated equation which, through the Coulomb interaction, couples one- and two-particle operators. To make any progress in solving it one must

somehow approximate the latter by simpler functions. The usual procedure is to replace two-particle correlations by suitable products of one-particle functions, let us write:

$$\begin{aligned} \langle a_{\vec{p}, l_1}^\dagger a_{\vec{p}+\vec{q}, l_1} a_{\vec{p}, l}^\dagger a_{\vec{p}+\vec{k}-\vec{q}, l} \rangle &= \langle a_{\vec{p}, l_1}^\dagger a_{\vec{p}+\vec{q}, l_1} \rangle \langle a_{\vec{p}, l}^\dagger a_{\vec{p}+\vec{k}-\vec{q}, l} \rangle \\ + [ \langle a_{\vec{p}, l_1}^\dagger a_{\vec{p}+\vec{q}, l_1} a_{\vec{p}, l}^\dagger a_{\vec{p}+\vec{k}-\vec{q}, l} \rangle - \langle a_{\vec{p}, l_1}^\dagger a_{\vec{p}+\vec{q}, l_1} \rangle \langle a_{\vec{p}, l}^\dagger a_{\vec{p}+\vec{k}-\vec{q}, l} \rangle ] \end{aligned} \quad (2.23)$$

Here the average of an operator product is expressed as the product of two averages, plus a second term ( the bracketed portion of Eq.(2.23) ) which represents the fluctuations about the average values. The key approximation of *self-consistent-field* (SCF) method is to neglect the fluctuation terms in Eq.(2.23), i.e., to make the replacements:

$$\begin{aligned} \langle a_{\vec{p}, l_1}^\dagger a_{\vec{p}+\vec{q}, l_1} a_{\vec{p}, l}^\dagger a_{\vec{p}+\vec{k}-\vec{q}, l} \rangle &\approx \langle a_{\vec{p}, l_1}^\dagger a_{\vec{p}+\vec{q}, l_1} \rangle \langle a_{\vec{p}, l}^\dagger a_{\vec{p}+\vec{k}-\vec{q}, l} \rangle \\ \langle a_{\vec{p}, l_1}^\dagger a_{\vec{p}+\vec{q}, l_1} a_{\vec{p}+\vec{q}, l}^\dagger a_{\vec{p}+\vec{k}, l} \rangle &\approx \langle a_{\vec{p}, l_1}^\dagger a_{\vec{p}+\vec{q}, l_1} \rangle \langle a_{\vec{p}+\vec{q}, l}^\dagger a_{\vec{p}+\vec{k}, l} \rangle \end{aligned} \quad (2.24)$$

This approximation is equivalent to using an effective Coulomb interaction of the form

$$V_{l-l'} = \sum_{\vec{p}, \vec{p}', \vec{q}} a_{\vec{p}+\vec{q}, l}^\dagger a_{\vec{p}, l} \frac{2\pi e^2}{q} e^{-q|l-l'|a} f(qd, l-l') \langle a_{\vec{p}-\vec{q}, l'}^\dagger a_{\vec{p}, l'} \rangle \quad (2.25)$$

in determining the equation of motion, rather than the interaction given in Eq.(2.10). The difference between the two interactions is clear. In Eq.(2.10), electrons respond to the instantaneous field generated by other carriers, whereas in Eq.(2.25) they feel the average field. From this description we can convince ourselves why the RPA is a good approximation in weakly coupled plasmas. In such system, many electrons are within range of one another ( $n \lambda_{FT} \gg 1$ , or  $r_s < 1$  ,

where  $\lambda_{FT}$  is the screening length ) hence the instantaneous field experienced by a typical electron does not deviate much from the average value. This is precisely what is required for Eq.(2.25) to be valid.

With the aid of Eq.(2.25) equation of motion takes the form:

$$\begin{aligned}
 i \frac{\partial}{\partial t} F_l(\vec{p} + \vec{k}, \vec{p}, t) &= (K_{\vec{p} + \vec{k}} - K_{\vec{p}}) F_l(\vec{p} + \vec{k}, \vec{p}, t) \\
 &+ \frac{ie}{m \omega} \vec{k} \cdot \vec{E} e^{-i \omega t} F_l(\vec{p} + \vec{k}, \vec{p}, t) \\
 &+ \sum_{\vec{q}} \frac{2\pi e^2}{q} \left[ \sum_{l_1} e^{-q |l - l_1| a} f(qd, l - l_1) n_{l_1}(\vec{q}, t) \right. \\
 &\left. - Z \sum_n e^{-q |(l - n)a - b|} g(qd) \sum_i e^{i\vec{q} \cdot \vec{R}_{ni}} \right] \times \\
 &[ F_l(\vec{p} + \vec{k} - \vec{q}, \vec{p}, t) - F_l(\vec{p} + \vec{k}, \vec{p} + \vec{q}, t) ] \tag{2.26}
 \end{aligned}$$

and  $n_l$  is the electron density on the  $l$  th layer

$$n_l(\vec{q}, t) = \sum_{\vec{p}} F_l(\vec{p} + \vec{q}, \vec{p}, t). \tag{2.27}$$

In order to obtain the expression for current, we replace the term with time derivative in Eq.(2.26) by

$$i \frac{\partial}{\partial t} F_l(\vec{p} + \vec{k}, \vec{p}, t) = \omega F_l(\vec{p} + \vec{k}, \vec{p}, t) \tag{2.28}$$

The meaning of Eq.(2.28) is that the scattering is elastic in energy because of the infinite mass of ions. Making use of Equations (2.19) and (2.20), we have the following expression for  $j_1(\omega)$

$$\vec{j}_1(\omega) = \frac{-Ze}{m\omega} \sum_{\vec{q}, l, n} \frac{2\pi e^2}{q} e^{-q} {}^{(l-n)a-b} g(qd) \vec{q} n^*_{l}(\vec{q}, \omega) \sum_i e^{i\vec{q} \cdot \vec{R}_m} \quad (2.29)$$

where  $n^*_{l}(\vec{q}, \omega)$  is the complex conjugate of the electron density  $n_l(\vec{q}, \omega)$ , and  $n^*_{l}(\vec{q}, \omega) = n_l(-\vec{q}, \omega)$ . In order to obtain Eq. (2.29), use has been made of the fact that

$$\sum_{\vec{q}, l} \sum_{l'} \frac{\vec{q}}{q} n_l(\vec{q}, t) n_{l'}(-\vec{q}, t) e^{-q} {}^{(l-l')a} f(qd, l-l') = 0. \quad (2.30)$$

Our expression for the average current  $j_1(\omega)$ , Eq.(2.16), is exact and it tells us that the induced current is uniquely determined by the density fluctuations. In the following section we shall develop a method to obtain  $n_l(\vec{q}, \omega)$  to the lowest order in the plasma parameter.

### 2.3. The Evaluation of the Conductivity

So far we have made no use of the fact that  $H^{e-e}, H^{e-I}$  are weak. We now evaluate all quantities in Eq.(2.26) to lowest order in the perturbations, i.e., first order in external field and  $H^{e-I}$  in  $n_l(\vec{q}, \omega)$ , and in consequence the current will be first order in external field and second order in electron-ion interaction. We will neglect the contribution of electron-electron scattering to the conductivity but include them fully in the screening effect.

Our first approximation is to assume the external field to be zero and seek for the change of static electron density matrix due to the electron-ion interaction,

$$(K_{\vec{p}+\vec{k}} - K_{\vec{p}}) F_l(\vec{p}+\vec{k}, \vec{p}, t)$$

$$= -\sum_{\vec{q}} \frac{2\pi e^2}{q} \left( \sum_{l_1} e^{-q |l-l_1|a} n_{l_1}(\vec{q}, t) - Z \sum_n e^{-q |(l-n)a-b|} \sum_i e^{i\vec{q} \cdot \vec{R}_{ni}} \right) \text{timeses}$$

$$\left[ F_l(\vec{p} + \vec{k}, \vec{p}, t) - F_l(\vec{p} + \vec{k}, \vec{p} + \vec{q}, t) \right] \quad (2.31)$$

In this approximation, a term of product in first order will be written as:

$$(nF)^1 = n^1 F^0 + n^0 F^1 \quad (2.32)$$

where the superscripts 0 and 1 indicate respectively, the zeroth and first order term in electron-ion interaction. For a uniform plasma, translational invariance ensures that the average  $\langle a^\dagger_{\vec{p}+\vec{q}} a_{\vec{p}} \rangle$  is zero unless  $q=0$ . Thus since  $q=0$  is excluded, the second term of Eq.(2.31) drops out. The first term only gives a contribution if  $\vec{k} = \vec{q}$ . This is a characteristic of the RPA: that only the  $\vec{k}^{th}$  Fourier component of the Coulomb potential contributes to the response of the system at wave vector  $\vec{k}$ . After reducing the second Coulomb term in Eq.(2.32) in a similar way, we obtain the final result:

$$(K_{\vec{p}+\vec{k}} - K_{\vec{p}}) F_l^1(\vec{p} + \vec{k}, \vec{p}) = (f_{\vec{p}+\vec{k}} - f_{\vec{p}}) \frac{2\pi e^2}{k} \times$$

$$\left[ \sum_{l_1} e^{-k |l-l_1|a} f(qd, l-l_1) n_{l_1}^1(\vec{k}) - Z \sum_n e^{-k |(l-n)a-b|} g(qd) \sum_i e^{i\vec{k} \cdot \vec{R}_{ni}} \right] \quad (2.33)$$

where use has been made of the approximation

$$F_l^0(\vec{p} + \vec{k}, \vec{p}, t) = f_{\vec{p}} \delta_{\vec{k}, 0} \quad (2.34)$$

In Eq.(2.34)  $f_p$  is the Fermi distribution function which is independent of layer index

$$f_p = \frac{1}{e^{\beta(K\vec{p} - \mu)} + 1} \quad (2.35)$$

$\beta$  is the Boltzman constant and  $\mu$  is the chemical potential. In order to solve Eq.(2.30) we sum over  $\vec{p}$  on both side of the above equation and making use of Eq.(2.27), we obtain the electron density corresponding to the density matrix  $F^1$ .

$$n_l^1(\vec{k}) = \frac{2\pi e^2}{k} Q(\vec{k}, 0) \left( \sum_{l_1} e^{-k |l-l_1|a} f(qd, l-l_1) n_{l_1}^1(\vec{k}) \right. \\ \left. - Z \sum_n e^{-k |(l-n)a-b|} g(qd) \sum_i e^{i\vec{k} \cdot \vec{R}_n} \right) \quad (2.36)$$

To solve Eq.(2.36) we use the discrete Fourier transformation in  $l$

$$n(k_z) = \sum_l n_l e^{ik_z a} \quad (2.37)$$

We thus obtain  $n_l(\vec{k})$  for the electrons,

$$n_l(\vec{k}) = a \int_{-\frac{\pi}{a}}^{\frac{\pi}{a}} \frac{dk_z}{2\pi} n(\vec{k}, k_z) e^{ik_z la} \quad (2.38)$$

and similarly for the ions:

$$e^{i\vec{k} \cdot \vec{R}_n} = a \int_{-\frac{\pi}{a}}^{\frac{\pi}{a}} \frac{dk_z}{2\pi} e^{ik_z(na+b)} e^{i\vec{k} \cdot \vec{R}_i(k_z)} \quad (2.39)$$

Clearly  $k_z$  is restricted to the first Brillouin zone. By the above transformation we obtain

$$n^1(\vec{k}, k_z) = - \frac{\frac{2\pi e^2}{k} Q(\vec{k}, 0) Z \sum_i e^{i\vec{k} \cdot \vec{R}_i} S_I(\vec{k}, k_z) g(qd)}{\epsilon(\vec{k}, k_z, 0)} \quad (2.40)$$

where

$$Q(k, \omega) = \int \frac{d\vec{p}}{4\pi^2} \frac{f_{\vec{p}+\vec{k}} - f_{\vec{p}}}{K_{\vec{p}+\vec{k}} - K_{\vec{p}} - \omega - i\alpha} \quad (\alpha \rightarrow 0^+) \quad (2.41)$$

and

$$\epsilon(q, k_z, \omega) = 1 + \frac{2\pi e^2}{k} [f_0(qd) + (S_e(q, k_z) - 1) f_1(qd)] Q(q, \omega) \quad (2.42)$$

with

$$S_e = \sum_l e^{-k|l-t|a} e^{i(l-t)\theta} = \frac{\sinh(ka)}{\cosh(ka) - \cos(\theta)} \quad (2.43)$$

and

$$S_I = \sum_n e^{-k|(l-n)a-b|} e^{i(l-n)\theta - \gamma\theta} = e^{i\gamma\theta} \frac{\sinh[k(a-b)] + e^{-i\theta} \sinh(kb)}{\cosh(ka) - \cos\theta} \quad (2.44)$$

where  $\theta = k_z a$  and  $\gamma = \frac{b}{a}$ . Here  $f_0(qd)$ ,  $f_1(qd)$  are given as:

$$f_0(qd) = \left[ \frac{2}{qd} \left( 1 + \frac{(\frac{qd}{2\pi})^2}{2(1+(\frac{qd}{2\pi})^2)} \right) - \frac{2}{(qd)^2} \frac{(1-e^{-qd})}{[1+(\frac{qd}{2\pi})^2]^2} \right] \quad (2.45)$$

and

$$f_1(qd) = \frac{(\frac{2}{qd})^2 \sinh^2(\frac{qd}{2})}{[1+(\frac{qd}{2\pi})^2]^2} \quad (2.46)$$

After simple substitution of Eqs.(2.34-2.42) into Eq.(2.33), we obtain

$$F_l^{-1} = -Ze^2 \int_{-\pi}^{\pi} \frac{d\theta}{k} \frac{f_{\vec{p}+\vec{k}} - f_{\vec{p}}}{K_{\vec{p}+\vec{k}} - K_{\vec{p}}} e^{i\theta} \frac{S_I(k, \theta) g(qd)}{\epsilon(k, \theta, 0)} \sum_i e^{i\vec{k} \cdot \vec{R}_i(\theta)} \quad (2.47)$$

We immediately see from Eq.(2.47) that the effective ion potential  $\frac{2\pi e^2}{k \epsilon(0)}$  is

screened by the self-consistent field of the electrons.

Next we look for the time dependent part of the single electron density matrix element  $F_l^2(\vec{p}, \vec{p} + \vec{k}, t)$  under the influence of the external field and of the ions. By a linearization procedure we get

$$\begin{aligned}
 & (i \frac{\partial}{\partial t} + K_{\vec{p}} - K_{\vec{p} + \vec{k}}) F_l^2(\vec{p} + \vec{k}, \vec{p}, t) \\
 &= \frac{2\pi e^2}{k} \sum_l e^{-k |l-l'| a} f(qd, l-l') n_l^2(\vec{k}, t) (f_{\vec{p}} - f_{\vec{p} + \vec{k}}) \\
 &+ \frac{ie}{m \omega} \vec{k} \cdot \vec{E} e^{i \omega t} F_l^1(\vec{p}, \vec{p} + \vec{k}) \tag{2.48}
 \end{aligned}$$

where terms not linear in the screened ion potential have been neglected. Assuming that all the quantities have same time-dependent factor  $e^{-i \omega t}$ , we obtain

$$\begin{aligned}
 & (\omega + K_{\vec{p}} - K_{\vec{p} + \vec{k}}) F_l^2(\vec{p} + \vec{k}, \vec{p}, \omega) \\
 &= \frac{2\pi e^2}{k} \sum_l e^{-k |l-l'| a} f(qd, l-l') n_l^2(\vec{k}, \omega) (f_{\vec{p}} - f_{\vec{p} + \vec{k}}) \\
 &+ \frac{ie}{m \omega} \vec{k} \cdot \vec{E} F_l^1(\vec{p}, \vec{p} + \vec{k}) \tag{2.49}
 \end{aligned}$$

where  $n^2(\vec{k}, \omega)$  is the electron density corresponding to density matrix  $F^2$ , it is essentially the induced electron density under the influence of the external field and of the ions. Moving the quantity  $(\omega - K_{\vec{p} + \vec{k}} + K_{\vec{p}})$  in Eq.(2.49) to the left hand side and summing over  $\vec{p}$ , using Eqs.(2.27) and (2.47), we obtain

$$n_l^2(\vec{q}, \omega) = \frac{2\pi e^2}{q} Q(q, \omega) \sum_l e^{-k |l-l'| a} f(qd, l-l') n_l^2(\vec{q}, \omega)$$

$$+ \frac{ie^2}{m\omega^2} \frac{\vec{q} \cdot \vec{E}}{q} [Q(q, \omega) - Q(q, 0)] \int_{-\pi}^{\pi} d\theta e^{i\theta} \frac{S_I(k, \theta) g(qd)}{\epsilon(k, \theta, 0)} \sum_i e^{i\vec{k} \cdot \vec{R}_i(\theta)} \quad (2.50)$$

Performing the Fourier transformation, we obtain,

$$n^2(\vec{q}, \theta, \omega) = \frac{ie^2}{m\omega^2} (\vec{q} \cdot \vec{E}) \frac{2\pi}{q} \frac{[Q(q, \omega) - Q(q, 0)]}{\epsilon(q, \theta, \omega) \epsilon(q, \theta, 0)} S_I(k, \theta) g(qd) \sum_i e^{i\vec{k} \cdot \vec{R}_i(\theta)} \quad (2.51)$$

Using the definition for the dielectric function, our final result for  $N^2(\vec{q}, \theta, \omega)$  can be written as:

$$n^2(\vec{q}, \theta, \omega) = -\frac{iZe}{m\omega^2} \vec{q} \cdot \vec{E} \frac{S_I(q, \theta) g(qd)}{f_0(qd) + (S_e(q, \theta) - 1) f_1(qd)} \times \left| \frac{1}{\epsilon(q, \theta, 0)} - \frac{1}{\epsilon(q, \theta, \omega)} \right| \sum_i e^{i\vec{q} \cdot \vec{R}_i(\theta)} \quad (2.52)$$

Combining Eqs.(2.29) and (2.52) we obtain

$$\vec{j}_1(\omega) = -\frac{iZ^2 e^4}{m^2 \omega^3} \int_{-\pi}^{\pi} d\theta \sum_l \int \frac{d\vec{q}}{4\pi^2 q} \vec{q} (\vec{q} \cdot \vec{E}) \frac{S_I(q, \theta) |g(qd)|^2}{f_0(qd) + (S_e(q, \theta) - 1) f_1(qd)} \left| \frac{1}{\epsilon(q, \theta, 0)} - \frac{1}{\epsilon(q, \theta, \omega)} \right| \sum_l e^{-i\theta} \sum_n e^{-q|(l-n)a-b|} \sum_i e^{-i\vec{q} \cdot \vec{R}_i(\theta)} \sum_j e^{i\vec{q} \cdot \vec{R}_{nj}} \quad (2.53)$$

We use the identity

$$e^{i\vec{q} \cdot \vec{R}_{nj}} = \int_{-\frac{\pi}{a}}^{\frac{\pi}{a}} \frac{adk'_z}{2\pi} e^{ik'_z(na+b)} e^{i\vec{q} \cdot \vec{R}_j(k'_z)} e^{ik'_z la} e^{-ik'_z la} \quad (2.54)$$

and substitute it in Eq.(2.53). We first sum over  $l$  and obtain that  $k_z = k'_z$  (or  $\theta = \theta'$ ) Then summing over  $n$  gives the last part in Eq.(2.53) to be equal to

$S_I^*(q, \theta)$ . Upon making use of the normalization<sup>[83]</sup>,

$$\frac{1}{A} \sum_{ij} e^{i\vec{q} \cdot [\vec{R}_i(k_z) - \vec{R}_j(k_z)]} = n_I = \frac{n}{Z}. \quad (2.55)$$

where A is 2D area of the system. We finally we have

$$\vec{j}_1(\omega) = \frac{-i 2\pi n e^4}{m^2 \omega^3} \int_{-\pi}^{\pi} \frac{d\theta}{2\pi} \int \frac{d\vec{q}}{4\pi^2} \frac{\vec{q}}{q} \vec{q} \cdot \vec{E}$$

$$\frac{|S_I(q, \theta) g(qd)|^2}{f_0(qd) + (S_e(q, \theta) - 1) f_1(qd)} \left| \frac{1}{\epsilon(q, \theta, 0)} - \frac{1}{\epsilon(q, \theta, \omega)} \right|. \quad (2.56)$$

Add  $j_1(\omega)$  and  $j_2(\omega)$  together to obtain:

$$\vec{j}(\omega) = \sigma_0(\omega) \left[ 1 - \frac{2\pi Z e^2}{m \omega^2} \vec{I}(\omega) \text{ right} \right] \cdot \vec{E} \quad (2.57)$$

where

$$\vec{I}(\omega) = \int_{-\pi}^{\pi} \frac{d\theta}{2\pi} \int_0^{\infty} \frac{d\vec{q}}{4\pi^2} \frac{\vec{q}}{q} \frac{|S_I(q, \theta) g(qd)|^2}{f_0(qd) + (S_e(q, \theta) - 1) f_1(qd)} \times$$

$$\left| \frac{1}{\epsilon(q, \theta, 0)} - \frac{1}{\epsilon(q, \theta, \omega)} \right|. \quad (2.58)$$

Since our system is isotropic, i.e.,  $\vec{j}$  is parallel to  $\vec{E}$ , conductivity is given in terms of  $I(\omega) = \frac{\vec{q} \cdot \vec{I} \cdot \vec{q}}{q^2}$  which is given by:

$$I(\omega) = \frac{1}{4\pi} \int_{-\pi}^{\pi} \frac{d\theta}{2\pi} \int_0^{\infty} dq \, q^2 \frac{|S_I(q, \theta) g(qd)|^2}{f_0(qd) + (S_e(q, \theta) - 1) f_1(qd)} \times$$

$$\left| \frac{1}{\epsilon(q, \theta, 0)} - \frac{1}{\epsilon(q, \theta, \omega)} \right| \quad (2.59)$$

Therefore our final expressions for the high-frequency conductivity in our model is

given by

$$\vec{j}(\omega) = \sigma_0(\omega) \left[ 1 - \frac{2\pi Z e^2}{m \omega^2} I(\omega) \right] \vec{E}. \quad (2.60)$$

Let us consider some interesting cases of our result.

(a). Pure two-dimensional approximation. Under this approximation, the wave function is written as:

$$|\xi(z-la)|^2 = \delta(z-la) \quad (2.61)$$

In this case, electrons can only move on the planes at  $z=la$  but localized in  $z$ -direction. Eq.(2.61) is equivalent to set  $d=0$  in our result Eq.(2.59). For the limit  $d=0$ ,  $g(qd) = f_0(qd) = f_1(qd) = 1$ , thus our result is reduced to that obtained by Tzoar and Zhang<sup>[4]</sup>,

$$I(\omega) = \frac{1}{4\pi} \int_{-\pi}^{\pi} \frac{d\theta}{2\pi} \int_0^{\infty} dq \, q^2 \frac{|S_I(q, \theta)|^2}{S_e(q, \theta)} \left| \frac{1}{\epsilon'(q, \theta, 0)} - \frac{1}{\epsilon'(q, \theta, \omega)} \right| \quad (2.62)$$

where  $\epsilon'$  is the dielectric function calculated under pure two-dimensional approximation.

(b) Eq.(2.62) can be reduced further as we approach the limit  $a \rightarrow \infty$ . For very large  $a$ ,  $S_e$  and  $S_I$  reduce to unity and  $e^{-qb}$  respectively while the angular integral

$$\int_{-\pi}^{\pi} \frac{d\theta}{2\pi} = 1$$

In this case  $I(\omega)$  reduces to:

$$I(\omega) = \frac{1}{4\pi} \int_0^\infty dq \, q^2 e^{-2qb} \left| \frac{1}{\epsilon(q,0)} - \frac{1}{\epsilon(q,\omega)} \right| \quad (2.63)$$

This is the result for the single layer case in which the separation between the electron and ion is  $b$ . Therefore, in the weak coupling case, i.e., when the period of the system  $a$  is much larger than the wave-length of density oscillation in the plane, each layer supports its own electron motion. If we neglect the separation  $b$  in Eq.(2.63), we recover to the result given by Tzoar et al<sup>[26]</sup>

$$I(\omega) = \frac{1}{4\pi} \int_0^\infty dq \, q^2 \left| \frac{1}{\epsilon(q,0)} - \frac{1}{\epsilon(q,\omega)} \right| \quad (2.64)$$

We will seek an analytical solution of this integral under some approximation in small and large frequencies.

(c) The difference between Eq.(2.59) and (2.62) is only a quantitative one. We know that the first important characteristic of superlattice structure is the layered electron gas arranged in a *periodic array*. The finite spatial spreading of the electron wave function in the well is of secondary importance because it exists in heterostructures or a single layer and this property was studied in detail even without the existence of other layers. Therefore, as we will see later from our plot, the qualitative behavior of our system will not change if we ignore the electron wave function. However, the quantitative difference is not small.

(d) As a last point of this section, we consider the lowest order correction due to the spreading of electron wave function in determining the modes of collective excitation. The collective excitation is given by

$$\epsilon(q, \theta, \omega) = 0 \quad (2.65)$$

Now for small  $qd$  ( strong coupling system )  $f_0, f_1$  is given as:

$$f_0(qd) = 1 - 0.257(qd) + 0.141(qd)^2 \quad (2.66)$$

and

$$f_1(qd) = 1 + 0.033(qd)^2 \quad (2.67)$$

The long wave length spectrum of density fluctuations is

$$Q(q, \omega) \approx \frac{nq^2}{m\omega^2} \quad (2.68)$$

From Eq.(2.65), the plasma frequency is obtained:

$$\omega^2 = \Omega_p^2 - \frac{0.514\pi n q e^2}{m}(qd) + \frac{2\pi n q e^2}{m}(0.141 + 0.033S(q, \theta))(qd)^2 \quad (2.69)$$

where  $\Omega_p$  is the plasma frequency for the pure 2D approximation

$$\Omega_p^2 = \frac{2\pi n q e^2}{m} S(q, \theta) \quad (2.70)$$

Therefore, the lowest order correction is to shift the plasma frequency downward.

We may note the bulk plasma oscillation at long wavelength is given as

$$\omega_p^2 = \frac{4\pi n_b e^2}{m} \text{ which is independent of wavenumber } q.$$

## 2.4. Scattering Time and Effective Mass

### A. Single-layer determination.

For single layer  $I(\omega)$  is expressed by Eq.(2.64). Using this equation we can write the conductivity as following:

$$\sigma(\omega) = \sigma_0(\omega) \left[ 1 + \frac{\frac{2\pi Ze^2}{m\omega^2} I(\omega)}{1 - \frac{2\pi Ze^2}{m\omega^2} I(\omega)} \right]^{-1} \quad (2.71)$$

The high frequency limit is given by the condition  $|I(\omega)| \ll \omega$  and we thus obtain the approximate expression for conductivity ( to lowest order of  $I(\omega)$  )

$$\sigma(\omega) = \frac{ine^2}{m\omega \left( 1 + \frac{2\pi Ze^2}{m\omega^2} I_1(\omega) + i \frac{2\pi Ze^2}{m\omega^2} I_2(\omega) \right)} \quad (2.72)$$

where  $I_1(\omega)$  and  $I_2(\omega)$  are respectively the real and imaginary parts of  $I(\omega)$ . On the other hand, Drude formula for conductivity can be written as:

$$\sigma(\omega) = \frac{ine^2}{m^* \left( \omega + \frac{i}{\tau} \right)} = \frac{ine^2}{m\omega \left( 1 + \frac{\Delta m}{m} + \frac{i}{\omega\tau} \right)} \quad (2.73)$$

where  $\tau$  is the scattering time,  $m^* = m + \Delta m$  and we have neglected the high order term  $\frac{\Delta m}{m\omega\tau}$ . By comparing our Eq.(2.72) with Eq.(2.73) we can identify

$$\frac{\Delta m}{m} = \frac{Zr_s}{2^{1/2}} N(\Omega, r_s) \quad (2.74)$$

and

$$\frac{1}{\tau} = \frac{Zr_s 4K_F}{2^{1/2}} R(\Omega, r_s) \quad (2.75)$$

where  $K_F$  is the electron Fermi energy,  $\Omega = \frac{\hbar\omega}{4K_F}$ ,  $r_s = \frac{me^2}{\hbar^2 k_F}$ . Using the dimen-

sionless variable  $z = \frac{q}{2k_F}$ , we can write  $N(\Omega, r_s)$ ,  $R(\Omega, r_s)$  as

$$N(\Omega, r_s) = \frac{1}{\Omega^2} \int dz z^2 \left| \frac{1}{\epsilon(z, \Omega)} - \frac{\epsilon_1(z, \Omega)}{\epsilon_1^2(z, \Omega) + \epsilon_2^2(z, \Omega)} \right| \quad (2.76)$$

and

$$R(\Omega, r_s) = \frac{1}{\Omega} \int dz z^2 \left| \frac{\epsilon_2(z, \Omega)}{\epsilon_1^2(z, \Omega) + \epsilon_2^2(z, \Omega)} \right| \quad (2.77)$$

where  $\epsilon_1$  and  $\epsilon_2$  are the real and imaginary parts of  $\epsilon(\omega)$ .

Tzoar et al<sup>[26]</sup> had evaluated the integrals (2.74) and (2.75) numerically for a variety of parameters. Here we would like to evaluate these integrals analytically for small and large  $\Omega$ . By using the RPA result<sup>[23]</sup> for  $Q(q, \Omega)$  at temperature  $T=0$ , the integral equation (4.5) after much algebra, can be cast in the form: (see Appendix 2A)

$$R(\Omega, r_s) \approx A + \frac{r_s^2 \pi}{2(1+r_s)^2} \Omega \quad \text{for } \Omega < \frac{1}{4} \quad (2.78)$$

and

$$R(\Omega, r_s) \approx \frac{\pi r_s}{8\Omega} \quad \text{for } \Omega \gg 1. \quad (2.79)$$

Here

$$A = \frac{\pi}{2} r_s - \frac{r_s^2}{r_s^2 - 1} + \left( \frac{\pi}{2} - \arcsin\left(\frac{1}{r_s}\right) \right) \frac{2r_s^2 - r_s^4}{(r_s^2 - 1)^{3/2}} \quad (r_s > 1)$$

$$A = \frac{\pi}{2} r_s - \frac{r_s^2}{1 - r_s^2} + \frac{3r_s^4 - 2r_s^2}{(1 - r_s^2)^{3/2}} \ln\left(\frac{1 + (1 - r_s^2)^{1/2}}{r_s}\right) \quad (r_s < 1). \quad (2.80)$$

Actually, Eq.(2.78) matches the numerical work very well for small  $\Omega$  and  $\Omega$  beyond 2.0. The integral (2.76) is rather complicated; however, we are interested in

small  $\Omega$  behavior and this can be done by using the dispersion relation

$$\operatorname{Re}\left(\frac{1}{\epsilon(\Omega)}\right) = 1 + \frac{2}{\pi} P \int_0^\infty \frac{\Omega_1 d \Omega_1}{\Omega_1^2 - \Omega^2} \operatorname{Im}\left(\frac{1}{\epsilon(\Omega_1)}\right). \quad (2.81)$$

We obtain

$$N(\Omega, r_s) = \frac{2}{\pi \Omega^2} \int z^2 dz \frac{\left( P \int_0^\infty \frac{d \Omega_1}{\Omega_1} \operatorname{Im}\left(\frac{1}{\epsilon(\Omega_1)}\right) - P \int_0^\infty \frac{\Omega_1 d \Omega_1}{\Omega_1^2 - \Omega^2} \right)}{\Omega_1^2 - \Omega^2} \operatorname{Im}\left(\frac{1}{\epsilon(\Omega_1)}\right) \quad (2.82)$$

Use Eq.(2.76) we obtain

$$N(\Omega, r_s) = -\frac{r_s^2}{(1+r_s)^3} \ln \Omega = -\frac{2B}{\pi} \ln \Omega \quad (2.83)$$

where B is the slope of  $R(\Omega, r_s)$  for small  $\Omega$ . Equation (4.11) tells us that as  $\Omega$  approaches zero, the particles will become very heavy, so the mobility goes to zero. Our analytical results are in full agreement with the numerical calculations of reference 35.

### B. Periodic layered system.

In this case we have to evaluate the following two integrals

$$R(\Omega, r_s, \theta, \gamma) = \frac{1}{\Omega} \int_{-\pi}^{\pi} \frac{d \theta}{2\pi} \int dz z^2 \times \frac{|S_I(z, \theta) g(qd)|^2}{f_0(qd) + (S_e(z, \theta) - 1) f_1(qd)} \frac{\epsilon_2(z, \theta, \Omega)}{|\epsilon(z, \theta, \Omega)|^2} \quad (2.84)$$

and

$$N(\Omega, r_s, \theta, \gamma) = \frac{1}{\Omega^2} \int \frac{d\theta}{2\pi} \int dz z^2 \times \frac{|S_I(z, \theta)g(qd)|^2}{f_0(qd) + (S_e(z, \theta) - 1)f_1(qd)} \left| \frac{1}{\epsilon(z, 0)} - \frac{\epsilon_1(z, \theta, \Omega)}{|\epsilon(z, \theta, \Omega)|^2} \right| \quad (2.85)$$

Again, a good approximate solution can be obtained for small and large  $\Omega$  by the same calculation as in Appendix 2A. Algebraic calculation gives us

$$R(\Omega, r_s, \theta, \gamma) \approx A_m + B_m \Omega \quad \text{for} \quad \Omega < \frac{1}{4} \quad (2.86)$$

for large  $\Omega$  we obtain:

$$R(\Omega, r_s, \theta, \gamma) \approx \frac{\pi r_s}{8\Omega} |g(2k_F d \sqrt{\Omega})|^2 e^{-4k_F b \sqrt{\Omega}} (1 + e^{-4k_F (a-2b)\sqrt{\Omega}}) \quad (2.87)$$

$A_m$  and  $B_m$  are expressed as follows ( here m refers to the many-layer system )

$$A_m = \frac{r_s}{\pi} \int_0^\pi d\theta \int_0^1 dz \frac{|S_I(z, \theta)g(2k_F dz)|^2}{\left| 1 + \frac{r_s (f_0(qd) + (S_e - 1)f_1(2k_F dz))}{z} \right|^2 (1-z^2)^{1/2}} \quad (2.88)$$

and

$$B_m = \frac{r_s^2 \pi |g(2k_F d)|^2 \sinh(2k_F a)}{2[1 + r_s (f_0(2k_F d) - f_1(2k_F d))] (G^2 - 1)^{3/2}} \left[ (G^2 + \frac{1}{2})M + \frac{3JG}{2} \right] \quad (2.89)$$

with

$$G = \frac{r_s \sinh(2k_F a)}{1 + r_s (f_0(2k_F d) - f_1(2k_F d))} + \cosh(2k_F a)$$

$$M = \sinh^2(2k_F (a - b)) + \sinh^2(2k_F b)$$

$$J = 2\sinh(2k_F(a-b))\sinh(2k_F b) \quad (2.90)$$

Clearly as  $a \rightarrow \infty, b \rightarrow 0, d \rightarrow 0$ , we have  $A_m \rightarrow A, B_m \rightarrow B$ . We easily see that the value of the expression in the parentheses on the right-hand side of Eq.(2.87) approaches unity when frequencies are very high. For the special case  $a = 2b$ , this value is 2 since electrons are scattered equally by two adjacent ion layers. For finite  $a$  and  $b$ , but  $d \rightarrow 0$  our result is just that obtained by Tzoar and Zhang<sup>84</sup>. We may estimate the quantitative difference of our result from that of reference 84. To do this we expand Eq.(2.88) to the lowest order of  $qd$

$$A_m = A'_m + \Delta A_m = \frac{r_s}{\pi} \int_0^\pi d\theta \int_0^1 dz \frac{|S_I(z, \theta)|^2}{\left[1 + \frac{r_s S_e}{z}\right]^2 (1-z^2)^{1/2}} + \Delta A_m \quad (2.91)$$

where  $A'_m$  is the value of  $A_m$   $|_{d \rightarrow 0}$ , and  $\Delta A_m$  is the lowest order correction due to the finite spatial spreading of the wave function which is obtained as:

$$\Delta A_m = \frac{0.514k_F dr_s}{\pi} \int_0^\pi d\theta \int_0^1 z dz \frac{|S_I(z, \theta)|^2}{\left[1 + \frac{r_s S_e}{z}\right]^3 (1-z^2)^{1/2}} + \Delta A_m \quad (2.92)$$

It is easy to see that  $\Delta A_m$  is a small quantity because the factor  $0.514k_F d$  and  $\frac{z}{1 + \frac{r_s S_e}{z}}$  are both small compare to one. Numerical calculation shows  $\frac{\Delta A_m}{A_m}$

about 10 to 20 percent. This small amount of enhancement is due to the collisions in z-direction. Same estimation can be done for  $B_m$ , the difference in  $B_m$  is much less noticeable. For high frequency, Eq.(2.87) is not suitable for expansion in  $d$  since it appears as a product with  $\sqrt{\Omega}$  which is large in question. But we can see from our numerical calculation that for  $\Omega \gg 1$ , there is no difference between pure 2D system and present treatment.

Again we are interested in the low-frequency behavior of the change of effective mass. The dispersion relation gives us

$$N(\Omega r_s) = -\frac{2}{\pi} B_m \ln \Omega \quad (2.93)$$

We immediately see the mass function of the superlattice has same strong frequency dependence as the single-layer system, particularly at rather small  $\Omega$  it decreases very rapidly. The origin of this variation was pointed out by Tzoar et al<sup>[26]</sup>.

It is difficult to obtain the general solution for  $R(\Omega r_s)$  for the whole range of  $\Omega$ . However, we have calculated the integral (2.84) numerically for several parameters. The results are plotted in Figures 2.1-2.5

## 2.5. Discussion

In this chapter, we have derived the expressions for the effective mass and inverse collision time of type-I superlattices in the long-wavelength and high frequency limits due to electron-ion scattering. Analytical solutions for these integrals are obtained for low- and high-frequency limits. Numerical calculation reveals the relative differences between the single-layer case and superlattice case. This difference is essentially due to interference of different layers. In order to have noticeable interferences, the form factors  $S_e$  and  $S_I$  in the integrands of Eqs.(2.84) and (2.85) should be different from unity. It is easy to see that different layers become uncoupled if  $(q_{\max} a)$  is much larger than unity, where  $\frac{q_{\max}}{2k_F}$  is the upper limit of the integral of Eq.(2.84) and  $q_{\max}$  can be written as

$$q_{\max} = k_F [ 1 + ( 1 + 4\Omega )^{1/2} ]$$

At low frequencies, the inverse collision time of the superlattice is reduced relative to that of the single layer due to an increase in the static screening of neighboring layers. On the other hand we find an increase in the inverse collision time at intermediate frequencies. Here the dynamical screening effect of the superlattice allows the excitations of an electron-hole pair to take place on any layer  $l$ , even if the photon is being absorbed at a specific layer  $l'$ . This process becomes negligibly small when the spacing  $a$  increases, and in the limit of  $a \rightarrow \infty$  we obtain the inverse collision time of the superlattice be identical to that of the single layer. Finally, for very high frequencies ( $q_{\max}a \gg 1$ ), as expected we have no interference effect between the layers in the superlattice and we find that as  $\omega \rightarrow \infty$  the inverse collision time for the superlattice asymptotically approaches that of the single layer. The quantitative behaviors are shown in Fig.(2.1).

In Figures (2.2-2.4) we show quantitatively how the finite spreading of the electron wave function affects the absorption process. We found that the inverse collision time increases with the width of electron spreading. The physical interpretation for this behavior is that the average electron-ion interaction is an increasing function of the width  $d$ . In other words, the quantity  $g(qd)$  is always great than unit and increase with  $qd$ . For small  $qd$ , the lowest order correction from  $g(qd)$  is:

$$g(qd) = \frac{2}{qd} \left[ \frac{qd}{2} + \frac{1}{6} \left( \frac{qd}{2} \right)^3 \right] \left( 1 - \frac{(qd)^2}{2\pi^2} \right) = 1 + \left( \frac{qd}{2} \right)^2 \left[ \frac{1}{6} - \frac{1}{\pi^2} \right] \quad (2.94)$$

Therefore the correction for finite spreading at low energy is proportional to  $(qd)^2$ .

For large  $qd$  we have:

$$g(qd) = \frac{8\pi^2}{qd} e^{\frac{qd}{2}} \quad (2.95)$$

In this case, the ratio of absorption with spreading to that of a pure two-dimensional system will be very large. However, the absorption for either system is asymptotically approaches zero. In Fig.(2.5) we present two plasmon dispersion curves for two different widths of the electron wave function.

## 2.6. Appendix 2A

We use the two-dimensional polarizability at  $T=0$  as given by Stern<sup>[23]</sup>. We denote  $\epsilon_1$  as the real part of the dielectric function and  $\epsilon_2$  as the imaginary part of the dielectric function.

$$\epsilon_1(\Omega, z) = 1 + \frac{r_s}{2z^2} \left( 2z - C_+ \sqrt{\left(z + \frac{\Omega}{z}\right)^2 - 1} - C_- \sqrt{\left(z - \frac{\Omega}{z}\right)^2 - 1} \right) \quad (2A1)$$

and

$$\epsilon_2(\Omega, z) = \epsilon_{21} - \epsilon_{22} = \frac{r_s}{2z^2} \left( D_- \sqrt{1 - \left(z - \frac{\Omega}{z}\right)^2} - D_+ \sqrt{1 - \left(z + \frac{\Omega}{z}\right)^2} \right) \quad (2A2)$$

where  $C_{\pm}$  is nonzero only if  $|z \pm \Omega/z| > 1$  and  $D_{\pm}$  is nonzero only if  $|z \pm \Omega/z| < 1$ . At low frequency, only single particle excitation contribute. For small  $\Omega$ ,  $|z \pm \Omega/z| < 1$  is equivalent to

$$\Omega - \Omega^2 < z < 1 \mp \Omega - \Omega^2$$

and  $|z \pm \Omega/z| > 1$  is equivalent to

$$z > 1 \mp \Omega - \Omega^2$$

Therefore  $C_-$  is definitely zero in the entire region of integration for  $\epsilon_2$ . Since

there is a  $\frac{1}{\Omega}$  factor in front of the integral we should keep the terms up to  $\Omega^2$  to retain the  $\Omega$ -dependence in lowest order. Now

$$\begin{aligned}
 R(\Omega) &= \frac{1}{\Omega} \int_{\Omega-\Omega^2}^{1-\Omega-\Omega^2} z^2 dz \frac{\epsilon_{21} - \epsilon_{22}}{\epsilon(z)^2 + \epsilon_2(z, \Omega)^2} + \frac{1}{\Omega} \int_{1-\Omega-\Omega^2}^{1+\Omega-\Omega^2} z^2 dz \frac{\epsilon_{21}}{\epsilon(z, \Omega)^2 + \epsilon_2(z, \Omega)^2} \\
 &= \frac{1}{\Omega} \int_{\Omega-\Omega^2}^{1+\Omega-\Omega^2} z^2 dz \frac{\epsilon_{21}}{\epsilon(z)^2 + \epsilon_2(z, \Omega)^2} - \frac{1}{\Omega} \int_{\Omega-\Omega^2}^{1-\Omega-\Omega^2} z^2 dz \frac{\epsilon_{22}}{\epsilon(z)^2 + \epsilon_2(z, \Omega)^2} \\
 &+ \frac{1}{\Omega} \int_{1-\Omega-\Omega^2}^{1+\Omega-\Omega^2} z^2 dz \frac{\epsilon_{21}}{\epsilon(z, \Omega)^2 + \epsilon_2(z, \Omega)^2} - \frac{1}{\Omega} \int_{1-\Omega-\Omega^2}^{1+\Omega-\Omega^2} z^2 dz \frac{\epsilon_{21}}{\epsilon(z)^2 + \epsilon_2(z, \Omega)^2} \quad (2A3)
 \end{aligned}$$

Let's denote R by  $\frac{1}{\Omega}[I - II + III]$  where I represents the first two integrals in Eq.(2A3) and II (III) represents the second and third integral in Eq.(2A3). Please note the difference of the denominators II and III. Let us consider I first. We see I has the property that  $I = F(\Omega) - F(-\Omega)$ . Therefore  $I = a\Omega$  for small  $\Omega$  and b can be written as:

$$a = \left. \frac{\partial F(\Omega)}{\partial \Omega} \right|_{\Omega=0} \quad (2A4)$$

where

$$F(\Omega) = \int_{\Omega-\Omega^2}^{1+\Omega-\Omega^2} z^2 dz \frac{0.5r_s [1 - (z - \frac{\Omega}{z})^2]^{1/2}}{(z+r_s)^2 + r_s^2 \Omega^2 z^{-2} (1-z^2)^{-2}} \quad (2A5)$$

Use the formula

$$\frac{\partial}{\partial t} \int_{a(t)}^{b(t)} g(x, t) dx = \int_{a(t)}^{b(t)} \frac{\partial g(x, t)}{\partial t} dx$$

$$+ g(b, t) \frac{\partial b(t)}{\partial t} - g(a, t) \frac{\partial a(t)}{\partial t} \quad (2A6)$$

We obtain

$$\begin{aligned} a &= \frac{r_s}{2} \int_0^1 z^2 dz \frac{\partial}{\partial t} \left[ \frac{[1 - (z - \frac{\Omega}{z})^2]^{1/2}}{(z + r_s)^2 + r_s^2 \Omega^2 z^{-2} (1 - z^2)^{-2}} \right] \Big|_{\Omega=0} \\ &= \frac{r_s}{2} \int_0^1 \frac{z^2 dz}{[1 - z^2]^{1/2} (z + r_s)^2} = \frac{r_s}{2} \int \frac{z dz}{[1 - z^2]^{1/2}} \left[ \frac{1}{z + r_s} - \frac{r_s}{(z + r_s)^2} \right] \\ &= \frac{r_s}{2} \int \frac{dz}{[1 - z^2]^{1/2}} \left[ 1 - \frac{2r_s}{z + r_s} + \frac{r_s^2}{(z + r_s)^2} \right] \end{aligned} \quad (2A7)$$

These three terms are all elementary integration. The result are in Eq.(2.80)

Next we consider II

$$II = \int_{1-\Omega-\Omega^2}^{1+\Omega-\Omega^2} z^2 dz \frac{0.5r_s [1 - (z - \frac{\Omega}{z})^2]^{1/2}}{(z + r_s)^2 + r_s^2 \Omega^2 z^{-2} (1 - z^2)^{-2}} \quad (2A8)$$

The term with  $\Omega^2$  in denominator contribute to absorption with  $\Omega^2$  and can be neglected. Now we expand III for small  $\Omega$ :

$$\begin{aligned} III &= \int_{1-\Omega-\Omega^2}^{1+\Omega-\Omega^2} dz \frac{0.5r_s [1 - (z - \frac{\Omega}{z})^2]^{1/2}}{\left[ 1 + \frac{r_s}{z} - \frac{r_s}{2z^2} [(z + \frac{\Omega}{z})^2 - 1]^{1/2} \right]^2 + \frac{r_s^2}{4z^4} [1 - (z - \frac{\Omega}{z})^2]} \\ &= \int_{1-\Omega-\Omega^2}^{1+\Omega-\Omega^2} z^2 dz \frac{0.5r_s [1 - (z - \frac{\Omega}{z})^2]^{1/2}}{(z + r_s)^2 + r_s^2 \Omega z^{-4} - (1 + \frac{r_s}{z}) \frac{r_s}{z^2} [(z + \frac{\Omega}{z})^2 - 1]^{1/2}} \end{aligned} \quad (2A9)$$

In this integral  $z$  is evaluated near 1 so  $(z + \frac{\Omega}{z})^2$  is close to 1 and we can treat

$[(z + \frac{\Omega}{z})^2 - 1]^{1/2}$  as a small quantity. Thus

$$III = \frac{r_s}{2} \int_{1-\Omega-\Omega^2}^{1+\Omega-\Omega^2} z^2 dz \frac{[1 - (z - \frac{\Omega}{z})^2]^{1/2}}{(z + r_s)^2} \left( 1 + \frac{r_s}{z(z + r_s)} \sqrt{(z + \frac{\Omega}{z})^2 - 1} \right) \quad (2A10)$$

We immediately see that the first term just cancel II and finally we should evaluate the second term in Eq.(2A10). After letting  $z=1+x$  we have for  $I'=III-II$

$$I' = r_s^2 \int_{-\Omega-\Omega^2}^{\Omega-\Omega^2} dx \frac{\sqrt{\Omega^2 - x^2}}{(1+r_s)^3} = \frac{r_s^2 \Omega^2}{(1+r_s)^3} \left( \sin^{-1}(1-\Omega) + \sin^{-1}(1+\Omega) \right) = \frac{\pi r_s^2 \Omega^2}{(1+r_s)^3} \quad (2A11)$$

Now we consider the behavior of  $R(\Omega)$  at large  $\Omega$ . In this region  $\epsilon$  can be approximated as 1 and  $\epsilon_{22}=0$ . we have

$$R(\Omega) = \frac{r_s}{2\Omega} \int_{\sqrt{\Omega-0.5}}^{\sqrt{\Omega+0.5}} dz \sqrt{1 - (z - \frac{\Omega}{z})^2} \quad (2A12)$$

Set  $z = \sqrt{\Omega} + x$  and neglect the  $\frac{x^2}{\Omega}$

$$R(\Omega) = \frac{r_s}{2\Omega} \int_{-0.5}^{0.5} dz \sqrt{1 - 4z^2} = \frac{\pi r_s}{8\Omega} \quad (2A13)$$

For many layered system, because of the third integration in z-direction, the expression for  $a_m$  can only be obtained in terms of numerical integration which is given in Eq.(2.88). However the expression for  $b_m$  can still be obtained analytically. The equation similar to Eq.(2A11) reads:

$$(III - II)_m = r_s^2 \int_{-\Omega-\Omega^2}^{\Omega-\Omega^2} dx \sqrt{\Omega^2 - x^2} \int \frac{d\theta}{2\pi} \frac{|S_I(\theta, 2k_F a)|^2}{(1+r_s S_e(\theta, 2k_F a))^3} \quad (2A14)$$

The result for x-integration is still  $\pi\Omega^2$ . The integral over  $\theta$  can be cast into following:

$$\int \frac{d\theta}{2\pi} \frac{|S_I(\theta, 2k_F a)|^2}{(1+r_s S_e(\theta, 2k_F a))^3} = \int \frac{d\theta}{2\pi} \frac{A + B \cos\theta + C \cos^2\theta}{(G - \cos\theta)^3} \quad (2A15)$$

where

$$G = \cosh(2k_F a) + r_s \sinh(2k_F a)$$

$$A = \cosh(2k_F a) [ \sinh^2(2k_F b) + \sinh^2(2k_F (a-b)) ]$$

$$B = 2 \sinh(2k_F (a-b)) \sinh(2k_F b) - [ \sinh^2(2k_F b) + \sinh^2(2k_F (a-b)) ]$$

$$C = 2 \sinh(2k_F (a-b)) \sinh(2k_F b)$$

Or Eq.(2A15) can be rewritten as:

$$\frac{A'}{2\pi} \int \frac{d\theta}{(G - \cos\theta)^3} + \frac{B'}{2\pi} \int \frac{d\theta}{(G - \cos\theta)^2} + \frac{C}{2\pi} \int \frac{d\theta}{G - \cos\theta} \quad (2A16)$$

In Eq.(2A16),  $A' = A + BG + CG^2$  and  $B' = -B - 2CG$ . The integration in Eq.(2A16) is elementary and the result is shown in the text.

## Chapter III

### TWO-COMPONENT LAYERED ELECTRON GAS

#### 3.1. Introduction

The calculation on conductivity and resistivity for a two-component electron gas in bulk system was first performed by Tzoar and Platzman<sup>[86]</sup>. They particularly focused their attention on the effect of dynamical correlation. Later on they extended their discussion to 2D two-component system<sup>[31]</sup>. If electrons and holes are located in the alternating layers which are arranged to a periodic array. The new system should show an intermediate behavior between 3D and 2D plasmas, as mentioned in the general introduction.

The real system for such a model is InAs-GaSb superlattice. The junction between GaSb and InAs is characterized by the unusual situation that the conduction band of InAs is lower than the upper valence band edge of GaSb ( see Fig. 1.2 ). Therefore there is a energy range in which charge carriers crossing the interface change from electron-like to hole-like character. Unlike type-I superlattice, both type of carriers (electron and hole) are primarily confined in the GaAs region and ionized impurities remain in th GaAlAs region, here electrons mainly exist in InAs while holes in GaSb region. Most theoretical and experimental research was on electronic properties and subband structure. We have given wide references about the research in this area in Chapter 1.

In this chapter, we shall investigate for the first time the response of a two-component layered electron gas to a long-wavelength high-frequency electromagnetic radiation. The high-frequency conductivity of such a system reflects many of its important physical and optical properties. In Chapter 2 we treat the ion as fixed scatterers and use a method of kinetic description. That formalism can be used for the two-component systems only if one accounts for the mobility of the holes. We choose to use the Kubo's formula for conductivity and the temperature-dependent Green's function technique instead. We treat the electrons and holes on equal footing, and only restrict ourselves to the approximation that both electrons and holes are confined in sheets of zero thickness. If the energy of the incident photons is less than the energy difference between the ground state and the first excited state, and the mean spreading of wave function is less than the layer thickness, our approximation is realistic and can be used as a model for theoretical calculation which should be valid in and can be compared with real systems. Within this model, we shall obtain an exact expression for the conductivity and resistivity. They are dependent on frequency, plasma parameter  $r_s$ , spatial separation  $a$  and density per unit area  $n$ . We will evaluate the resistivity numerically. The result will be useful for interpreting the far-infrared Drude type conductivity of 2D two-component layered electron gas.

### 3.2. General Formalism Of The Problem

Calculations of the current-current correlations and the conductivity in a free-electron gas have been worked out in much detail and are well documented [19]. The calculation for the superlattice system is remarkably similar<sup>[6]</sup>. We evalu-

ate the conductivity treating the electron-hole collision within the Born approximation (high-frequency conductivity), however treating the self-consistent fields of fluctuating electron and hole gas exactly in the random-phase approximation (RPA). Our expression will include full dynamical screening of the electrons and holes.

Let us consider electrons of density  $n_e$  per unit area and mass  $m_e$  occupying layers which are positioned at  $z = ja$  and holes of density  $n_h$  per unit area and mass  $m_h$  occupying layers which are positioned at  $z = ja + b$ . Where  $j$  can be any integer,  $a$  is the length of the unit cell in z-direction and  $b$  is the separation between electrons and holes on each cell. We start from the general expression of long wavelength conductivity for a system of charged particles as given by Kubo <sup>24</sup> which reads

$$\sigma_{\mu\nu}(\omega) = \int_0^{\infty} e^{i\omega t} dt \int_0^{\beta} \langle j_{\mu}(t - i\lambda) j_{\nu}(0) \rangle d\lambda \quad (3.1)$$

where  $\omega$  is the frequency of electromagnetic wave and we set  $\hbar$  equal to unity for notational convenience. Here,

$$j_{\mu}(t) = e^{iHt} j_{\mu}(0) e^{-iHt} \quad (3.2)$$

is the current operator in Heisenberg representation and the average of an operator is defined by

$$\langle O \rangle = Tr [ e^{\beta(\Omega + \sum_s \mu_s N_s - H)} O ] \quad (3.3)$$

where  $H$  is the total Hamiltonian of the system and  $\Omega$  is defined by

$$e^{-\beta\Omega} = Tr [ e^{\beta(\sum_s \mu_s N_s - H)} ] \quad (3.4)$$

In Eqs.(3.3) and (3.4)  $\mu_s$  and  $N_s$  are, respectively, the chemical potential and

number operator of  $s$  species in the system, and  $\beta$  the inverse of the temperature in energy units. In order to render Eqn.(3.1) in a more convenient form we integrate it by parts:

$$\begin{aligned}
 \sigma_{\mu\nu}(\omega) &= \int_0^\infty e^{i\omega t} dt \int_0^\beta \langle j_\mu(t-i\lambda) j_\nu(0) \rangle d\lambda \\
 &= \int_0^\infty \frac{de^{i\omega t}}{i\omega} \int_0^\beta \langle j_\mu(t-i\lambda) j_\nu(0) \rangle d\lambda \\
 &= -\frac{1}{i\omega} \int_0^\beta \langle j_\mu(-i\lambda) j_\nu(0) \rangle d\lambda \\
 &\quad - \int_0^\infty e^{i\omega t} \frac{dt}{i\omega} \int_0^\beta d\lambda \frac{\partial}{\partial t} \langle j_\mu(t-i\lambda) j_\nu(0) \rangle \\
 &= \sigma_{\mu\nu}^0(\omega) + \sigma_{\mu\nu}^1(\omega)
 \end{aligned} \tag{3.5}$$

where

$$\sigma_{\mu\nu}^0(\omega) = -\frac{1}{i\omega} \int_0^\beta d\lambda \langle j_\mu(-i\lambda) j_\nu(0) \rangle = \frac{ie^2}{a\omega} \left[ \frac{n_e}{m_e} + \frac{n_h}{m_h} \right] \delta_{\mu\nu} \tag{3.6}$$

and

$$\begin{aligned}
 \sigma_{\mu\nu}^1(\omega) &= -\frac{1}{i\omega} \int_0^\infty e^{i\omega t} dt \int_0^\beta d\lambda \frac{\partial}{\partial t} \langle j_\mu(t-i\lambda) j_\nu(0) \rangle \\
 &= -\frac{1}{\omega} \int_0^\infty e^{i\omega t} dt \int_0^\beta d\lambda \frac{\partial}{\partial \lambda} \langle j_\mu(t-i\lambda) j_\nu(0) \rangle \\
 &= -\frac{1}{\omega} \int_0^\infty e^{i\omega t} dt \langle j_\mu(t) j_\nu(0) - j_\mu(t-i\beta) j_\nu(0) \rangle
 \end{aligned}$$

Now the second term in the bracket can be converted to

$$\begin{aligned}
 \langle j_\mu(t - i\beta) j_\nu(0) \rangle &= \langle e^{\beta H} j_\mu(t) e^{-\beta H} j_\nu(0) \rangle \\
 &= \text{Tr} \left[ e^{\beta(\Omega + \sum_s \mu_s N_s)} e^{-\beta H} e^{\beta H} j_\mu(t) e^{-\beta H} j_\nu(0) \right] \\
 &= \text{Tr} \left[ e^{\beta(\Omega + \sum_s \mu_s N_s - H)} j_\mu(0) j_\nu(t) \right] \\
 &= \langle j_\mu(0) j_\nu(t) \rangle
 \end{aligned}$$

and we obtain

$$\sigma_{\mu\nu}^1(\omega) = -\frac{1}{i\omega} \int_0^\infty dt e^{i\omega t} \langle [j_\mu(t), j_\nu(0)] \rangle \quad (3.7)$$

The wave function for electrons is given by:

$$\psi_j^e(\vec{p}, \vec{r}, z) = e^{i\vec{p}\cdot\vec{r}} \xi(z - ja) \quad (3.8)$$

and similarly for holes

$$\psi_j^h(\vec{p}, \vec{r}, z) = e^{i\vec{p}\cdot\vec{r}} \xi(z - ja - b) \quad (3.8a)$$

where  $\vec{p}, \vec{r}$  are respectively, the 2-D momentum and position vector,  $j$  is index for  $j$ th cell.  $\xi(z - ja)$  is defined in following way such that all the particles are confined in the sheets of zero thickness.

$$|\xi(z - ja)|^2 = \delta(z - ja) \quad (3.9)$$

By this, the current operator and interaction operator can be expressed as

$$\vec{j}(k) = \sum_{\vec{p}, j, s} \frac{e_s}{m_s} \vec{p} a_{\vec{p}+\vec{k}, j}(s) a_{\vec{p}, j}(s) \quad (3.10)$$

where summation over  $s$  means that  $s$  can be either electron or hole, and

$$H_I = \frac{1}{2} \sum_{\vec{q}, \vec{p}, \vec{p}', j, j'} \sum_{s, s'} \frac{2\pi}{q} e_s e_{s'} e^{-q |j-j'| a} \times$$

$$a_{\vec{p}+\vec{q}, j}(s) a_{\vec{p}-\vec{q}, j}(s') a_{\vec{p}', j}(s') a_{\vec{p}, j}(s) \quad (3.11)$$

Therefore

$$\sigma_{\mu\nu}^1(\omega) = \frac{1}{\omega} \sum_{\vec{p}, s} \sum_{\vec{p}', s'} \frac{e_s}{m_s} \frac{e_{s'}}{m_{s'}} p_{\mu} p'_{\nu} \int_0^{\infty} dt e^{i\omega t} \times$$

$$\langle a_{\vec{p}+\vec{k}, j}(s) a_{\vec{p}, j}(s), a_{\vec{p}-\vec{k}, j}(s) a_{\vec{p}, j}(s) \rangle \quad (3.12)$$

### 3.3 Relation Between Electrical Conductivity and Finite Temperature Green's Function.

Now in order to facilitate the temperature dependent Green's function formalism, we define a function

$$Y_{\mu\nu}(z) = \int_{-\infty}^{\infty} \frac{d\omega}{\omega-z} (1-e^{-\beta\omega}) \phi_{\mu\nu}(\omega) \quad (3.13)$$

which is analytic in the entire z-plane except for a cut on the real axis  $\phi_{\mu\nu}$  is real and given as

$$\phi_{\mu\nu} = \sum_{nn'} \exp[\beta(\Omega + \sum_s \mu_s N_s - E_n)] \langle n | j_{\mu}(0) | n' \rangle \langle n' | j_{\nu}(0) | n \rangle \delta(E_{n'} - E_n - \omega) \quad (3.14)$$

where n and n' represent eigenstates of Hamiltonian and number operator with

$$H |n\rangle = E_n |n\rangle, \text{ and } N_s |n\rangle = N_s^{(n)} |n\rangle \quad (3.15)$$

and  $N_s^{(n)} = N_s^{(n')}$  in the above equation due to the fact that  $j_{\mu}$  commutes with the number operator. If we represent explicitly the average in Eq.(3.14) as a sum

over states and use the fact that  $N_s^{(n)} = N_s^{(n')}$  we obtain

$$\sigma_{\mu\nu}(\omega) = \frac{1}{i\omega} Y_{\mu\nu}^+(\omega) \quad (3.16)$$

where for any function  $f(z)$  in the complex  $z$ -plane, we denote

$$f^{\pm}(\omega) = \lim_{z \rightarrow \omega \pm i\epsilon} f(z); \quad \text{with } (\epsilon=0^+) \quad (3.17)$$

In order to obtain the function  $Y(z)$  of Eq.(2.15), we define a Green's function

$$M_{\mu\nu}(u) = \langle T(j_{\mu}(u)j_{\nu}(0)) \rangle \quad \text{with } (-\beta < u < \beta) \quad (3.18)$$

where  $T$  is the Dyson ordering operator and

$$j_{\mu}(u) = e^{uH} j_{\mu}(0) e^{-uH} \quad (3.19)$$

It is easy to show that  $M(u)$  is a periodic function, i.e  $M(u+\beta) = M(u)$ . Therefore its "Fourier Transform" with respect to  $u$

$$M_{\mu\nu}(n) = \int_0^{\beta} du e^{\frac{i2\pi nu}{\beta}} M_{\mu\nu}(u) \quad (3.20)$$

with  $n = \text{any integer}$ , and we obtain

$$M_{\mu\nu}(n) = \int \frac{d\omega}{\omega - \frac{i2\pi n}{\beta}} (1 - e^{-\beta\omega}) \phi_{\mu\nu}(\omega) \quad (3.21)$$

We can now immediately see that the problem of determining  $Y(\omega)$  is now transformed into that of evaluating first the finite temperature Green's function  $M(u)$ . By comparison of Eq. (3.21) with Eq. (3.13), we realize that  $Y(z)$  is the analytical continuation of  $M(n)$  from the infinite set of points  $\frac{i2\pi n}{\beta}$  ( $n > 0$ ) on the positive imaginary axis of  $z$  to the entire upper-half-plane of  $z$ . The result is the desired relation between the electric conductivity and the finite temperature

Green's function. There exist an effective perturbation theory method for obtaining the finite temperature Green's function and next section is devoted to the evaluation of this function.

### 3.4. Many Body Perturbation Theory in Layered System

We turn now to the calculation of  $M(n)$  using perturbation expansion, and then resumming all diagrams which contribute to the conductivity of the quantum plasma when the number of particles in the Bohr (Debye) sphere is large, the frequency is high compare to the collision frequency and the wave-length of the incident field is large compare to Bohr (Debye) radius. Thus in resumming the diagrams of the perturbation expansion, we consider processes proportional to the numbers of particles,  $N$ , as finite and include them to all orders while those process which are not proportional to  $N$  are treated small [87].

Let us write our Green's function in the second quantization formalism in the interaction representation as,

$$M_{\mu\nu}(u) = \frac{1}{LA} \sum_{j,j'} \sum_{s,s'} \frac{e_s e_{s'}}{m_s m_{s'}} \sum_{\vec{p},\vec{p}'} p_{\mu} p'_{\nu} \times$$

$$\frac{\langle T [a_{\vec{p}+\vec{k},j}(s,u) a_{\vec{p},j}(s,u) a_{\vec{p}-\vec{k},j}(s',0) a_{\vec{p},j}(s',0) U(\beta)] \rangle_0}{\langle U(\beta) \rangle_0} \quad (3.22)$$

where Eq.(3.10) has been used,  $L$  is the total number of cells,  $A$  is the 2D area and the symbol  $\langle \rangle_0$  corresponds to the average defined in Eq.(3.3) for noninteracting particles

$$U(\beta) = \exp \left[ - \int_0^{\beta} du H_I(u) \right] \quad (3.23)$$

Using the expansion

$$U(\beta) = \sum_{n=0}^{\infty} \frac{(-1)^n}{n!} \int_0^{\beta} \dots \int_0^{\beta} du_1 \dots du_n T_u [H_I(u_1) \dots H_I(u_n)] \quad (3.24)$$

and Wick's theorem, we obtain a perturbation expansion for  $M(u)$  in which every term corresponding to a Feymann diagram. There is a theorem shows

$$M_{\mu\nu}(u) = \frac{1}{LA} \sum_{j,j',s,s'} \frac{e_s e_{s'}}{m_s m_{s'}} \sum_{\vec{p},\vec{p}'} p_{\mu} p'_{\nu} \times$$

$$\langle T [a_{\vec{p}+\vec{k},j}(s,u) a_{\vec{p},j}(s,u) a_{\vec{p}-\vec{k},j}(s',0) a_{\vec{p}',j}(s',0) U(\beta)] \rangle_{0c} \quad (3.25)$$

in which c indicates that only the contributions from connected diagrams are taken, and

$$a_{\vec{p}}(u) = e^{u(H_0 - \sum_s \mu_s N_s)} a_{\vec{p}} e^{-u(H_0 - \sum_s \mu_s N_s)} \quad (3.26)$$

$$a(u) = e^{u(H_0 - \sum_s \mu_s N_s)} a e^{-u(H_0 - \sum_s \mu_s N_s)} \quad (3.26a)$$

### 3.5. Basic Rules For Evaluation of Diagram

In techniques for evaluating the diagrams arising from a perturbation theory expansion of Green's function, the single particle Green's function plays an important and basic role. The basic rules for the perturbation of  $M(k, \mu)$  were given by Luttinger and Ward<sup>[88]</sup>, by their technique we indicate by a solid line with  $p, j, s$ ,  $\zeta_l$  the  $j$ th layer free electron or hole propagator of wave-vector  $p$  and energy  $\zeta_l$  ( we restrict ourselves to fermions only ).

$$G_{\vec{p}}(\zeta_l, j, s) = \frac{1}{\zeta_l(j, s) - E_{\vec{p}}(j, s)} \quad (3.27)$$

with

$$\zeta_l(j, s) = \frac{i \pi(2l+1)}{\beta} + \mu_{j, s}; \quad l = \text{any integer} \quad (3.28)$$

and

$$E_{\vec{p}}(j, s) = \frac{\vec{p}^2}{2m_{j, s}} \quad (3.29)$$

and by dotted line the interaction  $\frac{2\pi}{q}$  to each vertex. We assign a charge  $e_s$  given by the  $s$  label of the particle. In the high-frequency and long-wavelength region, we take into account a generalized version of diagrams considered by Ron and Tzoar <sup>[19]</sup>. Our generalization corresponds to considering all species in equivalent manner, see Fig.3.1.

### 3.6. Effective Interaction

Using the perturbation expansion of Eq.(3.25), we now use an effective interaction to represent the electron-electron ( electron-hole ) Coulombic interaction. Using a wavy line to represent the effective interaction we see that it satisfies the integral equation represented in Fig.3.1, the analytical expression of which is

$$v_{j, j}^{ss'}(q, \alpha_m) = V_{j, j}^{ss'}(q, \alpha_m) + \sum_{j_1, s_1} e_{s_1}^2 V_{j, j_1}^{ss_1}(q) Q_{s_1}(q, \alpha_m) v_{j_1, j}^{s_1 s'}(q, \alpha_m) \quad (3.30)$$

where (e means electron and h means hole in following expressions)

$$V_{j, j}^{ss'}(q) = \frac{2\pi}{q} e^{-q |j-j'| a} \quad ( \text{for } s=e, s'=e \text{ or } s=h, s'=h ) \quad (3.31)$$

or

$$V_{j,j}^{ss'}(q) = \frac{2\pi}{q} e^{-q|(j-j')a-b|} \quad (for \quad s=e, \quad s'=h) \quad (3.31a)$$

and

$$\alpha_m = \frac{2\pi mi}{\beta} \quad (3.32)$$

In Eq.(3.30),  $Q_s(q, \alpha_m)$  is the density fluctuation of  $s$  species given by

$$\begin{aligned} Q_s(q, \alpha_m) &= \frac{1}{A} \sum_{\vec{p}} \frac{1}{\beta} \sum_l G_{\vec{p}+\vec{q}}(\zeta_l + \alpha_m, s) G_{\vec{p}}(\zeta_l, s) \\ &= \frac{1}{4\pi^2} \int d\vec{p} \frac{f_{\vec{p}+\vec{q}}(s) - f_{\vec{p}}(s)}{E_{\vec{p}+\vec{q}}(s) - E_{\vec{p}}(s) - \alpha_m} \end{aligned} \quad (3.33)$$

here  $f_{\vec{p}}$  is the Fermi distribution function of  $s$  species

$$f_{\vec{p}} = \frac{1}{\exp(\beta E_{\vec{p}}(s) - \beta \mu_s) - 1} \quad (3.33)$$

In Eqs.(3.29-3.33), use has made of the fact that  $G, Q, E$  are independent of layer index  $j$ .

The integral equation (3.30) can be solved as following. We write down two coupled equations for electron-hole and hole-hole interactions.

$$\begin{aligned} v_{j,j}^{eh}(q, \alpha_m) &= V_{j,j}^{eh}(q, \alpha_m) + \sum_{j_1} e^2 V_{j,j_1}^{ee}(q) Q(q, \alpha_m) v_{j_1,j}^{eh}(q, \alpha_m) \\ &\quad + \sum_{j_1} e^2 V_{j,j_1}^{eh}(q) B(q, \alpha_m) v_{j_1,j}^{hh}(q, \alpha_m) \end{aligned} \quad (3.34)$$

and

$$v_{j,j}^{hh}(q, \alpha_m) = V_{j,j}^{hh}(q, \alpha_m) + \sum_{j_1} e^2 V_{j,j_1}^{he}(q) Q(q, \alpha_m) v_{j_1,j}^{eh}(q, \alpha_m)$$

$$+ \sum_{j_1} e^2 V_{j,j_1}^{hh}(q) B(q, \alpha_m) v_{j_1,j}^{hh}(q, \alpha_m) \quad (3.35)$$

We carry out the following Fourier transformation:

$$v^{eh}(q, k_z) = \sum_j v_{j,j}^{eh} e^{ik_z((j-j)a-b)} \quad (3.36)$$

By making use of Eqs.(3.30) and (3.30a), we obtain following two equations,

$$v^{eh}(q, k_z) = VS' + e^2 VS v^{eh}(q, k_z) + e^2 VBS v^{hh}(q, k_z) \quad (3.37)$$

and

$$v^{hh}(q, k_z) = VS + e^2 VS^* Q v^{eh}(q, k_z) + e^2 VBS v^{hh}(q, k_z) \quad (3.38)$$

where  $V = \frac{2\pi}{q}$  and Q,B refer to, respectively the 2-D density fluctuation of elec-

tron and hole.  $S'$  and  $S$  are respectively the form factors which can be expressed as following

$$S = \sum_j e^{-q|j|a} e^{-ik_z ja} = \sinh \frac{(qa)}{\cosh(qa) - \cos(k_z a)} \quad (3.39)$$

and

$$S' = \sum_j e^{-q|ja-b|} e^{-ik_z ja} = \frac{\sinh(q(a-b)) + e^{-ik_z a} \sinh(qb)}{\cosh(qa) - \cos(k_z a)} \quad (3.40)$$

After simple algebra we have

$$v^{eh}(q, k_z) = \frac{V S'}{\epsilon(q, k_z, \omega)} \quad (3.41)$$

and

$$v^{hh}(q, k_z) = \frac{V [S - e^2 V Q (S^2 - |S'|^2)]}{\epsilon(q, k_z, \omega)} \quad (3.42)$$

Where we have defined a "dielectric function",

$$\begin{aligned} \epsilon(q, k_z, \omega) = & 1 - \frac{2\pi e^2}{q} S(Q(q, \omega) + B(q, \omega)) \\ & + \left(\frac{2\pi e^2}{q}\right)^2 Q(q, \omega) B(q, \omega) (S^2 - |S|^2) \end{aligned} \quad (3.43)$$

It is easy to obtain  $v^{eh}$  and  $v^{ee}$  with the same method, we have:

$$v^{he}(q, k_z) = \frac{V S^*}{\epsilon(q, k_z, \omega)} \quad (3.44)$$

and

$$v^{ee}(q, k_z) = \frac{V [S - e^2 V B (S^2 - |S|^2)]}{\epsilon(q, k_z, \omega)} \quad (3.45)$$

Because the system has no invariance under translation  $z \rightarrow z + na + b$ , our effective interaction becomes a tensor. For type-I superlattice where the periodic array is formed by only the electron layers (ions are treated as fixed scatterers) and the system is invariant under translation  $z \rightarrow z + na$ . The effective interaction for type-I superlattices is simply a scalar.

We would like to point out that  $\epsilon$  in our formalism is not really the total response function of our system to an external field though we define it as "dielectric function". The induced charge densities can be easily worked out by density-density correlation calculation and one gets two expressions for electrons and holes,

$$\rho^e(q, k_z, \omega) = \frac{v^{ext} Q [1 - e^2 V B (S - S e^{ik_z b})]}{\epsilon(q, k_z, \omega)} \quad (3.46)$$

and

$$\rho^h(q, k_z, \omega) = \frac{e^{-ik_z b} v^{ext} B [1 - e^{2VQ} (S - S^* e^{-ik_z b})]}{\epsilon(q, k_z, \omega)} \quad (3.47)$$

Again, the induced charge density has two components because the total fields at electron-layer and hole-layer do not simply differ by a phase factor. However, if we are interested in the eigenvalues of the collective excitation of the system, we find them to be given by the roots of  $\epsilon(q, k_z, \omega)$ , the "dielectric function". Also, one should note that the weighting of the roots of the different components is different, as can be seen from Eqs.(3.46) and (3.47).

### 3.7. Evaluation of the Conductivity

Now we calculate the contributions of diagrams given in Fig.3.1. We assert that these are the leading asymptotic terms for long-wavelength [12]. Using the prescription of Luttinger and Ward [88] for many species system under consideration we obtain,

$$M_{\mu\nu}(\omega_n) = M_{\mu\nu}(k=0, \omega_n) = \frac{1}{LA} \sum_{j, j', s, s'} \frac{e_s}{m_s} \frac{e_{s'}}{m_{s'}} \sum_{\vec{p}, \vec{p}'} p_{\mu} p'_{\nu} \sum_{i=1}^5 K_{pp'}^i(\omega_n, j, j', s, s') \quad (3.48)$$

here  $K_{pp'}^i(\omega_n, j, j', s, s')$  corresponds to  $i^{th}$  diagram of Fig.3.2.

$$K_{pp'}^1(\omega_n, j, j', s, s') = \delta_{j, j'} \delta_{ss'} \frac{e_s^2}{LA \beta} \sum_{mq} v_{j, j}^{ss}(q, \alpha_m) \delta_{\vec{p}, \vec{p}+q} \frac{1}{\beta} \sum_l G_{\vec{p}}(\zeta_l, s) G_{\vec{p}}(\zeta_l + \omega_n, s) G_{\vec{p}+q}(\zeta_l + \omega_n + \alpha_m, s) G_{\vec{p}+q}(\zeta_l + \alpha_m, s) \quad (3.49)$$

$$K_{pp'}^2(\omega_n, j, j', s, s') = \delta_{j, j'} \delta_{ss'} \delta_{pp'} \frac{e_s^2}{LA \beta} \sum_{qm} v_{j, j}^{ss}(q, \alpha_m)$$

$$\frac{1}{\beta} \sum_l [G_{\bar{p}}(\zeta_l, s)]^2 G_{\bar{p}-\bar{q}}(\zeta_l - \alpha_m, s) G_{\bar{p}}(\zeta_l - \omega_n, s) \quad (3.50)$$

$$K_{pp}^3(\omega_n, j, j', s, s') = \delta_{j, j'} \delta_{ss'} \delta_{pp'} \frac{e_s^2}{LA\beta} \sum_{qm} v_{j, j'}^{ss}(q, \alpha_m)$$

$$\frac{1}{\beta} \sum_l [G_{\bar{p}}(\zeta_l, s)]^2 G_{\bar{p}+\bar{q}}(\zeta_l + \alpha_m, s) G_{\bar{p}}(\zeta_l + \omega_n, s) \quad (3.51)$$

$$K_{pp}^4(\omega_n, j, j', s, s') = \frac{e_s^2 e_{s'}^2}{L^2 A^2 \beta} \sum_{qm} v_{j, j'}^{ss'}(q, \alpha_m) v_{j', j}^{s's}(q, \alpha_m - \omega_n)$$

$$\frac{1}{\beta^2} \sum_l G_{\bar{p}}(\zeta_l, s) G_{\bar{p}}(\zeta_l - \omega_n, s) G_{\bar{p}-\bar{q}}(\zeta_l - \alpha_m, s)$$

$$\sum_l G_{\bar{p}}(\zeta_l, s') G_{\bar{p}}(\zeta_l - \omega_n, s') G_{\bar{p}-\bar{q}}(\zeta_l - \alpha_m, s') \quad (3.52)$$

$$K_{pp}^5(\omega_n, j, j', s, s') = \frac{e_s^2 e_{s'}^2}{L^2 A^2 \beta} \sum_{qm} v_{j, j'}^{ss'}(q, \alpha_m) v_{j', j}^{s's}(q, \alpha_m - \omega_n)$$

$$\frac{1}{\beta^2} \sum_l G_{\bar{p}}(\zeta_l, s) G_{\bar{p}}(\zeta_l - \omega_n, s) G_{\bar{p}-\bar{q}}(\zeta_l - \alpha_m, s)$$

$$\sum_l G_{\bar{p}}(\zeta_l, s') G_{\bar{p}}(\zeta_l + \omega_n, s') G_{\bar{p}+\bar{q}}(\zeta_l + \alpha_m, s') \quad (3.53)$$

We now carry out the summation over  $l$  and  $l'$  by converting the sums into integrals. After some complicated algebra, ( see an example in Appendix 3A ) we obtain

$$M_{\mu\nu}(\omega_n) = M_{\mu\nu}^a(\omega_n) + M_{\mu\nu}^b(\omega_n) \quad (3.54)$$

where  $M^a$  is the sum of the first three diagrams

$$M_{\mu\nu}^a(\omega_n) = \frac{1}{L\beta\omega_n^2} \int \frac{\vec{d}q}{4\pi^2} q_{\mu} q_{\nu} \sum_{j,s,m} \frac{e_s^4}{m_s^2} v_{j,j}^{ss'}(q, \alpha_m) [Q_s(\alpha_m + \omega_n) - Q_s(\alpha_m)] \quad (3.55)$$

or we would like to write it in a more symmetric form

$$M_{\mu\nu}^a(\omega_n) = -\frac{1}{2L\beta\omega_n^2} \int \frac{\vec{d}q}{4\pi^2} q_{\mu} q_{\nu} \sum_{ss'} \frac{e_s^4 e_{s'}^2}{m_s^2} \times \sum_{j,j} \sum_m v_{j,j}^{ss'}(\alpha_m + \omega_n) v_{j,j}^{s's}(\alpha_m) D_{ss'}(\alpha_m, \omega_n) \quad (3.56)$$

with

$$D_{ss'}(\alpha_m, \omega_n) = [Q_s(\alpha_m + \omega_n) - Q_s(\alpha_m)] [Q_{s'}(\alpha_m + \omega_n) - Q_{s'}(\alpha_m)]$$

and  $M_b$  is the sum of last two diagrams

$$M_{\mu\nu}^b(\omega_n) = \frac{1}{2L\beta\omega_n^2} \int \frac{\vec{d}q}{4\pi^2} q_{\mu} q_{\nu} \sum_{ss'} \frac{e_s^3 e_{s'}^3}{m_s m_{s'}} \sum_{j,j} \sum_m v_{j,j}^{ss'}(\alpha_m) v_{j,j}^{s's}(\alpha_m + \omega_n) D_{ss'}(\alpha_m, \omega_n) \quad (3.57)$$

Finally the sum of all five diagrams gives

$$M_{\mu\nu}(\omega_n) = -\frac{1}{2L\beta\omega_n^2} \int \frac{\vec{d}q}{4\pi^2} q_{\mu} q_{\nu} \sum_{s,s'} \frac{e_s^3 e_{s'}^2}{m_s} \left[ \frac{e_s}{m_s} - \frac{e_{s'}}{m_{s'}} \right] \sum_{j,j} \sum_m v_{j,j}^{ss'}(\alpha_m + \omega_n) v_{j,j}^{s's}(\alpha_m) D_{ss'}(\alpha_m, \omega_n) \quad (3.58)$$

Taking into account the symmetry of the expression Eq.(3.58) with respect to the mutual interchange of electron-hole, summing over  $s$  and  $s'$ , we get,

$$M_{\mu\nu}(\omega_n) = -\frac{e^6}{2L\beta\omega_n^2} \left| \frac{1}{m_e} - \frac{1}{m_h} \right|^2 \int \frac{d\vec{q}}{4\pi^2} q_{\mu} q_{\nu} \times$$

$$\sum_{j,j'} \sum_m v_{j',j}^{eh}(\alpha_m + \omega_n) v_{j,j'}^{he}(\alpha_m) D_{eh}(\alpha_m, \omega_n) \quad (3.59)$$

Eq.(3.58) or (3.59) shows that the  $s=s'$  part in Eq(3.58) just cancels Eq(3.57). The physical meaning of this cancellation is that the only absorption in our system is due to the electron-hole collisions, i.e., the only possible intermediate states are an electron pair and a hole pair . Electron-electron or hole-hole interactions does not contribute to the absorption process but only screens the effective interaction. Therefore, our conductivity  $\sigma_2$  vanishes with vanishing electron-hole interaction. In other words, we will not have any absorption if the parameter  $b \rightarrow \infty$ .

Instead of the sum over  $j$  and  $j'$  in Eq.(3.59), we would rather use the integral over  $k_z$ , for this we use discrete Fourier transformation.

From Eqs.(3.25-3.27), the effective electron-hole interaction can written as:

$$v_{j,j'}^{eh} = \int_{-\frac{\pi}{a}}^{\frac{\pi}{a}} \frac{adk_z}{2\pi} \frac{\frac{2\pi}{q} S'(q, k_z) e^{ik_z(a(j-j)-b)}}{\epsilon(q, k_z, \omega)} \quad (3.60)$$

Substituting it into Eq.(3.59), we have,

$$M_{\mu\nu}(\omega_n) = -\frac{e^6}{2L\beta\omega_n} \left( \frac{1}{m_e} + \frac{1}{m_h} \right)^2 \int \frac{d\vec{q}}{q} q_{\mu} q_{\nu} \int \frac{a^2 dk'_z dk_z}{(2\pi)^2} S'(q, k_z) S^*(q, k_z)$$

$$\sum_{j,j'} e^{i(j-j')(k_z - k'_z)a} \sum_m \frac{D_{eh}(\omega_n, \alpha_m)}{\epsilon_q(\alpha_m, k_z) \epsilon_q(\alpha_m + \omega_n, k_z)} \quad (3.61)$$

making use of the identity:

$$\sum_{j,j'} e^{i(j-j')k_z - k'_z} = 4\pi^2 \delta^2(a(k_z - k'_z)) \quad (3.62)$$

therefore we get the following expression

$$M_{\mu\nu}(\omega_n) = -\frac{\pi}{\beta\omega_n^2} \int \frac{d\vec{q}}{q^2} q_\mu q_\nu \int \frac{adk_z}{2\pi} |S(q, k_z)|^2 e^6 \left(\frac{1}{m} + \frac{1}{m_h}\right)^2$$

$$\sum_m \frac{[Q(\alpha_m + \omega_n) - Q(\alpha_m)] [B(\alpha_m + \omega_n) - B(\alpha_m)]}{\epsilon(\alpha_m) \epsilon(\alpha_m + \omega_n)} \quad (3.63)$$

where the use has been made of the fact

$$\delta(a(k_z - k'_z)) |_{k_z=k'_z} = \sum_j e^{ija(k_z - k'_z)} |_{k_z=k'_z} = L$$

Our result given by Eq.(3.63) which is derived from the sum of  $M^a$  and  $M^b$  (Eq.(3.18) and (3.20)) shows cancellation of all contributions which do not have simultaneously an electron-pair and a hole-pair in its final state. Thus as expected, electron-electron or hole-hole interactions does not contribute to a long wavelength photon absorption.

Eq.(3.63) are not suitable for analytical continuation to the upper  $z$  half-plane. In order to perform the continuation, one has to evaluate the summation over  $m$  <sup>[19]</sup>. After some algebra and using Eqs.(2.15), (2.17), (2.20) and (3.40) we obtain

$$\sigma_{\mu\nu}^1(\omega) = \frac{i\pi e^6}{\omega^3} \left( \frac{1}{m_e} + \frac{1}{m_h} \right)^2 \int \frac{d\vec{q}}{q^2} q_\mu q_\nu \int \frac{adk_z}{2\pi} |S(q, k_z)|^2 \frac{P}{2\pi i} \int dx \coth\left(\frac{\beta x}{2}\right)$$

$$\left( \frac{[Q(x^+ + \omega, q) - Q(x^+, q)] [B(x^+ + \omega, q) - B(x^+, q)]}{\epsilon(x^+ + \omega, q) \epsilon(x^+, q)} \right)$$

$$\left. - \frac{[Q(x^{++}, \omega, q) - Q(x^-, q)] [B(x^{++}, \omega, q) - B(x^-, q)]}{\epsilon(x^{++}, \omega, q) \epsilon(x^-, q)} \right\} \quad (3.64)$$

Here P stands for principal value and

$$x^\pm = x \pm i\eta, \quad (\eta \rightarrow 0)$$

Now we make use of Eq.(2.5). Our final result for complex conductivity is

$$\sigma(\omega) = \sigma^0(\omega) + \sigma^1(\omega) = \sigma^0(\omega) \left[ 1 + \frac{I(\omega)}{\omega} \right] \quad (3.65)$$

where

$$I(\omega) = \frac{\pi^2 e^4}{n \omega} \left( \frac{1}{m_e} + \frac{1}{m_h} \right) \int q dq \int \frac{adk_z}{2\pi} |S(q, k_z)|^2 \frac{P}{2\pi} i \int dx \coth\left(\frac{\beta x}{2}\right)$$

$$\left\{ \frac{[Q(x^{++}, \omega, q) - Q(x^+, q)] [B(x^{++}, \omega, q) - B(x^+, q)]}{\epsilon(x^{++}, \omega, q) \epsilon(x^+, q)} - \frac{[Q(x^{++}, \omega, q) - Q(x^-, q)] [B(x^{++}, \omega, q) - B(x^-, q)]}{\epsilon(x^{++}, \omega, q) \epsilon(x^-, q)} \right\} \quad (3.66)$$

This is the exact expression in which we have used the fact that  $Q, B$  depend only on absolute value of  $\vec{q}$  and that  $\sigma_{\mu\nu}(\omega) = \delta_{\mu\nu} \sigma(\omega)$  for isotropic system. This result is rather complicated but in principle can be evaluated analytically or numerically for specific problem. The result is applicable both for classical and quantum plasmas for any mass ratio of the species of the system, and for any temperature, where the average potential energy of interaction per particle should be less than the average kinetic energy.

### 3.8. Relaxation Time and Resistivity

In order to obtain the relaxation time we rewrite Eq.(3.42) as:

$$\sigma(\omega) = \sigma^0 \left[ \frac{1}{1 - \frac{I / \omega}{1 + I / \omega}} \right] \quad (3.67)$$

The high-frequency limit is given by the condition  $|I(\omega)| \ll \omega$  and we thus obtain the approximate expression for the conductivity:

$$\sigma(\omega) = \frac{\sigma^0}{1 - \frac{I_1(\omega) + iI_2(\omega)}{\omega}} \quad (3.68)$$

Here  $I_1$  and  $I_2$  are respectively the real and imaginary parts of  $I(\omega)$ . Now let us compare Eq.(4.2) with the Drude formula for conductivity:

$$\sigma(\omega) = \frac{ine^2}{m^* (\omega + \frac{i}{\tau})} \quad (3.69)$$

We find the effective reduced mass;

$$\frac{m^*}{m} = [1 - I_1(\omega)] \quad \text{with} \quad m = \frac{m_e m_h}{m_e + m_h} \quad (3.70)$$

and the relaxation time:

$$\tau^{-1} = -\frac{I_2(\omega)}{\omega} \quad (3.71)$$

Here only linear corrections due to  $I_1$  and  $I_2$  are retained. however, using Eq.(4.1) we obtain for the general case the result:

$$\frac{m^*}{m} = \frac{1}{(1 + \frac{I_1}{\omega}) [1 + \frac{I_2^2}{(\omega + I_1)^2}]} \quad (3.72)$$

and

$$\tau^{-1} = - \frac{I_2}{1 + \frac{I_1}{\omega}} \quad (3.73)$$

In the following, we are only interested in absorption properties which related to relaxation time  $\tau$ . or the collision frequency  $\nu = \tau^{-1}$ . The absorption properties of the plasma can be best described by the resistivity, i.e.,  $R(\omega) = \text{Re}[\frac{1}{\sigma(\omega)}]$  where  $\text{Re}$  stands for the real part and  $\sigma$  is given by Eq.(3.42). The frequency dependent resistivity is given by:

$$R = \frac{1}{\tau n e^2} \left[ \frac{1}{m_e} + \frac{1}{m_h} \right]^{-1} \quad (3.74)$$

Using the analytical properties of  $Q, B$ , and "dielectric function" respectively, we can write

$$R(\omega) = \frac{\pi e^2}{\omega n^2} \left( \frac{1}{m_e} + \frac{1}{m_h} \right)^2 \int q dq \int_{-\pi}^{\pi} \frac{d\theta}{2\pi} |S(q, \theta)|^2$$

$$\frac{P}{2} \int dx \left[ \coth \frac{\beta x}{2} - \coth \frac{\beta(x + \omega)}{2} \right] F(x, x + \omega) \quad (3.75)$$

where  $\theta = ak_z$  and

$$F(x, x + \omega) = \frac{F_1 + F_2 + F_3}{|\epsilon(x)|^2 |\epsilon(x + \omega)|^2} \quad (3.76)$$

with

$$F_1 = [B_2(x + \omega) + B_2(x)] [(\epsilon_1(x + \omega)\epsilon_1(x) + \epsilon_2(x + \omega)\epsilon_2(x)) (Q_2(x + \omega) + Q_2(x))]$$

$$-(\epsilon_1(x) \epsilon_2(x + \omega) - \epsilon_1(x + \omega) \epsilon_2(x)) (Q_1(x + \omega) - Q_1(x)) \quad (3.77)$$

and

$$F_2 = [B_2(x) - B_2(x + \omega)] [(\epsilon_1(x + \omega) \epsilon_1(x) - \epsilon_2(x + \omega) \epsilon_2(x)) (Q_2(x + \omega) - Q_2(x)) - (\epsilon_1(x) \epsilon_2(x + \omega) + \epsilon_1(x + \omega) \epsilon_2(x)) (Q_1(x + \omega) - Q_1(x))] \quad (3.78)$$

and

$$F_3 = 2[B_1(x + \omega) - B_1(x)] [\epsilon_1(x + \omega) \epsilon_2(x) Q_2(x + \omega) - \epsilon_1(x) \epsilon_2(x + \omega) Q_2(x) - (Q_1(x + \omega) - Q_1(x)) \epsilon_2(x) \epsilon_2(x + \omega)] \quad (3.79)$$

Where  $\epsilon_1$  and  $\epsilon_2$  represent, respectively, the real and imaginary parts of the "dielectric function". Similarly  $Q_1$  and  $Q_2$  ( $B_1$  and  $B_2$ ) represent respectively the real and the imaginary parts of  $Q(B)$ . We shall next investigate the effect of the small mass ratio (i.e.  $\frac{m_e}{m_h} < 1$ ) on the conductivity at low temperature. We would

like to use following dimensionless variables,

$$z = \frac{q}{2k_F}, \quad \Omega = \frac{\omega}{4E_F}, \quad X = \frac{x}{4E_F}, \quad \Theta = \frac{1}{4E_F \beta}$$

and

$$B = \frac{2\pi e^2}{q} B, \quad Q = \frac{2\pi e^2}{q} Q, \quad F = \left(\frac{2\pi e^2}{q}\right)^2 F,$$

where  $E_F$  is the Fermi energy for electrons, by this we get

$$R = \frac{16}{e^2 \Omega} \int_{-\pi}^{\pi} \frac{d\theta}{2\pi} \int_0^{\infty} z^3 dz |S(z, \theta)|^2$$

$$\frac{P}{2} \int_{-\infty}^{\infty} dX \left[ \coth\left(\frac{X}{2\Theta}\right) - \coth\left(\frac{X + \Omega}{2\Theta}\right) \right] F(X, \Omega + X) \quad (4.80)$$

For the case  $kT \ll E_F$ , we can use the limit ( $T \rightarrow 0$ ) and get:

$$R = \frac{16}{e^2 \Omega} \int_{-\pi}^{\pi} \frac{d\theta}{2\pi} \int_0^{\infty} z^3 dz |S(z, \theta)|^2 \int_0^{\Omega} dX F(X, \Omega - X) \quad (3.81)$$

We would first like to examine the behavior of R qualitatively in the low frequency region where the static approximation is applicable [86]. We treat the screening effect due to the self-consistent field statically. This approximation drastically simplifies  $F(X, \Omega + X)$ . Let  $\frac{X}{\Omega} = \nu$ , we get

$$R = \frac{32}{e^2} \int_{-\pi}^{\pi} \frac{d\theta}{2\pi} \int_0^{\infty} z^3 dz \frac{|S(z, \theta)|^2}{\epsilon(z, \theta, 0)^2} \int_0^1 d\nu \left[ B_2(\Omega\nu) Q_2(\Omega(1-\nu)) + B_2(\Omega(1-\nu)) Q_2(\Omega\nu) \right] \quad (3.82)$$

Using RPA result [30] for Q and B,

$$Q_2(\Omega(1-\nu)) = \frac{r_s}{2z^2} \left( \sqrt{1 - (z - \frac{\Omega(1-\nu)}{z})^2} \theta(1 - (z - \frac{\Omega(1-\nu)}{z})^2) - \sqrt{1 - (z + \frac{\Omega(1-\nu)}{z})^2} \theta(1 - (z + \frac{\Omega(1-\nu)}{z})^2) \right) \quad (4.83)$$

and

$$B_2(\Omega\nu) = \frac{\alpha r_s}{2z^2} \left( \sqrt{1 - (z - \frac{\alpha\Omega\nu}{z})^2} \theta(1 - (z - \frac{\alpha\Omega\nu}{z})^2) - \sqrt{1 - (z + \frac{\alpha\Omega\nu}{z})^2} \theta(1 - (z + \frac{\alpha\Omega\nu}{z})^2) \right) \quad (4.84)$$

where  $r_s = \frac{m_e e^2}{k_F}$ ,  $\alpha = \frac{m_h}{m_e}$ , and  $\theta(x)$  is the regular step function, i.e.,

$$\theta(x)=1 \quad \text{for } x > 0 \quad \text{and} \quad \theta(x)=0 \quad \text{for } x < 0 \quad (4.85)$$

We immediately see that  $Q'_2|_{\Omega=0}=0$  and  $B'_2|_{\Omega=0}=0$ , therefore the lowest order term at low frequencies is following:

$$R = A_1 \Omega^2 \quad (3.86)$$

with

$$A_1 = \frac{1}{2} \frac{\partial^2 R}{\partial \Omega^2} \Big|_{\Omega=0}$$

The coefficient  $A_1$  can be obtained numerically or analytically. In the later case, one must take the second derivative after the integration over  $z$  and  $v$  is done. If we first take the derivative of the integrand in Eq.(3.82), we obtain a new integrand which will have singular behavior at  $z=1$ . For an analytical result for  $A_1$  one has to change the variables  $z, v$  to new variables  $z', v'$  for four different terms in the product  $Q'_2 B'_2$  of Eq.(3.82). However, even after carrying out the transformation we are left with numerical integration and thus we evaluated  $A_1$  numerically using Eq.(3.82). We found that  $A_1$  increases when period or  $r_s$  are decreased or when the mass ratio  $\alpha$  is increased. These properties can be seen from our plot, Figs.3.3-3.5.

This  $\Omega^2$  behavior of the resistivity is due to the lack of phase-space for the absorption process. We should remember that we consider an electron-hole system in which both electrons and holes have their own Fermi sphere. The photon is absorbed by mutually exciting an electron pair and a hole pair. The energy supplied by the photon is  $\omega$ , a negligible quantity, thus the two pairs must be in the vicinity of their Fermi sea where the density of states is negligibly small. The

momentum to this process is supplied by the Coulomb collision of the electron and hole which in our formalism is given by  $q$ . Thus the momentum  $q$  is limited to be in the range between 0 and  $2k_F$ . As stated above, the density of states vanishes with vanishing  $\omega$  and it can be shown, using density of states arguments, that the joint density of states for electron-hole excitation divided by  $\omega$  is proportional to  $\omega^2$ .

### 3.9. Discussion

It is difficult to evaluate analytically the resistivity, as given by Eq.(3.81). Here we take into account dynamical screening of the plasma which is a complex function of  $q$ ,  $k_z$  and  $\omega$ . Thus one does not necessarily expect that the integral in Eq.(3.81) will depend solely on the imaginary part of the electron and hole pair distribution function respectively as it appears in Eq.(3.82). Indeed we find that when the electron and hole can be thought of as scattered by a retarded potential, we should have the general expression including terms proportional to the product of two imaginary parts of electron (hole) density fluctuations as fully written in Eqs.(3.71-3.75). We evaluated Eq.(3.81) numerically for some value of parameters and the results are plotted in Fig.3.3-3.5. Comparing our result with that for electron-hole droplet obtained by Tzoar and Platzman<sup>[86]</sup>, the peak in the resistivity at low frequency does not appear here. This peak results from the excitation of the low frequency mode of the heavy species screened by the light species, known as ion acoustic mode. From the analysis of the imaginary part of inverse dielectric function for two dimensional system which consists of electrons and holes, we found that the ion acoustic mode carries much less oscillator strength than in the 3D case.

If the frequency is very low, or the incident photon energy is in the same order of magnitude as electronic thermal energy, one can not use the limit  $T \rightarrow 0$  in the calculation. We should also include the contribution to the resistivity from thermal excitation up to order  $\Theta^2$ . To do this, we should add to our resistivity following term:

$$R' = \frac{16}{e^2 \Omega} \int_{-\pi}^{\pi} \frac{d\theta}{2\pi} \int z^3 dz |S(z, \theta)|^2$$

$$\frac{P}{2} \int_{-\infty}^{\infty} dX \left[ \coth\left(\frac{X}{2\Theta}\right) - \coth\left(\frac{X+\Omega}{2\Theta}\right) \right] F'(X, X+\Omega) \Big|_{\Omega=0} \quad (3.87)$$

We see that the only nonvanishing term in  $F'$  is  $F'_1$  at  $\Omega=0$ . The temperature dependence of  $Q'_2, B'_2$  can be neglected because they will give us high order terms. Thus we only consider the temperature dependence of the statistical factor and expand it as:

$$\frac{1}{\Omega} [\coth\left(\frac{X}{2\Theta}\right) - \coth\left(\frac{X+\Omega}{2\Theta}\right)] \Big|_{\Omega=0} = \frac{1}{2\Theta} \frac{1}{\sinh^2\left(\frac{X}{2\Theta}\right)} \quad (3.88)$$

Let  $u = \frac{X}{\Theta}$ , we have

$$R' = \frac{32}{e^2} \int_{-\pi}^{\pi} \frac{d\theta}{2\pi} \int z^3 dz |S(z, \theta)|^2 \times$$

$$\int_0^{\infty} \frac{du}{\sinh^2\left(\frac{u}{2}\right)} \frac{Q'_2(z, \Theta u) B'_2(z, \Theta u)}{|f(z, \theta, \Theta u)|^2} \quad (3.89)$$

Where  $Q'_2(z, \Theta u)$  is given in Eqs.(3.83),

$$Q'_2(z, \Theta u) = \frac{r_s}{2z^2} \left[ \sqrt{1 - \left(z - \frac{\Theta u}{z}\right)^2 \theta} \left(1 - \left(z - \frac{\Theta u}{z}\right)^2\right) - \right.$$

$$\sqrt{1 - \left(z + \frac{\Theta u}{z}\right)^2 \theta \left(1 - \left(z + \frac{\Theta u}{z}\right)^2\right)} \quad (3.90)$$

and

$$B'_2(z, \theta u) = \alpha Q'_2(z, \alpha \Theta u)$$

Clearly  $Q'_2|_{\Theta=0}=0$  and  $B'_2|_{\Theta=0}=0$ , the lowest order term in Eq.(3.90) is  $A_2\Theta^2$  as expected. Therefore we find at low frequency and low temperature, the resistivity behaves like,

$$R = A_1\Omega^2 + A_2\Theta^2 \quad (3.91)$$

Where  $A_2 = \frac{1}{2} \frac{\partial^2 R}{\partial \Theta^2} |_{\Theta=0}$ . Again the explicit form of  $A_2$  can be obtained numerically or analytically with the similar method for  $A_1$ . We have checked the  $\Theta^2$  properties and obtained  $A_2$  numerically. The results are shown in Fig.3.3. We finally note that the  $\Omega^2, T^2$  dependence of Eq.(3.91) is not limited to superlattices and is quite general<sup>[85,89,90]</sup>.

The dependences of absorption on mass ratio are given in Fig.3.4. We found the relative magnitude of the maximum absorption decreases as the mass ratio decreases (i.e., the mass of hole increases). This maximum moves towards the low frequency region as expected. For the case  $\frac{m_e}{m_h}=0.01$ , we basically recover the the result for type-I superlattices except in the low frequency region. Here we would like to point out that there is a fundamental difference between electron-hole and electron-random ion systems. The ions only provide the electrons with a momentum relaxation mechanism. However the holes, besides providing momentum

relaxation, contribute to the electric current in two other ways; first they carry current themselves, which results in negligible contribution at large hole mass. Second, they participated in the screening which for large hole mass manifests itself in retaining the contribution to the static screening which influence the conductivity at low and intermediate frequencies. Therefore, as the mass of the hole becomes much heavier than the mass of the electron we reach the following limit:

$$[B(x + \omega) \pm B(x)] \rightarrow \pm i n \delta(x) \quad (3.92)$$

and  $F_3$  vanishes while  $F_2$  equals  $F_1$  (see Eqs.(3.77-3.79). We must let  $B(x)$  equal to zero everywhere in the "dielectric function", then we recover our result for electron-ion system <sup>21</sup>;

$$R = \frac{1}{2n\omega} \int_0^\pi \frac{d\theta}{\pi} \int q^2 dq \frac{|S'(q, \theta)|^2}{S(q, \theta)} \text{Im} \left( \frac{1}{\epsilon(0)} - \frac{1}{\epsilon(\omega)} \right) \quad (3.93)$$

Finally, we have checked the absorption intensity as a function of frequency for different thickness of unit cell  $a$ . For intermediate frequencies, we find an increase in absorption intensity with decreasing  $a$ . First, the scattering fields increase very rapidly with decreasing  $a$ . Second, the dynamical screening effect of the superlattice allows the excitation of an electron-hole pair to take place on any cell  $j$ , even if the photon is being absorbed at a specific cell  $j'$ . The second process only becomes negligibly small at extremely low and high frequencies. For high frequencies, the interference effect between the cells becomes unimportant. For very small frequencies, absorption intensities for different thickness all approach zero and the difference between them is less noticeable in comparison with type-I superlattices. However, there is also a difference in period dependence of absorption intensities between type-I and type-II superlattices at low frequencies. We

know that the absorption intensity  $R$  is proportional to  $\frac{|v^{scat}|^2}{|\epsilon(q, \Omega)|^2} |_{\Omega \rightarrow 0}$ . As the period changes to a smaller value, both  $v^{scat}$  and  $\epsilon(q, \Omega)$  increases. For type-I superlattice, the static screening of neighboring layers is dominant and we found a reduction in the absorption when the period  $a$  became smaller. For type-II superlattice, due to the dynamical properties of the holes as mentioned above, the screening is less effective compared with the increase in scattering potential when the period is decreased. Therefore the absorption is enhanced by decreasing the period. The results for period dependence on the absorption are plotted in Fig.3.5.

In conclusion, we have found the conductivity of type-II superlattices in the high-frequency and long-wavelength limit. We have given the expressions for effective reduced mass and relaxation time. We have discussed the dependences of absorption on mass ratio and spacing of superlattices. The functional form of resistivity at very low frequencies and low temperature is found to be  $A_1 \Omega^2 + A_2 \Theta^2$  from our numerical calculation which is consistent with the analysis of phase space argument. Finally we have pointed out some differences of our present system with the 3D electron-hole systems and with type-I superlattices.

### 3.10. Appendix 3A

We wish to represent here an example of calculation of one diagram of Fig.3.1, namely 3.1d. To calculate the contribution of this diagram to  $M_{\mu\nu}(\omega_n)$  we first substitute K of Eq.(3.52) into Eq.(3.48) and replace  $G_p$  by its representation, Eq.(3.27);

$$M_{\mu\nu}(\omega_n) = \sum_{s,s'} \frac{e_s^3 e_{s'}^3}{m_s m_{s'}} \sum_{\vec{p}, \vec{p}'} p_{\mu} p'_{\nu}$$

$$\sum_q \frac{1}{\beta} \sum_m U_q^{ss'}(\alpha_m) U_q^{s's}(\alpha_m - \omega_n) L_p(\alpha_m, \omega_n, s) L_{p'}(\alpha_m, \omega_n, s') \quad (3A1)$$

where

$$L_p(\alpha_m, \omega_n, s) = \frac{1}{\beta} \sum_l \frac{1}{\zeta_l(s) - E_p(s)} \frac{1}{\zeta_l(s) - \omega_n - E_p(s)} \frac{1}{\zeta_l(s) - \alpha_m - E_{p-q}(s)} \quad (3A2)$$

Now to perform the summation we replace  $\zeta_l$  by  $\zeta$  and write  $L_p$  as an integral along path C given in Fig.3.6

$$L_p(\alpha_m, \omega_n, s) = \frac{1}{2\pi i} \int_C \frac{d\zeta}{e^{\beta(\zeta - \nu_s)} + 1} \frac{1}{\zeta - E_p(s)} \frac{1}{\zeta - \omega_n - E_p(s)} \frac{1}{\zeta - \alpha_m - E_{p-q}(s)} \quad (3A3)$$

This integral can be evaluated by Cauchy's theorem to give

$$L_p(\alpha_m, \omega_n, s) = -\omega_n^{-1} [e^{\beta(E_p - \mu_s)} + 1]^{-1} [-\alpha_m - E_{p-q}(s) + E_p(s)]^{-1}$$

$$+ \omega_n^{-1} [e^{\beta(E_p + \omega_n - \mu_s)} + 1]^{-1} [-\omega_n - \alpha_m - E_{p-q}(s) + E_p(s)]^{-1}$$

$$+[e^{\beta(E_p + \omega_n - \mu_s)} + 1]^{-1} [-\omega_n + \alpha_m + E_{p-q}(s) + E_p(s)]^{-1} [\alpha_m - E_{p-q}(s) + E_p(s)]^{-1} \quad (3A4)$$

If we now realize that

$$e^{\beta\omega_n} = e^{\beta\alpha_m} = e^{i2\pi} = 1$$

and use the definition of Eq.(3. ), we get

$$L_p(\alpha_m, \omega_n, s) = \frac{1}{\omega_n} [f_{\vec{p}-\vec{q}(s)} - f_{\vec{p}}(s)] \times \\ \left( [\alpha_m - \omega_n - E_{\vec{p}}(s) + E_{\vec{p}-\vec{q}}(s)]^{-1} - [\alpha_m - E_{\vec{p}}(s) - E_{\vec{p}-\vec{q}}(s)]^{-1} \right) \quad (3A5)$$

Thus

$$M_{\mu\nu}(\omega_n) = \frac{1}{\omega_n^2} \sum_{s,s'} \frac{e_s^3 e_{s'}^3}{m_s m_{s'}} \frac{1}{(2\pi)^3} \int d\vec{q} \times \\ \frac{1}{\beta} \sum_m U_q^{ss}(\alpha_m) U_q^{ss}(\alpha_m - \omega_n) R_\mu(\alpha_m, \omega_n, s) L_\nu(\alpha_m, \omega_n, s') \quad (3A6)$$

and

$$R_\mu(\alpha_m, \omega_n, s) = \frac{1}{(2\pi)^3} \int_0^\infty d\vec{p} (p + \frac{1}{2}\vec{q}\mu) \left( f_{\vec{p}+\frac{\vec{q}}{2}} - f_{\vec{p}-\frac{\vec{q}}{2}} \right) \times \\ \left( [\alpha_m - \omega_n - E_{\vec{p}}(s) - E_{\vec{p}-\vec{q}}(s)]^{-1} - [\alpha_m - E_{\vec{p}}(s) - E_{\vec{p}-\vec{q}}(s)]^{-1} \right) \quad (3A7)$$

If we use Eq.(3.33) we obtain

$$R_\mu(\alpha_m, \omega_n, s) = \frac{1}{2} q_\mu [Q_q(\alpha_m - \omega_n, s) - Q_q(m, s)] \quad (3A8)$$

and finally

$$M_{\mu\nu}^4(\omega_n) = \frac{1}{4L\beta\omega_n^2} \int \frac{d\vec{q}}{4\pi^2} q_{\mu} q_{\nu}$$

$$\sum_j \sum_{jss'm} \frac{e_s^3 e_{s'}^3}{m_s m_{s'}} v_{j,j}^{ss'}(\alpha_m) v_{j,j}^{ss}(\alpha_m + \omega_n) D_{ss'}(\alpha_m, \omega_n) \quad (3A9)$$

and  $D_{ss'}$  is defined after Eq.(3.65).

## Chapter IV

### ELECTRON-LO-PHONON SYSTEM

#### 4.1. Introduction

Early interest in the electron-phonon interaction in quasi-two-dimensional electron system arose in the context of the transport behavior of silicon electron inversion layers at room temperatures is limited basically by the electron-acoustic phonon interaction<sup>[2,91,92]</sup>. Many of these semiconductor superlattices are made of weakly polar III-V or II-VI compound semiconductor materials (eg., GaAs-AlGaAs and InAs-GaSb). In view of the two-dimensional electron confinement in these system, one expects that the effects of the electron-LO phonon coupling on the absorption properties will be important. In fact, a number of theoretical<sup>[93-100]</sup> and experimental works<sup>[101-106]</sup> have already been done in various aspects of the electron-LO phonon interaction effects on the polarons and electronic properties of two-dimensional systems.

In this chapter we shall consider the electron-LO phonon interaction, which is not of much significance in silicon. Most of the work involving electron-LO phonon interaction in the quasi-two-dimensional electron system is no the III-V semiconductors system like GaAs heterostructure, GaAs-GaAlAs superlattice, InSb space charged layer, etc. All these materials are weakly polar in nature (the Frohlich coupling constant is around 0.1 for these materials). However, this weak coupling

may very well give rise to some interesting observable effect, particularly because interaction effects are usually enhanced in systems of lower dimensionality. For strongly polar semiconductor, we expect that effect of electron-LO phonon interaction will be very important. We shall calculate the collision frequency of electrons in superlattice systems due to the electron-LO phonon interaction.

We use the Kubo's formula for conductivity and the temperature-dependent Green's function technique. We restrict ourselves to the approximation that electrons are confined in sheets of zero thickness. If the energy of the incident photons is less than the energy difference between the ground state and the first excited state, and the mean spreading of wave function is less than the layer thickness, our approximation is realistic and can be used as a model for theoretical calculation which should be valid in and can be compared with real systems. Within this model, we have obtained an exact expression for the conductivity. It is dependent on frequency, plasma parameter  $r_s$ , spatial separation  $a$  and the electron-LO phonon coupling. We have evaluated the relaxation time numerically for a weakly interacting polar system (GaAs-GaAlAs) as well as a strongly interacting polar system (PbTe-PbEuTeSe).

The model we use is simple: A purely two-dimensional confined electron gas is interacting via the Frohlich Hamiltonian with the bulk LO phonons of the relevant semiconductor material. Here we neglect coupling to all other kinds of phonons as well as to interface phonon. We have two reasons for ignoring the effects of the interface phonons. One is experimental--light scattering experiments<sup>[107]</sup> seem to indicate that the bulk LO phonon are the only phonons that couple to the two-dimensional confined electrons. The second one is theoretical--the

superlattice system that we are considering consist of two lattice-matched semiconductors (eg., GaAs and AlGaAs) with rather similar lattice dielectric properties which make the existence of purely interface phonon modes (with their own distinct frequencies) rather unlikely<sup>[93,100]</sup>.

## 4.2. Hamiltonian of the System

Let us consider electrons of density  $n$  per unit area and mass  $m$  occupying layers positioned at  $z=la$  ( $l=0, \pm 1, \pm 2, \dots$ ) where  $a$  is the period of the superlattice system along z-direction. We use a simplified model in which electrons can only move in the x-y planes. The wave function of the electron in  $l$  th layer is

$$\phi_l(\vec{p}, \vec{r}, z) = e^{i\vec{p} \cdot \vec{r}} \xi(z - la) \quad (4.1)$$

where  $\vec{p}, \vec{r}$  are respectively the 2D momentum and position vector along the x-y plane.  $\xi_l(z)$  is defined in such a way that it gives  $\delta$ -function like distribution:

$$|\xi_l(z)|^2 = \delta(z - la) \quad (4.2)$$

We define our model by writing down the Hamiltonian which includes a description of the basic excitations and their interactions. This Hamiltonian of our electron-phonon system is given as:

$$H = H_e + H_{ph} + H_{ee} + H_{eph} \quad (4.3)$$

where  $H_e$  and  $H_{ph}$  are the Hamiltonians for the conduction electrons and LO phonons. The  $H_{ee}$  is the electron-electron interaction and  $H_{eph}$  the electron-LO-phonon interaction in the layered system. We have for these terms the explicit forms

$$H_e = \sum_{\vec{p}, l} E_p a_{\vec{p}, l}^\dagger a_{\vec{p}, l} \quad (4.4a)$$

$$H_{ph} = \sum_{\vec{Q}} \omega_{\vec{Q}} b_{\vec{Q}}^\dagger b_{\vec{Q}} \quad (4.4b)$$

where  $\vec{Q} = (\vec{q}, q_z)$  is a three dimensional vector because our two dimensional electron gas only interact with the bulk phonon of the compound. Here  $E_p = \frac{p^2}{2m}$  is the kinetic energy of an electron having momentum  $\vec{p}$ .  $\omega_{\vec{Q}}$  is the wave number dependent longitudinal optical frequency and  $a_{\vec{p}, l}^\dagger, a_{\vec{p}, l}$  ( $b_{\vec{Q}}^\dagger, b_{\vec{Q}}$ ) represent, respectively, the electron (phonon) creation and destruction operators with momentum  $\vec{p}$  ( $\vec{Q}$ ) on  $l$ th layer.

The electron-electron interaction is of the form

$$H_{ee} = \frac{1}{2} \sum_{\vec{q}, \vec{p}, \vec{p}', l} \sum_{\vec{p}'} V_q e^{-q|l-l'|} a_{\vec{p}+\vec{q}, l}^\dagger a_{\vec{p}-\vec{q}, l}^\dagger a_{\vec{p}', l} a_{\vec{p}', l} \quad (4.5a)$$

Here the coupling term  $V_q = \frac{2\pi e^2}{q \epsilon_\infty}$  is the Fourier transform of the Coulomb interaction for planar electrons.

For  $H_{eph}$  we have

$$H_{eph} = \sum_{\vec{Q}, l} C_l(\vec{q}, q_z) a_{\vec{p}+\vec{q}, l}^\dagger a_{\vec{p}, l} (b_{\vec{Q}}^\dagger + b_{-\vec{Q}}) \quad (4.5b)$$

where  $C_l(\vec{q}, q_z)$  is the Frohlich coupling between planar electron on the  $l^{th}$  layer and the bulk LO phonon which is given as:

$$C_l(\vec{q}, q_z) = i \left[ \frac{2\pi e^2 \omega_{LO}}{(q^2 + q_z^2)} \left( \frac{1}{\epsilon_\infty} - \frac{1}{\epsilon_0} \right) \right]^{1/2} \int dz e^{iq_z z} \xi_l(z) \xi_l^*(z) \quad (4.6)$$

For  $\delta$ -function distribution, Eq(2.6) simply becomes:

$$C_l(\vec{q}, q_z) = i \left( \frac{2\pi e^2 \omega_{LO}}{(q^2 + q_z^2)} \left( \frac{1}{\epsilon_\infty} - \frac{1}{\epsilon_0} \right) \right)^{1/2} e^{iq_z la} \quad (4.7)$$

Where  $\omega_{LO}$  is the longitudinal optical phonon frequency at zero wave-number and  $\epsilon_\infty$   $\epsilon_0$  are respectively the high-frequency and static dielectric constants of the relevant semiconductors.

### 4.3. Evaluation Of The Conductivity

To evaluate the conductivity, we start from the Kubo's<sup>[73]</sup> formula for conductivity which reads:

$$\sigma_{\mu\nu}(\omega) = \int_0^\infty e^{i\omega t} dt \int_0^\beta \langle j_\mu(t - i\lambda) j_\nu(0) \rangle d\lambda \quad (4.8)$$

where  $\omega$  is the frequency of electromagnetic wave and we set  $\hbar$  equal to unity for notational convenience. Here,

$$j_\mu(t) = e^{iHt} j_\mu(0) e^{-iHt} \quad (4.9)$$

is the current operator in Heisenberg representation and the average of an operator is defined by

$$\langle O \rangle = Tr [ e^{\beta(\Omega + \sum_s \mu_s N_s - H)} O ] \quad (4.10)$$

where H is the total Hamiltonian of the system and  $\Omega$  is defined by

$$e^{-\beta\Omega} = Tr [ e^{\beta(\sum_s \mu_s N_s - H)} ] \quad (4.11)$$

In equations (4.10) and (4.11)  $\mu_s$  and  $N_s$  are, respectively, the chemical potential and number operator of s species in the system, and  $\beta$  the inverse of the temperature in energy units. In order to render Eqn.(4.8) in a more convenient form we integrate it by parts and obtain

$$\sigma_{\mu\nu}(\omega) = \sigma_{\mu\nu}^0(\omega) + \sigma_{\mu\nu}^1(\omega) \quad (4.12)$$

where

$$\sigma_{\mu\nu}^0(\omega) = -\frac{1}{i\omega} \int_0^\beta d\lambda \langle j_\mu(-i\lambda) j_\nu(0) \rangle = \frac{ie^2 n}{\omega m} \delta_{\mu\nu} \quad (4.13)$$

and

$$\sigma_{\mu\nu}^1(\omega) = \frac{1}{\omega} \int_0^\infty dt e^{i\omega t} \langle [j_\mu(t), j_\nu(0)] \rangle \quad (4.14)$$

In Eq.(4.13), the square brackets denote the commutator. By this, the current operator can be expressed as

$$\vec{j}(k) = \frac{e}{m} \sum_{\vec{p}, l} \vec{p} a_{\vec{p}+\vec{k}, j}^\dagger a_{\vec{p}, j} \quad (4.15)$$

Calculation of the current-current correlations and the conductivity in the layered structure have been worked out in much detail in chapter 2 and 3. Here we will follow the same method as used in chapter 3. We evaluate the conductivity treating electron phonon collision within the Born approximation (high-frequency conductivity), however treating the self-consistent field of the fluctuating electron gas and phonons exactly in the random-phase-approximation. Under these approximations, we consider the class of diagrams of Fig.4.1a-4.1e. Our expression includes the full dynamical screening of the electron-phonon systems. The wavy line in Fig.4.1a-4.1e is the effective interaction of an electron in  $l$  th layer with an electron in  $l'$  th layer which is determined by following integral equation (Fig.4.2):

$$\begin{aligned}
v_{ll}(q, \alpha_m) &= V_{ll}(q) + \sum_{q_z} C_l(q, q_z) C_{l_1}^*(q, q_z) D_{\vec{Q}}(\alpha_m) \\
&+ \sum_{q_z \neq l_1} C_l(q, q_z) C_{l_1}^*(q, q_z) D_{\vec{Q}}(\alpha_m) Q(q, \alpha_m) v_{l_1 l}(q, \alpha_m) \\
&+ \sum_{l_1} V_{ll_1} Q(q, \alpha_m) v_{l_1 l}(q, \alpha_m)
\end{aligned} \tag{4.16}$$

Where

$$V_{ll}(q) = \frac{2\pi e^2}{q \epsilon_\infty} e^{-q |l-l_1| a} \tag{4.17}$$

and

$$\alpha_m = \frac{2\pi m i}{\beta} \quad m = 0, \pm 1, \pm 2, \dots \tag{4.18}$$

In Eq.(4.16),  $Q_s(q, \alpha_m)$  is the density fluctuation of 2D electron gas which is independent of layer index given by

$$Q(q, \alpha_m) = \frac{1}{4\pi^2} \int d\vec{p} \frac{f_{\vec{p}+\vec{q}} - f_{\vec{p}}}{E_{\vec{p}+\vec{q}} - E_{\vec{p}} - \alpha_m} \tag{4.19}$$

here  $f_{\vec{p}}$  is the Fermi distribution function:

$$f_{\vec{p}} = \frac{1}{\exp(\beta E_{\vec{p}} - \beta \mu) + 1} \tag{4.20}$$

And  $D_{\vec{Q}}(\alpha_m)$  is the free phonon propagator:

$$D_{\vec{Q}}(\alpha_m) = \frac{\omega_Q}{\alpha_m^2 - \omega_Q^2} \tag{4.21}$$

Since the momentum transfer  $q$  is of order of the Fermi momentum which in turn is much smaller than lattice momentum, we ignore entirely the dispersion of

the of the phonons and replace  $\omega_Q$  by  $\omega_{LO}$ .

$$D_{\bar{Q}}(\alpha_m) = D(\alpha_m) = \frac{\omega_{LO}}{\alpha_m^2 - \omega_{LO}^2} \quad (4.22)$$

Therefore, the summation over  $q_z$  in Eq.(4.16) can be carried out, we obtain,

$$\begin{aligned} v_{ll'}(q, \alpha_m) = & V_{ll'}(q) + \psi_{ll'}(q)D(\alpha_m) + \sum_{l_1} \psi_{ll'}(q)D(\alpha_m)Q(q, \alpha_m)v_{l_1 l'}(q, \alpha_m) \\ & + \sum_{l_1} V_{ll_1}Q(q, \alpha_m)v_{l_1 l'}(q, \alpha_m) \end{aligned} \quad (4.23)$$

where

$$\psi_{ll'}(q) = \frac{2\pi e^2}{q} \omega_{LO} \left[ \frac{1}{\epsilon_\infty} - \frac{1}{\epsilon_0} \right] e^{q|l-l'|a} \quad (4.24)$$

Now the integral equation (4.23) can be solved by Fourier transformation ( note  $v_{ll'}$  only depend on  $l-l'$  )

$$v(q, k_z, \alpha_m) = \sum_{l'} v_{ll'}(q, \alpha_m) e^{ik_z(l-l')a} \quad (4.25)$$

We obtain,

$$v(q, k_z, \alpha_m) = \frac{V_q S(q, k_z) + \psi(q, k_z)D(\alpha_m)}{1 - Q(q, \alpha_m)[V_q S(q, k_z) + \psi(q, k_z)D(\alpha_m)]} \quad (4.26)$$

where

$$\psi(q, k_z) = \frac{2\pi e^2}{q} S(q, k_z) \omega_{LO} \left[ \frac{1}{\epsilon_\infty} - \frac{1}{\epsilon_0} \right] \quad (4.27)$$

and

$$S(q, k_z) = \sinh \frac{(qa)}{\cosh(qa) - \cos(k_z a)} \quad (4.28)$$

Let us define a dielectric function

$$\epsilon(q, \alpha_m) = 1 - V_q Q(q, \alpha_m) S(q, k_z) \quad (4.29)$$

and the "true" phonon propagator

$$\begin{aligned} \tilde{D}(\alpha_m) &= \frac{D(\alpha_m)}{1 - \frac{\psi(q, k_z) D(\alpha_m) Q(q, \alpha_m)}{\epsilon(q, \alpha_m)}} \\ &= \frac{\omega_{LO}}{\alpha_m^2 - \omega_{LO}^2 - \frac{\omega_{LO} \psi(q, k_z) Q(q, \alpha_m)}{\epsilon(q, \alpha_m)}} \end{aligned} \quad (4.30)$$

therefore

$$v(q, \alpha_m) = \frac{V_q S(q, k_z)}{\epsilon(q, \alpha_m)} + \frac{\psi(q, k_z) \tilde{D}(\alpha_m)}{\epsilon(q, \alpha_m)^2} \quad (4.31)$$

Thus we express our effective interaction by two terms, the first term is the screened Coulomb potential due to the collective motion of the electrons. The second term represents the renormalized phonon interaction at a vertex with the electron through a screened phonon-electron interaction  $\frac{\psi(q, \alpha_m)}{\epsilon(q, \alpha_m)}$ . After some

algebra, our final result for conductivity reads:

$$\sigma(\omega) = \sigma^0(\omega) + \sigma^1(\omega) = \sigma^0(\omega) \left[ 1 - \frac{1}{\omega} I(\omega) \right] \quad (4.32)$$

where

$$I(\omega) = \frac{\pi}{nm \omega} \int q^3 dq \int \frac{adk_z}{2\pi} \frac{\psi(q, k_z)}{V_q S(q, k_z)} \frac{P}{2\pi} i \int dx \coth\left(\frac{\beta x}{2}\right) F(q, x, \omega) \quad (4.33)$$

where

$$\begin{aligned}
 F(q, x, \omega) = & [\tilde{D}(x) - \tilde{D}^*(x)] \frac{1}{\epsilon(q, x + \omega)} + \left[ \frac{1}{\epsilon(q, x)} - \frac{1}{\epsilon^*(q, x)} \right] \tilde{D}(x + \omega) \\
 & - \left[ \frac{\tilde{D}(x)}{\epsilon(q, x)} - \frac{\tilde{D}^*(x)}{\epsilon^*(q, x)} \right] - \frac{\psi(q, k_z)}{V_q S(q, k_z)} \left[ \frac{\tilde{D}(x + \omega)}{\epsilon(q, x + \omega)^2} [\tilde{D}(x) - \tilde{D}^*(x)] \right. \\
 & \left. + \tilde{D}(x + \omega) \left[ \frac{\tilde{D}(x)}{\epsilon(q, x)^2} - \frac{\tilde{D}^*(x)}{\epsilon^*(q, x)^2} \right] - \frac{2\tilde{D}(x + \omega)}{\epsilon(q, x + \omega)} \left[ \frac{\tilde{D}(x)}{\epsilon(q, x)} - \frac{\tilde{D}^*(x)}{\epsilon^*(q, x)} \right] \right]
 \end{aligned} \tag{4.33a}$$

Here P stands for principal value and

$$f(x) \rightarrow f(x + i\eta), \quad (\eta \rightarrow 0) \tag{4.34}$$

Eq.(4.33) is the exact expression in which we have use the fact that  $Q$  depend only on absolute value of  $\vec{q}$  and that  $\sigma_{\mu\nu}(\omega) = \delta_{\mu\nu} \sigma(\omega)$  for isotropic system. This expression is our principal result. This algebraically complicated result can be evaluated numerically for any frequency, temperature and electron-LO phonon coupling. Our next task is to investigate the frequency and temperature variation of the relaxation time and to explore the role of coupling between the LO phonon and plasma oscillation and other effects presented at finite carrier concentration.

#### 4.4. Relaxation Time and Resistivity

The collision process is described by the real part of the conductivity as written in Eq.(4.32-33). We see immediately that the only absorption is from the electron-phonon scattering. The phonon propagator  $\tilde{D}$  plays an important role in our result. The dispersion relation of the coupled plasmon-LO-phonon modes is given by the poles of  $\tilde{D}$ . By using Eqs.(4.27),(4.29) and  $\omega_{TO}^2 = \frac{\epsilon_\infty}{\epsilon_0} \omega_{LO}^2$ , we may

write  $\tilde{D}$  in the following form

$$\tilde{D}(\omega) = \frac{\omega_{LO} \epsilon(q, \omega)}{(\omega^2 - \omega_{LO}^2 + i \delta \omega) - (\omega^2 - \omega_{TO}^2 + i \delta \omega) \frac{2\pi e^2}{q \epsilon_\infty} Q(q, \omega) S(q, k_z)} \quad (4.35)$$

where  $\omega_{TO}$  is the transverse optical phonon frequency. Here  $\delta$  is the half width of the free phonon<sup>[88]</sup>. We find that the poles of the the dressed phonon propagator are identical to the roots of the dielectric function given by:

$$\tilde{\epsilon}(q, \omega) = \epsilon_\infty \frac{\omega^2 - \omega_{LO}^2 + i \delta \omega}{\omega^2 - \omega_{TO}^2 + i \delta \omega} - \frac{2\pi e^2}{q} Q(q, \omega) S(q, k_z) \quad (4.36)$$

In our later numerical work we shall use Eq.(4.35) for our calculation of F of Eq.(4.33b). Let us rewrite Eq.(4.30) as:

$$\sigma(\omega) = \sigma^0 \left( \frac{1}{1 + \frac{I / \omega}{1 - I / \omega}} \right) \quad (4.37)$$

The high-frequency limit is given by the condition  $|I(\omega)| \ll \omega$  and we thus obtain the approximate expression for the conductivity:

$$\sigma(\omega) = \frac{\sigma^0}{1 + \frac{I_1(\omega) + i I_2(\omega)}{\omega}} \quad (4.38)$$

Here  $I_1$  and  $I_2$  are respectively the real and imaginary parts of  $I(\omega)$ . The relaxation time and effective mass are related to conductivity by the Drude formula:

$$\sigma(\omega) = \frac{ine^2}{m^* (\omega + \frac{i}{\tau})} \quad (4.39)$$

We find the effective mass;

$$m^* = m \left[ 1 + \frac{I_1(\omega)}{\omega} \right] \quad (4.40)$$

and the relaxation time:

$$\tau^{-1} = I_2(\omega) \quad (4.41)$$

Here only linear corrections due to  $I_1$  and  $I_2$  are retained. however, using Eq.(4.37) we obtain for the general case the result:

$$\frac{m^*}{m} = \frac{1}{\left(1 + \frac{I_1}{\omega}\right) \left[1 + \frac{I_2^2}{(\omega + I_1)^2}\right]} \quad (4.42)$$

and

$$\tau^{-1} = \frac{I_2}{1 + \frac{I_1}{\omega}} \quad (4.43)$$

Using the analytical properties of  $Q, \tilde{D}$ , and the dielectric function respectively, we can write:

$$\frac{1}{\tau} = \frac{1}{\omega n m} \int q^3 dq \int_{-\pi}^{\pi} \frac{d\theta}{2\pi} \psi(q, \theta) \times \frac{P}{2} \int dx \left[ \coth \frac{\beta x}{2} - \coth \frac{\beta(x + \omega)}{2} \right] F(x, x + \omega) \quad (4.44)$$

where  $\theta = ak_z$  and

$$F(x, x + \omega) = F_1(x, x + \omega) - F_2(x, x + \omega) \quad (4.45)$$

with

$$F_1(x, x + \omega) = \frac{2}{V_q S(q, k_z)} \left[ \text{Im} \tilde{D}(x) \text{Im} \frac{1}{\epsilon(x + \omega)} + \text{Im} \tilde{D}(x + \omega) \text{Im} \frac{1}{\epsilon(x)} \right] \quad (4.46)$$

and

$$F_2(x, x+\omega) = \frac{2\psi(q, k_z)}{(V_q S(q, k_z))^2} \left( \text{Im} \frac{\tilde{D}(x+\omega)}{\epsilon(x+\omega)^2} \text{Im} \tilde{D}(x) \right. \\ \left. + \text{Im} \frac{\tilde{D}(x)}{\epsilon(x)^2} \text{Im} \tilde{D}(x+\omega) - 2 \text{Im} \frac{\tilde{D}(x)}{\epsilon(x)} \text{Im} \frac{\tilde{D}(x+\omega)}{\epsilon(x+\omega)} \right) \quad (4.47)$$

The leading term at high-frequencies is given by  $F_1$ .  $F_2$  will contribute terms to the conductivity or absorption which are smaller by a factor  $\omega^{-2}$  with respect to those obtained from  $F_1$ . We observe that  $F_2$  represents simultaneous excitation of two phonon with a large shift in their energy which makes a small contribution to the conductivity at *high frequencies*. Even at frequencies  $\omega \approx \omega_{LO}$  our numerical calculations indicate that the contribution from  $F_2$  is still very small. Therefore, we neglect the contributions from  $F_2$ . Eq.(4.44) with Eq.(4.46) is our general result for the absorption which includes the effect of finite lifetime of the phonons. It is apparent that instead of having a  $\delta$  function behavior for  $\text{Im} \tilde{D}(x)$ , we have here a lorentzian like shape. This amounts to an average of the electron density fluctuation  $[\text{Im} \frac{1}{\epsilon}]$  over a range of frequencies of width  $|\Gamma_q^{-1}|$ . For the purpose of the calculation we would like to use following dimensionless variables,

$$z = \frac{q}{2k_F}, \quad \Omega = \frac{\omega}{4E_F}, \quad X = \frac{x}{4E_F}, \quad \Theta = \frac{1}{4E_F \beta}$$

$$D = 4E_F \tilde{D} \quad Q = \frac{2\pi e^2}{q \epsilon_\infty} Q \quad F = 4E_F \frac{2\pi e^2}{q \epsilon_\infty} F,$$

where  $E_F$  is the Fermi energy for electrons. By this we get

$$\frac{1}{\tau} = \frac{8\pi^2\omega_{LO}}{\Omega} \left[1 - \frac{\epsilon_\infty}{\epsilon_0}\right] \int_{-\pi}^{\pi} \frac{d\theta}{2\pi} \int_0^\infty z^3 dz S(z, \theta) \times$$

$$\frac{P}{2} \int_{-\infty}^\infty dX \left[ \coth\left(\frac{X}{2\Theta}\right) - \coth\left(\frac{X+\Omega}{2\Theta}\right) \right] F(X, \Omega+X) \quad (4.48)$$

For the case  $kT \ll E_F$ , we can use the limit ( $T \rightarrow 0$ ) and get:

$$\frac{1}{\tau} = \frac{8\pi^2\omega_{LO}}{\Omega} \left[1 - \frac{\epsilon_\infty}{\epsilon_0}\right] \int_{-\pi}^{\pi} \frac{d\theta}{2\pi} \int_0^\infty z^3 dz S(z, \theta) \int_0^\Omega dX F(X, \Omega-X) \quad (4.49)$$

We will evaluate this inverse collision time numerically for GaAs-GaAlAs and PbTe-PbEuTeSe systems.

#### 4.5 Mass Shift

In this project, we are mainly interested in the optical absorption in a layered system due to various mechanism. Therefore we will not give any quantitative result for the mass renormalization. However, here we would like to discuss briefly the qualitative behavior of  $\delta m = m^* - m$  as a function of  $\omega$ . For  $|I_1| \ll \omega$ ,  $\delta m$  can be cast into a simpler form after algebra and reads

$$\delta m = \frac{\pi}{n\omega^2} \int q^3 dq \int \frac{adk_z}{2\pi} \frac{\psi(q, k_z)}{V_q S(q, k_z)} \frac{P}{2\pi} \int dx \coth\left(\frac{\beta x}{2}\right) F_3(q, x, \omega) \quad (4.50)$$

where

$$F_3(x, x+\omega) = \frac{2}{V_q S(q, k_z)} \left[ \text{Im}\tilde{D}(x) \text{Re}\frac{1}{\epsilon(x+\omega)} + \text{Re}\tilde{D}(x+\omega) \text{Im}\frac{1}{\epsilon(x)} \right]$$

$$- \frac{2\psi(q, k_z)}{(V_q S(q, k_z))^2} \left[ \text{Re}\frac{\tilde{D}(x+\omega)}{\epsilon(x+\omega)^2} \text{Im}\tilde{D}(x) \right]$$

$$\left. + \operatorname{Re} \frac{\tilde{D}(x)}{\epsilon(x)^2} \operatorname{Im} \tilde{D}(x+\omega) - 2 \operatorname{Im} \frac{\tilde{D}(x)}{\epsilon(x)} \operatorname{Re} \frac{\tilde{D}(x+\omega)}{\epsilon(x+\omega)} \right\} \quad (4.51)$$

Here the various terms in the integrand Eq.(4.51) have alternating signs, thus large cancellations do occur. Let us determine the qualitative behavior of  $\delta m$  as a function of  $\omega$ . For  $\omega \rightarrow \infty$ ,  $\epsilon(x)$  and  $\epsilon(\omega+x)$  may be replaced by unity and  $\tilde{D}(x+\omega)$  asymptotically approaches zero as  $\omega^{-2}$ . We thus conclude that for  $\omega \rightarrow \infty$  the integral in Eq.(4.50) approaches a constant and hence  $\delta m \approx \omega^{-2}$ . On the other hand for  $\omega \rightarrow 0$  the integrand Eq.(4.51) behaves as  $\omega^2$ , and thus  $\delta m$  becomes a constant when  $\omega$  approaches zero.

#### 4.6. Discussion

In this chapter, we have calculated the high-frequency conductivity and relaxation time for superlattice system made out of polar or partially polar semiconductors. Here we treat electron-LO phonon scattering as the dominant scattering mechanism which contribute to the absorption. Our general expression for dynamical conductivity is given in Eqs.(4.32) and (4.33). The conductivity depends on the dressed phonon propagator  $\tilde{D}$  which is defined in Eq.(4.35). The poles of  $\tilde{D}$  are identical to the roots which determine the phonon-plasma coupled frequencies (see Eq.(4.36)). Essentially the same result indicate that the bulk conductivity depends on  $\tilde{D}$  rather than  $D$  was derived long ago by Ron and Tzoar<sup>[107]</sup>. However, the first calculation that demonstrated the difference of using  $\tilde{D}$  rather than  $D$  was given by Katayama and co-workers<sup>[108]</sup>. Our calculation indicates that for weak electron-phonon coupling, for semiconductors such as GaAs-GaAlAs, the intensity of  $\tilde{D}$  resides almost exclusively in the vicinity of the longitudinal optic phonon frequency. In this case using  $D$  rather than  $\tilde{D}$  in our expression for the

conductivity should yield a realistic approximation for the conductivity. Our numerical results indicate it to be true. For the case of strong electron-phonon coupling, for materials such as PbTe-PbEuTeSe, the intensity of  $\tilde{D}$  shows two broad resonances which can be identified as "dressed phonon" and "dressed plasmon". We find significant difference in our results if we use  $D$  rather than  $\tilde{D}$  in our expression for the conductivity. We thus may conclude that for polar material having strong electron-phonon coupling the dressed phonon propagator should be used.

In our Figures, we have plotted the real part of the conductivity and the inverse collision time as a function of the normalized frequency. From the real part of the conductivity, one can see clearly the scattering from two coupled modes. However for the inverse collision time the peak at low frequency is drastically reduced. This comes about since the inverse collision time is proportional to  $\omega^2\sigma_1$ , and the peak is at frequency  $\omega_0$  which is smaller than its effective width. Thus the factor  $\omega^2$  strongly suppressed the resonant effect for  $\tau^{-1}$  at  $\omega_0$ . In Fig.(4.2) We plot the the numerical results of the real part of the conductivity and the inverse collision time ( $\tau^{-1}$ ) for weakly polar material [ GaAs-GaAlAs ]. The difference between using the bare phonon propagator rather than the dressed phonon propagator is small. The absorption at frequencies below the LO phonon frequency is not noticeable for the case of weak electron-phonon coupling. We note however that the absorption at  $\omega$  larger than  $\omega_{LO}$  is reduced for the dressed phonon in comparison with the bare phonon, just as has been reported for the bulk case<sup>[108]</sup> In Fig.(4.3) we present our numerical results for the real part of conductivity and inverse collision time for PbTe-PbEuTeSe, which is a strongly interacting electron-phonon system. In this case, we found a large difference in the real

part of conductivity as well as in the inverse collision time between the bare phonon scattering and the dressed phonon scattering. For the case of strong electron-phonon coupling, the peak in real part of conductivity at low frequencies is due to the scattering from the low-lying mode in the density fluctuation of the electron-phonon system. In Fig.(4.4) the lower curve is obtained by changing  $a \rightarrow 2a, n \rightarrow 2n$  ( $\frac{n}{a} = \text{constant}$ , i.e, the volume density is fixed ) under this change both the real part of conductivity and the inverse collision time are greatly reduced due to the increasing in screening and decreasing in coupling between layers. In Fig.(4.5) we present our numerical results for the real part of the conductivity and the inverse collision time for PbTe-PbEuTeSe with the same parameters as in Fig.(4.3). Here for finite temperature,  $\tau^{-1}$  is finite in the small frequency limit, and the real part of the conductivity is greatly increased in this regime. The physical parameters used in our numerical calculation are the following:  
 $\epsilon_0^{PbTe} = 1333.0, \epsilon_\infty^{PbTe} = 33.0, \omega_{LO}^{PbTe} = 13.4 \text{ meV}, m^{PbTe} = 0.21 m_0, \epsilon_0^{GaAs} = 12.5,$   
 $\epsilon_\infty^{GaAs} = 10.8, \omega_{LO}^{GaAs} = 36 \text{ meV}, m^{GaAs} = 0.07 m_0$  where  $m_0$  is the free electron mass.

In conclusion, we have calculated the high-frequency conductivity of superlattice system with electron-LO phonon interaction. General result has been derived in terms of integral and numerical computation has been done for some typical parameters for type-I superlattices. We note that our work can be easily generalized to calculate, say, the collision frequency due to phonons of the electron and the holes respectively for type-II superlattices.

## Chapter V

### LIGHT SCATTERING FROM

### A TWO-COMPONENT LAYERED STRUCTURE

#### 5.1. Introduction

Recently, many light scattering experiments and theoretical investigation have been done on the superlattice structure which was formed by a layered electron gas (LEG)<sup>[36,109]</sup>. Olego et al.<sup>[68]</sup> observed the bulk plasmon of a LEG by inelastic light scattering from GaAs-(AlGa)As heterostructures. This experiment confirmed the random-phase-approximation (RPA) prediction<sup>[25,110]</sup> of the bulk plasmon dispersion relation. By imposing standard electromagnetic boundary conditions at the layers of a semi-infinite LEG, Giuliani and Quinn<sup>[75]</sup> predicted the existence and dispersion relation of surface plasmons if the dielectric media outside and inside the semi-infinite LEG are different. Jain and Allen<sup>[77]</sup> calculated the Raman intensities of the bulk and surface plasmons.

It has long been known that a two-component plasma has two branches to its longitudinal oscillation spectrum. In the high-frequency branch, the two carriers oscillate out of phase with the long wavelength limit at the square root of the sum of the squares of individual plasma frequencies of the two components, while in the lower branch the carriers oscillate in phase, exhibiting at long wavelengths

---

a linear dispersion like that of a sound wave, assuming the two carriers have opposite charge. Pines<sup>[111]</sup> first discussed the relevance of these modes to multicomponent, solid state plasma as occurring, for example, in bulk semiconductors. The high frequency branch has been called "optical plasmon" and the lower branch "acoustic plasmon", referring to its sound like long wavelength dispersion. Even though the mode corresponding to acoustic mode was observed<sup>[112,113]</sup> in ionic plasmas more than twenty years ago, no such acoustic branch has been detected in solid state plasmas in spite of the considerable experimental efforts<sup>[114]</sup>. The reason lies primarily in the large damping associated with this acoustic mode. In bulk plasma where all the experiments so far have been carried out, this acoustic mode lies in the low frequency regime and is inside the single particle excitation spectrum of the faster moving charge carrier and thus severely Landau damped ( apart from any collisional damping associated with phonon and impurities, which can be reduced by working at low temperature and by using sufficiently pure samples ).

In this chapter we give a microscopic theory for the Raman intensity of the bulk plasmons in LEG where two different carriers are localized on alternating layers. We shall determine the resonant modes at high and low frequencies. Our method involves the exact construction of the density-density correlation functions in RPA for such LEG. From this correlation functions, the Raman intensity is calculated. We will also generalize our result to the case of finite width of the electronic wave function. Finally, predictions will be made about the experimental condition to observe resonant scattering.

Results obtained in this chapter will indicate that the ideal solid state systems to look for the acoustic mode are these new and novel two-dimensional-

confined, spatially separated, multicomponent structures, in particular the semiconductor superlattices. We first find that in such a system all collective modes are acoustic and there always exists a high-frequency acoustic mode (outside the electron-hole continua of both components). We also find that when the superlattice period exceeds a critical value, such a system is capable of supporting another high frequency acoustic mode which is also undamped up to some critical wave vector. The frequency of the second mode is proportional to the wave vector with a proportionality constant (i.e., phase velocity  $c$ ) which is higher than Fermi velocities of both components. In this regime of superlattice period, there is no low frequency collective mode of the system lying between the two electron-hole continua. Thus by virtue of superlattice parameters, the ordinary plasmon become two acoustic plasmons. The one with high phase velocity is always undamped and the other one with low phase velocity will be either damped or undamped depends on the superlattice parameters. The controllability of the superlattice parameters is the main advantage of such a system and make it the most suitable candidate for the experiment to realize the acoustic plasmon in solid state.

The Raman scattering cross-section is completely characterized by the wave number transfer  $q$  and energy loss  $\omega$  in the scattering event. Here  $q = k_{in} - k_{out}$  and  $\omega = \omega_{in} - \omega_{out}$  (subscripts *in* and *out* refer to incoming and outgoing photons). For most light scattering experiments from the semiconductor plasmas the wave number transfer is smaller than the inverse screening length, i.e.,  $q \lambda_s < 1$ . For a one component isotropic plasma the cross-section is proportional to the density fluctuations of the electron gas. For the case  $q \lambda_s < 1$  the scattered intensity resides almost entirely in the plasma line.

## 5.2. Formalism For Scattering Cross-Section

We use the model of Visscher and Felicov<sup>7</sup> for a LEG, which has delta-function-localized carrier density in a plane. The carriers are free to move in the plane and the carriers in different planes interact only via the Coulomb potential. The possibility of tunneling between two planes as well as of interband excitations within a plane is ignored under the assumption that both carrier temperature and their Fermi energy are small compared to the subband splitting. Let us consider electrons of density  $n_e$  per unit area and mass  $m_e$  occupying layers which are positioned at  $z = ja$  and holes of density  $n_h$  per unit area and mass  $m_h$  occupying layers which are positioned at  $z = ja + b$ , where  $j$  can be any integer,  $a$  is the length of the unit cell in the z-direction and  $b$  is the separation between electrons and holes on each cell. The Hamiltonian that describes such a system is given by

$$H = H_1 + H_I \quad (5.1)$$

where the first term contains the kinetic energy of the carriers and their coupling to the radiation field. The second term is the Coulomb interaction of the many-particle system. In second quantized notation, they are given as:

$$H_1 = \frac{1}{2} \sum_{\vec{p}, j, s} \frac{(\vec{p} + \frac{e_s}{c} \vec{A})^2}{m_s} a_{\vec{p}, j}^\dagger(s) a_{\vec{p}, j}(s) \quad (5.2)$$

and

$$H_I = \frac{1}{2} \sum_{\vec{q}, \vec{p}, \vec{p}', j, j', s, s'} V_{j, j'}^{s, s'}(\vec{q}) e_s e_{s'} a_{\vec{p} + \vec{q}, j}(s) a_{\vec{p} - \vec{q}, j'}(s') a_{\vec{p}', j}(s') a_{\vec{p}, j}(s) \quad (5.3)$$

where  $\vec{p}$  is 2D momentum vector.  $a_{\vec{p}, j}^\dagger$  and  $a_{\vec{p}, j}$  represent, respectively, the elec-

tron creation and destruction operators with momentum  $\vec{p}$  on the  $l$ th layer. We set  $\hbar$  and the speed of light  $c$  equal to unity for notational convenience. The summation over  $s$  means that  $s$  can be either an electron or a hole.  $V_{j,j'}^{s,s'}(q)$  is the Fourier transform of the Coulomb interaction,

$$V_{j,j'}^{ss'}(q) = \frac{2\pi}{q} e^{-q|j-j'|a} \quad (for \quad s=e, \quad s'=e \quad or \quad s=h, \quad s'=h) \quad (5.4)$$

or

$$V_{j,j'}^{ss'}(q) = \frac{2\pi}{q} e^{-q|(j-j')a-b|} \quad (for \quad s=e, \quad s'=h) \quad (5.4a)$$

In calculating the scattering cross-section, we consider only the coupling of the incoming and outgoing radiation via the  $\vec{A}^2$  term in the Hamiltonian. This is a good approximation when  $E_F < \omega_{in} < mc^2$ , where  $E_F$  is the Fermi energy. This essentially nonrelativistic approximation leads to the following expression for the cross-section for a photon of wave number  $k_{in}$ , frequency  $\omega_{in}$  and polarization  $\epsilon$  to be scattered into a state with wave number  $k_{out}$ , frequency  $\omega_{out}$ , and polarization  $\epsilon'$ : ( Appendix 5A )

$$\frac{d\sigma}{d\omega d\Omega} = e^4 |\epsilon \cdot \epsilon'|^2 \frac{\omega_{out}}{\omega_{in}} \int_{-\infty}^{\infty} \frac{dt}{2\pi} e^{i\omega t} \sum_{j,j',s,s'} \frac{e^{ik_z(j-j')a}}{m_s m_{s'}} \langle n_{j,s}(\vec{q}t) n_{j',s'}(-\vec{q}) \rangle \quad (5.5)$$

In Eq.(5.5),  $n_{j,s}(\vec{q}t)$  is the Fourier transform of the density operator to the  $l$ th cell for the  $s$  species,  $n_{j,s}(t) = e^{iHt} n_{j,s}(0) e^{-iHt}$ , the bracket  $\langle \rangle$  represents the usual thermodynamic ensemble average. The factor  $e^{ik_z(j-j')a}$  is a coherence term which will generate perpendicular momentum conservation. The scattering cross-section is given in our Eq.(5.5) in terms of the time dependent density fluctuations of the

carriers in the different planes. In equilibrium Eq.(5) can be rewritten, using the fluctuations-dissipation theorem, as

$$\frac{d \sigma}{d \omega d \Omega} = e^4 |\epsilon \cdot \epsilon'|^2 \left( \frac{\omega_{out}}{\omega_{in}} \right) \frac{\rho(\omega)+1}{\pi} \text{Im} \int_0^\infty dt e^{i \omega t} \sum_{j,j'} e^{ik_z(j-j)a} \sum_{s,s'} \frac{\Pi_{s,s'}(j,j')}{m_s m_{s'}} \quad (5.6)$$

where  $\rho(\omega)=(\exp(\beta\omega)-1)^{-1}$  and  $\beta$  is the inverse temperature in energy unit. Here  $\Pi$  is given as

$$\Pi_{s,s'}(j,j') = \theta(t) \langle [n_{j,s}(\vec{q}t), n_{j',s'}(-\vec{q}t)] \rangle, \quad (5.7)$$

where  $\theta(t)$  is the standard step function and it obeys the following integral equation

$$\Pi_{s,s'}(j,j') = \Pi_{s,s'}^0 \delta_{s,s'} \delta_{j,j'} + \Pi_{s,s'}^0 \sum_{s'',j''} e_s e_{s''} V_{j,j''}^{s,s''} \Pi_{s'',s'}(j'',j') \quad (5.8)$$

where  $\Pi^0$  is the value of  $\Pi$  in the absence of the Coulomb interaction.

$$\Pi_{s,s'}^0(q, \omega) = \int \frac{d\vec{p}}{4\pi^2} \frac{f_{\vec{p}+\vec{q}}(s) - f_{\vec{p}}(s)}{E_{\vec{p}+\vec{q}}(s) - E_{\vec{p}}(s) - \omega - i\alpha} \quad (\alpha \rightarrow 0^+) \quad (5.8a)$$

Here  $f_p(s)$  is the Fermi distribution function for  $s$  component which is independent of layer index

$$f_p(s) = \frac{1}{e^{\beta(E_{\vec{p}}(s) - \mu_s)} + 1}$$

where  $\mu$  is the chemical potential and  $E_{\vec{p}}(s) = \frac{\vec{p}^2}{2m_s}$ . The dependence on  $q$  and  $\omega$  is suppressed in Eq.(5.8). To solve this equation, we make the following Fourier transformation

$$\Pi_{s,s'}(j,j') = \frac{1}{N} \sum_{q_z} e^{-iq_z(j-j')a} \Pi_{s,s'}(q_z) \quad (5.9)$$

where  $q_z$  can assume the values  $\frac{2\pi n}{Na}$ . Here  $N$  is the number of planes and  $n=0,1,\dots,N-1$ . ( At the end, we take the limit  $N \rightarrow \infty$ ). After some algebra, our result can be written as: (Appendix 5B )

$$\frac{d\sigma}{d\omega d\Omega} = \frac{e^2}{m_e^2} |\epsilon \cdot \epsilon'|^2 \left( \frac{\omega_{out}}{\omega_{in}} \right) \frac{q(\rho(\omega)+1) A}{\pi} \text{Im} F(q, k_z, \omega) \quad (5.10)$$

where  $A$  is the area of the plane and

$$F(q, k_z, \omega) = [ Q(1-VSB) + \alpha^2 B(1-VSQ) - \alpha QBV(S+S^*) ] \frac{V(q)}{D(q, k_z, \omega)} \quad (5.11)$$

Here  $\alpha = \frac{m_e}{m_h}$ ,  $V = \frac{2\pi e^2}{q}$  and  $Q, B$  refer respectively to the 2-D density fluctuation of electrons and holes, i.e.  $Q = \Pi_e^0$  and  $B = \Pi_h^0$ . Also,  $S$  and  $S^*$  are the form factors which can be expressed respectively as

$$S = \sum_j e^{-q|j|a} e^{-ik_z ja} = \frac{\sinh(qa)}{\cosh(qa) - \cos(k_z a)} \quad (5.12)$$

and

$$S^* = \sum_j e^{-q|ja-b|} e^{-ik_z ja} = \frac{\sinh(q(a-b)) + e^{-ik_z a} \sinh(qb)}{\cosh(qa) - \cos(k_z a)} \quad (5.13)$$

In Eq.(5.11) we defined a "dielectric function",

$$D(q, k_z, \omega) = 1 - V(q)S(Q(q, \omega) + B(q, \omega)) + V(q)^2 Q(q, \omega) B(q, \omega) (S^2 - |S^*|^2) \quad (5.14)$$

From Eq.(5.10) or (5.11), we see that the cross-section is given in terms of the susceptibilities of the electrons and the holes (i.e. Q and B) of the 2D electron gas. However, the cross-section is not proportional to the imaginary part of the inverse dielectric function of LEG formed by the electron-hole system. The light scattering cross-section depends on the current matrix element while the dielectric response depends on the matrix element of the density operator. ( see the mass dependence in our Eqs.(5.5) and (5.6) ). We point out that the light scattering intensity will peak at the zeros of  $D(q, k_z, \omega)$  which defines the resonance frequencies of the density response. However the scattered light intensity related to these frequencies can not be obtained from the residues of the density response but rather by using our Eqs.(5.10) and (5.11). [ Nevertheless, one can calculate the cross-section macroscopically using a susceptibility defined by  $\frac{n_{induced}}{\phi_{external}}$  provided the coupling of the external field to the charge density of the s species is made proportional to  $m_s^{-1}$  times the usual Coulomb interaction.<sup>[115]</sup> )

### 5.3. Dispersion Relation and Resonant Frequencies

The dispersion relation of the plasmon in LEG as well as the collective excitations observed in light scattering are given by the zeros of  $D(q, k_z, \omega)$ , i.e., when  $D(q, k_z, \omega)=0$ . This was investigated by Tselis and Quinn<sup>[77]</sup>. Sarma and Madhukar<sup>[116]</sup> had investigated the longitudinal collective spectrum of a spatially separated, two-dimensional plasma. We have generalized their results for a layered electron-hole structure.

(A). High-frequency regime ( $\omega \gg qv_{F1}, qv_{F2}$ )

Using the high-frequency expression for  $Q$  and  $B$ , we have

$$D(q, \omega, k_z) = 1 - \frac{S}{\omega^2} (\omega_{pe}^2 + \omega_{ph}^2) + \frac{\omega_{pe}^2 \omega_{ph}^2}{\omega^4} \left( S^2 - |S'|^2 - \frac{3Sqm_e m_h}{4e^2 n_e n_h} \left( \frac{n_e^2}{m_e^3} + \frac{n_h^2}{m_h^3} \right) \right) \quad (5.15)$$

where  $\omega_{ps}^2 = \frac{2\pi n_s e^2 q}{m_s}$  is the 2D plasma frequency for  $s^{th}$  component. The dispersion relation from Eq.(5.15) is

$$\omega_{\pm}^2 = \frac{S(\omega_{pe}^2 + \omega_{ph}^2)}{2} \pm \frac{1}{2} \left( (\omega_{pe}^2 + \omega_{ph}^2)^2 S^2 - 4\omega_{pe}^2 \omega_{ph}^2 [S^2 - |S'|^2 - \frac{3Sqm_e m_h}{4e^2 n_e n_h} \left( \frac{n_e^2}{m_e^3} + \frac{n_h^2}{m_h^3} \right)] \right)^{1/2} \quad (5.16)$$

Since we are only interested in the long-wavelength behavior of the collective modes, we shall consider the small  $q$  limit, i.e.,  $\frac{q}{k_F} \ll 1$ . However we still are left with two regions; (i), the intermediate-coupling limit, i.e.,  $qa, qb \ll 1$  and (ii), the weak-coupling limit, i.e.,  $qa, qb \gg 1$ .

i).  $qa, qb \ll 1$  but  $k_z \neq 0$ . In this situation

$$S = \frac{qa}{1 - \cos(k_z a)} \quad (5.17)$$

and

$$|S'|^2 = q^2 \frac{(a-b)^2 + b^2 + 2b(a-b)\cos(k_z a)}{[1 - \cos(k_z a)]^2} \quad (5.18)$$

Using Eqs.(17-18) in Eq.(16) we obtain following two collective modes:

$$\omega_{\pm} = C_{\pm} q \quad (5.19)$$

The coefficient  $C_{\pm}$  are given by

$$C_{\pm} = \left[ \frac{\pi e^2 a}{1 - \cos(k_z a)} \left( \frac{n_e}{m_e} + \frac{n_h}{m_h} \right) [1 \pm \sqrt{g}] \right]^{1/2} \quad (5.20)$$

with

$$g = 1 - \frac{m_e m_h n_e n_h (1 - \cos(k_z a))}{a (m_e n_h + m_h n_e)^2} \left( 2b \left( 1 - \frac{b}{a} \right) - \frac{3m_e m_h}{4e^2 n_e n_h} \left( \frac{n_e^2}{m_e^3} + \frac{n_h^2}{m_h^3} \right) \right)$$

Both modes are acoustic like, and for the  $\omega_-$  mode,  $b$  can not be zero since  $C_-$  becomes pure imaginary. The  $\omega_-$  mode can exist as an undamped, stable mode in the long-wavelengths only in a system where the two components of electron gas are spatially separated<sup>[112]</sup>. The separation  $b$  and the period  $a$  must satisfy the

condition by the requirement ( $C_- > v_{F1} = \frac{\sqrt{2\pi n_e}}{m_e}$ ) which is given by:

$$2b \left( 1 - \frac{b}{a} \right) > \left[ \frac{4}{m_e e^2} \left[ 1 + \frac{m_h n_e}{m_e n_h} - \frac{n_e m_h}{a e^2 m_e^2 n_h} (1 - \cos(k_z a)) \right] + \frac{3m_e m_h}{4e^2 n_e n_h} \left( \frac{n_e^2}{m_e^3} + \frac{n_h^2}{m_h^3} \right) \right] \quad (5.21)$$

For a fixed  $a$ , one can find the minimum separation  $b_c$ . The  $\omega_+$  mode always exist without any restriction.

The case with  $k_z = 0$  is different from above result. In such a case the term with the product  $QB$  vanishes and

$$\omega^2 = \frac{4\pi e^2}{a} \left( \frac{n_e}{m_e} + \frac{n_h}{m_h} \right) \quad (5.22)$$

This is just like a three-dimensional plasmon with effective plasma frequency

$$\Omega_{ps} = \frac{4\pi n_{Bs} e^2}{m_s}, \text{ the same form as that of bulk plasmons where } n_{Bs} = \frac{n_s}{a}.$$

ii).  $qa, qb \gg 1$ . In this limit,  $\omega_{\pm}$  are simply the respective two-dimensional plasma frequencies of the two components.

(B). Low-frequency regime ( $qv_{F1} > \omega > qv_{F2}$ )

For a system with a small mass ratio ( $\alpha \ll 1$ ), one may expect that there is a low-lying mode of the heavy holes screened by the electron. Using the appropriate limiting forms for the two polarizability functions ( see Eqs.(7-8) in ref.10.) in this regime. one can easily find that there can be just one solution of Eq.(14) satisfying  $qv_{F1} > \omega > qv_{F2}$ . This solution is necessarily complex (indicating the mode to be a damped one), since the polarization function of the light species has an imaginary part in this regime due to single particle excitations. For the collective mode to be physically meaningful damping has to be small and we shall assume this in our analysis. We write the solution of Eq.(14) in this low-frequency regime in the form

$$\omega = \omega_A - i \delta_A \tag{5.23}$$

where

$$\omega_A = \omega_{ph} \left[ \frac{S + (S^2 - |S'|^2) 2r_s \frac{k_{Fe}}{q}}{1 + 2Sr_s \frac{k_{Fe}}{q}} \right]^{1/2} \tag{5.24}$$

and

$$\delta_A = \frac{m_e r_s \omega_A^2}{q^2} \left( \frac{\frac{S \omega_A^2}{\omega_{ph}^2} - S^2 + |S'|^2}{S + 2r_s (S^2 - |S'|^2) \frac{k_{Fe}}{q}} \right) \quad (5.25)$$

where  $k_{Fe}$  is the Fermi wave-vector for the electron and  $r_s = \frac{m_e e^2}{k_{Fe}}$  is the electronic plasma parameter. For  $qa \ll 1$ ,  $\omega_A$  and  $\delta_A$  are proportional to  $q$  ( $k_z \neq 0$ ) and their ratio is

$$\frac{\delta_A}{\omega_A} = \frac{\sqrt{\alpha} r_s^{3/2} (k_{Fe} a)^2}{[k_{Fe} a + 4r_s k_{Fe}^2 b (a - b)]^{1/2} [1 - \cos(k_z a) + 2r_s k_{Fe} a]^{3/2}} \quad (5.26)$$

Here for  $\alpha < 1$  and  $r_s < 1$ ,  $\frac{\delta_A}{\omega_A}$  can be easily made to be smaller than unity.

The proportionality coefficient  $C_A$  for  $\omega_A$  must satisfy the condition  $v_{Fh} < C_A < v_{Fe}$ . This gives the condition for  $a$  and  $b$ ,

$$1 < \left( r_s k_{Fe} \frac{m_h}{m_e} \frac{a + 4b(a-b) r_s k_{Fe}}{1 - \cos(k_z a) + 2r_s a k_{Fe}} \right) < \frac{m_h^2 n_e}{m_e^2 n_h} \quad (5.27)$$

For  $qa, qb \gg 1$ ,  $\omega_A$  is just  $\omega_{ph}$  which is proportional to  $\sqrt{q}$ , and  $\delta_A$  is approximately zero. As pointed in Ref[112], this ion acoustic mode can even exist when the mass ratio is 1 because of the separation between two components. However, we have checked in this work that the spectral weight of the mode is rather small when the mass ratio is close to 1.

#### 5.4. Effect of finite spreading of the Electronic Wave Function

We now generalize our result to the case where electronic wave function has a finite spatial spreading instead of  $\delta$ -function like distribution. In this case our differential scattering cross-section can be written as

$$\frac{d\sigma}{d\omega d\Omega} = e^4 |\epsilon \cdot \epsilon'|^2 \left( \frac{\omega_{out}}{\omega_{in}} \right) \frac{\rho(\omega)+1}{\pi} \text{Im} \int_0^\infty dt e^{i\omega t} \times$$

$$\int dz dz' \sum_{j,j'} e^{ik_z(z-z')} \sum_{s,s'} \frac{\Pi_{s,s'}(j,j')}{m_s m_{s'}} \zeta_j^s(z) \zeta_j^{*s}(z) \zeta_{j'}^s(z') \zeta_{j'}^{*s}(z') \quad (5.28)$$

where  $\zeta_j^s(z)$  is the electronic wave function for  $s$  species on  $l$ th layer. where  $\Pi$  is still the 2D polarizability and it obeys the integral equation Eq.(5.8). However the Coulomb matrix element in that equation should be replaced by following quantities

$$V_{jj'}^{ss'} = \int dz \int dz' \zeta_j^{*s}(z) \zeta_j^s(z') V_{jj'}^{ss'}(q, z-z') \zeta_{j'}^s(z') \zeta_{j'}^{*s}(z) \quad (5.29)$$

As an example, we again use the model function Eq.(2.2) to study the effect of electronic wave function: By this function, the Coulomb matrix element can be obtained as:

$$V_{jj'}^{ss'} = \frac{2\pi e^2}{q} e^{-q|j-j'|a} f^{ss'}(j-j') \quad (5.30)$$

where  $f^{ss'}(j-j')$  is structure factor arising from the integration in the wells because of the finite spatial spreading of the wave function.

$$f^{ss'}(j-j') = \left( \frac{2}{qd_s} \right)^2 \sinh^2 \left( \frac{qd_s}{2} \right) \left[ 1 + \left( \frac{qd_s}{2\pi} \right)^2 \right]^{-2} (1 - \delta_{j,j'})$$

$$+ \left[ \frac{2}{qd_s} \left( 1 + \frac{\left( \frac{qd_s}{2\pi} \right)^2}{2 \left( 1 + \left( \frac{qd_s}{2\pi} \right)^2 \right)} \right) - \frac{2}{(qd_s)^2} \frac{(1 - e^{-qd_s})}{\left[ 1 + \left( \frac{qd_s}{2\pi} \right)^2 \right]^2} \right] \delta_{j,j'} \quad (5.31)$$

and

$$f^{ss'}(j-j') = \left(\frac{2}{qd_s}\right) \frac{\sinh\left(\frac{qd_s}{2}\right)}{1+\left(\frac{qd_s}{2\pi}\right)^2} \left(\frac{2}{qd_{s'}}\right) \frac{\sinh\left(\frac{qd_{s'}}{2}\right)}{1+\left(\frac{qd_{s'}}{2\pi}\right)^2} (1-\delta_{s,s'}) \quad (5.32)$$

where  $d_s$  is the spreading of the wave function for s component. Now Eq.(5.28) can be written as

$$\frac{d\sigma}{d\omega d\Omega} = e^4 |\epsilon \cdot \epsilon'|^2 \left(\frac{\omega_{out}}{\omega_{in}}\right) \frac{\rho(\omega)+1}{\pi} \text{Im} \int_0^\infty dt e^{i\omega t} \times \sum_{j,j'} e^{ik_z(j-j')a} \sum_{s,s'} \frac{\Pi_{s,s'}(j,j')}{m_s m_{s'}} g^{ss'}(k_z, d_s, d_{s'}) \quad (5.33)$$

where

$$g^{ss'}(k_z, d_s, d_{s'}) = \frac{\sin\frac{k_z d_s}{2}}{\frac{k_z d_s}{2}} \frac{1}{1 - \left(\frac{k_z d_s}{2\pi}\right)^2} \frac{\sin\frac{k_z d_{s'}}{2}}{\frac{k_z d_{s'}}{2}} \frac{1}{1 - \left(\frac{k_z d_{s'}}{2\pi}\right)^2} \quad (5.34)$$

Using the same method as described in Appendix 5B, our result can be written as:

$$\frac{d\sigma}{d\omega d\Omega} = \frac{e^2}{m_e^2} |\epsilon \cdot \epsilon'|^2 \left(\frac{\omega_{out}}{\omega_{in}}\right) \frac{q(\rho(\omega)+1)A}{\pi} \text{Im} F_w(q, k_z, \omega) \quad (5.35)$$

where

$$F_w(q, k_z, \omega) = \frac{V(q)}{D_w(q, k_z, \omega)} \times$$

$$[ Q(1-V^{ee}B)g^{ee} + \alpha^2 B(1-V^{hh}Q)g^{hh} - \alpha QB(V^{eh} + V^{eh*})g^{eh} ] \quad (5.36)$$

In Eq.(5.36) the "dielectric function" is given as,

$$D_w(q, k_z, \omega) = 1 - V^{ee}Q(q, \omega) - V^{hh}B(q, \omega)$$

$$+ Q(q, \omega) B(q, \omega) (V^{ee} V^{hh} - V^{eh} V^{he}) \quad (5.37)$$

The quantities  $V^{ss}$  is defined as following:

$$V^{ee} = V_q [ f_0^{ee} + (S-1) f_1^{ee} ] \quad (5.38)$$

$$V^{hh} = V_q [ f_0^{hh} + (S-1) f_1^{hh} ] \quad (5.39)$$

and

$$V^{eh} = V_q S f^{eh} \quad (5.40)$$

with

$$f_1^{ee} = \left( \frac{2}{qd_e} \right)^2 \sinh^2 \left( \frac{qd_e}{2} \right) \left[ 1 + \left( \frac{qd_e}{2\pi} \right)^2 \right]^{-2} \quad (5.41)$$

$$f_0^{ee} = \left( \frac{2}{qd_e} \left( 1 + \frac{\left( \frac{qd_e}{2\pi} \right)^2}{2 \left( 1 + \left( \frac{qd_e}{2\pi} \right)^2 \right)} \right) - \frac{2}{(qd_e)^2} \frac{(1 - e^{-qd_e})}{\left[ 1 + \left( \frac{qd_e}{2\pi} \right)^2 \right]^2} \right) \quad (5.42)$$

and

$$f^{eh} = \left( \frac{2}{qd_e} \right) \frac{\sinh \left( \frac{qd_e}{2} \right)}{1 + \left( \frac{qd_e}{2\pi} \right)^2} \left( \frac{2}{qd_h} \right) \frac{\sinh \left( \frac{qd_h}{2} \right)}{1 + \left( \frac{qd_h}{2\pi} \right)^2} \quad (5.43)$$

From our result we can that our previous result can be easily recovered by letting  $d_e \rightarrow 0$  and  $d_h \rightarrow 0$ . We would like to investigate some qualitative effect of finite width on our optical properties. To lowest order in  $qd$ ,  $f_1=1$  and  $f_0$  can be written as

$$f_0(qd) = 1 - 0.257(qd)$$

and

$$D_w(q, k_z, \omega) = D(q, k_z, \omega) + 0.257qV_q(Q_q(\omega)d_e + B_q(\omega)d_h) - V_q^2Q_q(\omega)B_q(\omega)0.257(d_e + d_h) \quad (5.44)$$

Therefore we obtain the shift in plasma frequency

$$\omega'_\pm = \omega_\pm - 0.128 [ \omega_{pe}^2(qd_e) + \omega_{ph}^2(qd_h) ] \mp 0.5 \frac{0.257q(d_e + d_h)(\omega_{pe}^2 - \omega_{ph}^2)^2 - \frac{0.771\omega_{pe}^2\omega_{ph}^2m_e m_h}{e^e n_e n_h} [d_e \frac{n_e^2}{m_e^3} - d_h \frac{n_h^2}{m_h^3}]}{(\omega_{pe}^2 + \omega_{ph}^2)^2 S^2 - 4\omega_{pe}^2\omega_{ph}^2[S^2 - |S|^2] - \frac{3Sqm_e m_h}{4e^2 n_e n_h} (\frac{n_e^2}{m_e^3} + \frac{n_h^2}{m_h^3})} \quad (5.45)$$

We found that effect of the width is to shift the resonance to a small frequency.

As we will see from our numerical work, this shift is rather small  $\frac{\Delta\omega}{\omega} \approx 2-3\%$ .

For Raman intensity, the change  $\text{Im} \frac{\Delta F}{F}$  can amount to 5-10%. Therefore we can conclude that there is no qualitative effect on Raman intensity.

### 5.5. Discussion

All the above analytical results for the resonance frequencies are limited for small range of parameters. We have calculated and plotted the dispersion curves for arbitrary values of  $qa, qb$  and  $k_z a$ . For  $a=2b$  and  $\alpha=0.87$  for InAs-GaSb system (Fig.5.1), we obtain two acoustic-like high-frequency modes. When  $q > 0.3k_{Fe}$ , one of the mode drops into the single particle excitation regime. We may note that we have  $\omega_-$  mode at the separation  $b$  smaller than the critical separation defined in Eq.(21). This is because Eq.(5.21) is valid only under the condition  $qa, qb \ll 1$  which is not accurate here. In Fig.5.2, we plot the dispersion curves for case of  $\alpha=0.2$ . The lower solid curve represents the ion acoustic wave.

The intensity of the Raman-scattered light as a function of its energy loss for a fixed value of in-plane momentum exchange  $q$  is given by the imaginary part of  $F(q, k_z, \omega)$  given in Eq.(5.11).  $k_z$  is the z-component of the wave vector of photon inside the LEG, a negligible quantity. In our Figs, we have plotted the dispersion curves and the Raman intensity for several different values of  $q$  and mass ratio. For small value of  $q$  ( i.e.,  $q < q_s$ , where  $q_s$  is the screening wave vector of the system ), the scattered light only exhibit the collective spectrum. If  $q$  is not small, we have scattering due to collective excitation as well as single particle excitation. If we decrease the value of the hole mass, the plasmon frequency will shift upward as expected.

We have calculated the cross-section from Eq.(5.10). An exact expression for 2D polarization function has been given by Stern<sup>[30]</sup> for infinite electron relaxation time  $\tau$ . We use this result in our calculation. When the Landau damping is small, we introduce a phenomenological collision time  $\tau$  to account for the collisional damping from background impurities and phonon scattering. Using a realistic  $\tau$  [117], we compute the dimensionless quantity  $ImF(q, k_z, \omega)$ . In Fig.5.3, we plot this quantity as a function of frequency, the two resonant peaks are respectively at  $\omega_+$  and  $\omega_-$ . To relate our results to experiment, we also carried out the integration over each of the resonances and define

$$I(q, k_z, \omega_r) = \int_{\omega_r - \Delta}^{\omega_r + \Delta} ImF(q, k_z, \omega) \frac{d\omega}{4E_{Fe}} \quad (5.46)$$

which is the area under each resonant peak ( $\omega_r$  is the resonant frequency  $\omega_+$  or  $\omega_-$  ). The integrated cross-section can be written as;

$$\left( \frac{d\sigma}{d\Omega} \right)_{\omega_r} = \frac{4E_{Fe} e^2}{m_e^2} |\epsilon \cdot \epsilon'|^2 \left( \frac{\omega_{out}}{\omega_{in}} \right) \frac{q(\rho(\omega)+1)A}{\pi} I(q, k_z, \omega_r) \quad (5.47)$$

We have denoted these values of  $I(q, k_z, \omega_r)$  on our dispersion curves in Fig.5.1 to see their dependence on  $q$  and  $b$ . we found that  $I_+, I_-$  and the ratio  $\beta = \frac{I_+}{I_-}$  strongly depend on the in-plane momentum transfer  $q = |\vec{q}|$  and the separation  $b$ . We choose carrier surface density  $n = 3.77 \times 10^{11} \text{cm}^{-2}$ ,  $k_z = 0.45 \times 10^6 \text{cm}^{-1}$  and  $\alpha = 0.87$  for InAs-GaSb system and use  $a = 2b$ . For  $b$  smaller than 200Å the  $\omega_-$  mode is inside the regime of single particle excitation. For  $b = 300\text{Å}$ , most spectral weight is carried by the  $\omega_-$  mode and  $\beta$  is an increasing function of  $q$ . For  $b > 400\text{Å}$ , most spectral weight is carried by the  $\omega_+$  mode and in this case  $\beta$  is a decreasing function of  $q$ . The interesting case is at  $b = 350\text{Å}$ , in this case the spectral weight of  $\omega_+$  and  $\omega_-$  mode is about same and  $\beta$  is almost independent of  $q$ . We think this is the suitable case to observe the  $\omega_-$  mode in experiment. We conclude that  $\omega_-$  mode only appears when  $b > b_c$ , but most spectral weight will be carried by  $\omega_-$  mode for the separation slightly greater than  $b_c$ . For  $b$  is much large than  $b_c$ ,  $\omega_c$  is the plasma frequency of the holes. In Figs.5.2 and 5.4, we present results of similar investigation for the ion acoustic mode. Here the ion acoustic mode described by the resonance at  $\omega_A$  will appear for small separation  $b$ , together with the plasma mode  $\omega_+$ . We found that the  $\omega_+$  mode usually carries more spectral weight than the  $\omega_A$  mode for the typical mass ratio of semiconductors. We found that for  $b = 80\text{Å}$  and  $q = 0.1k_{Fe}$ ,  $I_A$  is very close to  $I_+$ . In Fig.5.4 we see that the peak of  $\text{Im}F(q, k_z, \omega)$  at  $\omega_A$  is even high than that at  $\omega_+$ , but the width of  $\omega_A$  mode is narrow compared to the width of  $\omega_+$  mode. For  $b$  is increased to 120Å the spectral weight of  $\omega_+$  mode increases and spectral weight of  $\omega_A$  mode decreases

since  $\omega_A$  mode is important only at small separations.

From our Figs.(5.1-5.4) we find that light scattering can provide us with experimental verification of the modes of electron-hole superlattice systems. As for the case of the two-dimensional electron-hole systems, depending on the electron-hole separation, we obtain either the high frequency acoustic mode  $\omega_-$  or the usual ion-acoustic mode  $\omega_A$ . The plasma mode,  $\omega_+$ , always exist regardless of the electron-hole separation. The advantage of scattering experiments using superlattices is that the relative intensity of the plasmon versus the acoustic mode depends strongly on  $b$ , the separation parameter. Thus it would be possible to verify the dispersion relation of  $\omega_-$  or  $\omega_A$ . In contrast for the 2D electron-hole systems most of the intensity seems to reside in the plasma ( $\omega_+$ ) mode.

In Figs.(5.5-5.7), we plot the Raman intensity for several different widths of the wave function. As analytically estimated, the finite width gives an increase in scattering cross-section. This is because the width increases the electron-electron hole-hole and electron-hole interaction. In Fig.(5.8), we show the Raman intensity of ion-acoustic mode at low frequencies, we found that the effect of the width is even small compared to that of high frequency modes.

In conclusion we have calculated the Raman intensity for electron-hole layered structure. The regimes for different modes to exist are obtained, and our calculations and plots for the spectral intensity indicate that the  $\omega_-$  and the  $\omega_A$  modes can be observed experimentally.

## Appendix 5A

It has been shown that for multi-component system, the ratio of  $P \cdot A$  and  $A^2$  contribution to the light scattering matrix element is<sup>13</sup>

$$\frac{M_{P \cdot A}}{M_{A^2}} \approx \frac{\omega_{in}}{mc^2} \ll 1 \quad (5A1)$$

Therefore in our calculation we only consider the  $A^2$  contribution. The matrix element of light scattering is

$$M = \langle I | H_{\gamma} | F \rangle \quad (5A2)$$

where  $I, F$  refer to initial and final states and  $H_{\gamma} = \frac{e^2}{2} \sum_{s,j} \frac{A^2}{m_s} a_{\vec{p},j}(s) a_{\vec{p},j}(s)$ .

Using the property of delta-function-like carrier density in a plane and by standard calculation, we obtain

$$M = \frac{2\pi e^2}{\sqrt{\omega_{in} \omega_{out}}} \sum_{j,s} \frac{e^{ik_z ja}}{m_s} \langle I | n_{j,s}(\vec{q}) | F \rangle \quad (5A3)$$

where  $n_{j,s}(\vec{q}) = \sum_i e^{i\vec{q} \cdot \vec{r}_i(j,s)}$  and  $\vec{r}_i(j,s)$  is the coordinate of  $i$ th electron of  $s$ th component on  $j$ th cell. Now the cross-section can be written as:

$$\frac{d\sigma}{d\omega d\Omega} = e^4 \left( \frac{\omega_{out}}{\omega_{in}} \right) (\epsilon \cdot \epsilon')^2 \sum_F \left| \sum_{j,s} \frac{e^{ik_z ja}}{m_s} \langle I | n_{j,s}(\vec{q}) | F \rangle \right|^2 \delta(E_F - E_I - \omega) \quad (5A4)$$

where  $E_F, E_I$  are energies of initial and final states. By using the identity

$$\delta(E_F - E_I - \omega) = \int_{-\infty}^{\infty} dt e^{i(E_F - E_I - \omega)t} \quad (5A5)$$

We finally obtain

$$\frac{d \sigma}{d \omega d \Omega} = e^4 \left( \frac{\omega_{out}}{\omega_{in}} \right) (\epsilon \cdot \epsilon')^2 \sum_{j,j'} \sum_{s,s'} \frac{e^{i k_z (j-j') a}}{m_s m_{s'}} S_{j,j'}^{s,s'}(\vec{q}, \omega) \quad (5A6)$$

with

$$S_{j,j'}^{s,s'}(q, \omega) = \int_{-\infty}^{\infty} dt e^{i \omega t} \int d\vec{r} d\vec{r}' e^{-i \vec{q} \cdot (\vec{r} - \vec{r}')} \langle n_{j,s}(\vec{r}, t) n_{j',s'}(\vec{r}') \rangle \quad (5A7)$$

In Eq.(5A7),  $\vec{q}, \vec{r}'$  are two dimensional vectors in a plane.

## Appendix 5B

We substitute Eq.(5.9) in Eq.(5.6) and obtain

$$\frac{d \sigma}{d \omega d \Omega} = 2\pi A e^4 |\epsilon \cdot \epsilon'|^2 \left( \frac{\omega_{out}}{\omega_{in}} \right) \frac{\rho(\omega) + 1}{\pi} \times$$

$$\text{Im} \left[ \frac{\Pi_{ee}(k_z)}{m_e^2} + \frac{\Pi_{hh}(k_z)}{m_h^2} + \frac{\Pi_{eh}(k_z)}{m_e m_h} + \frac{\Pi_{he}(k_z)}{m_e m_h} \right] \quad (5B1)$$

To obtain the quantities  $\Pi_{ee}(k_z)$ ,  $\Pi_{hh}(k_z)$ ,  $\Pi_{eh}(k_z)$ ,  $\Pi_{he}(k_z)$ , we take Fourier transformation of Eq.(5.8) and have following coupled equations:

$$\Pi_{ee}(k_z) = Q + Q [S V \Pi_{ee}(k_z) - S' V \Pi_{he}(k_z)] \quad (5B2)$$

$$\Pi_{he}(k_z) = B [-S^* V \Pi_{ee}(k_z) + S V \Pi_{he}(k_z)] \quad (5B3)$$

$$\Pi_{hh}(k_z) = Q + Q [S V \Pi_{hh}(k_z) - S^* V \Pi_{eh}(k_z)] \quad (5B4)$$

$$\Pi_{eh}(k_z) = B [-S' V \Pi_{hh}(k_z) + S V \Pi_{eh}(k_z)] \quad (5B5)$$

In Eqs.(5B2-5B5), the quantities  $V, S, S', Q, B, D$  are all defined in the text. The solutions for Eqs.(5B2-5B5) are

$$\Pi_{ee}(k_z) = Q (1 - S V B) D^{-1} \quad (5B6)$$

$$\Pi_{he}(k_z) = -Q B S^* D^{-1} \quad (5B7)$$

$$\Pi_{hh}(k_z) = B ( 1 - S V Q ) D^{-1} \quad (5B8)$$

$$\Pi_{eh}(k_z) = -Q B S' D^{-1} \quad (5B9)$$

Substitute Eqs(5B6-5B9) into Eq.(5B1), we obtain Eq.(5.10).

## Captions

FIG. 1.1. Schematic diagram for type-I superlattice and its energy diagram.

FIG. 1.2. Schematic diagram for type-II superlattice

FIG. 2.1. Plot of  $R(\Omega, r_s)$  as a function of normalized frequency  $\Omega$  where  $r_s = 2^{1/2}$ ,  $d=0.0$ ,  $k_F = 2.5 \times 10^6 \text{cm}^{-1}$  and  $b=0.05 \times 10^{-6} \text{cm}$ . Discrete points denote single-layer case, solid lines represent superlattice cases. (a)  $a=2.5b$ . (b)  $a=3b$ . (c)  $a=6b$ . (d)  $a=10b$ . We notice that if  $\Omega$  is greater than 2, the value for single layer is almost same as the value of superlattice with  $a=10b$ .

FIG. 2.2. Plot of  $R(\Omega, r_s)$  as a function of normalized frequency  $\Omega$  where  $r_s = 2^{1/2}$ ,  $k_F = 2.5 \times 10^6 \text{cm}^{-1}$ ,  $a = 0.15 \times 10^{-6} \text{cm}$  and  $b=0.05 \times 10^{-6} \text{cm}$ . upper curve— $d = 0.09 \times 10^{-6} \text{cm}$ , lower curve— $d = 0.0$ .

FIG. 2.3. Plot of  $R(\Omega, r_s)$  as a function of normalized frequency  $\Omega$  where  $r_s = 2^{1/2}$ ,  $k_F = 2.5 \times 10^6 \text{cm}^{-1}$ ,  $a = 1.0 \times 10^{-6} \text{cm}$  and  $b=0.5 \times 10^{-6} \text{cm}$ . upper curve— $d = 0.6 \times 10^{-6} \text{cm}$ , middle curve— $d = 0.3 \times 10^{-6} \text{cm}$ , lower curve— $d = 0.0$ .

FIG. 2.4. Plot of  $R(\Omega, r_s)$  as a function of normalized frequency  $\Omega$  where  $r_s = 2^{1/2}$ ,  $k_F = 2.5 \times 10^6 \text{cm}^{-1}$ ,  $a = 0.5 \times 10^{-6} \text{cm}$  and  $b=0.25 \times 10^{-6} \text{cm}$ . upper curve— $d = 0.3 \times 10^{-6} \text{cm}$ , middle curve— $d = 0.15 \times 10^{-6} \text{cm}$ , lower curve— $d = 0.0$ .

FIG. 2.5. plasmon dispersion relation for type-I superlattice. where  $r_s = 2^{1/2}$ ,  $k_z = 0.5k_F$ ,  $k_F = 2.5 \times 10^6 \text{cm}^{-1}$ ,  $a = 0.5 \times 10^{-6} \text{cm}$  and  $b=0.25 \times 10^{-6} \text{cm}$ . upper curve— $d = 0.05 \times 10^{-6} \text{cm}$ , middle curve— $d = 0.20 \times 10^{-6} \text{cm}$ , lower curve— $d = 0.35 \times 10^{-6} \text{cm}$ .

FIG. 3.1. The class of diagrams which contribute the high-frequency conductivity of a multi-component system

FIG. 3.2. Integral equation for self-consistent fields.

FIG. 3.3. Plot of  $1.125e^2 R(\Omega, r_s)$  as a function of normalized frequency  $\Omega$  at low frequencies, where  $r_s = 2^{1/2}$ ,  $k_F = 2.5 \times 10^6 \text{cm}^{-1}$ ,  $b=0.7 \times 10^{-6} \text{cm}$  and  $a = 1.4 \times 10^{-6} \text{cm}$ .  $\frac{m_h}{m_e} = 1.1$ . (a)  $\Theta=0.0$ , (b)  $\Theta=0.03$ , (c)  $\Theta=0.05$ , (d)  $\Theta=0.08$ .

FIG. 3.4. Plot of  $1.125e^2R(\Omega r_s)$  as a function of normalized frequency  $\Omega$  where  $r_s = 2^{1/2}$ ,  $k_F = 2.5 \times 10^6 \text{cm}^{-1}$ ,  $b = 0.7 \times 10^{-6} \text{cm}$  and  $a = 2.0 \times 10^{-6} \text{cm}$ .  $\alpha = \frac{m_h}{m_e}$ . (a)  $\alpha = 1.1$ , (b)  $\alpha = 5.0$ , (c)  $\alpha = 10.0$ , (d)  $\alpha = 20.0$ , (e)  $\alpha = 100.0$ .

FIG. 3.5. Plot of  $1.125e^2R(\Omega r_s)$  as a function of normalized frequency  $\Omega$  where  $r_s = 2^{1/2}$ ,  $k_F = 2.5 \times 10^6 \text{cm}^{-1}$ ,  $b = 0.7 \times 10^{-6} \text{cm}$  and  $\alpha = 1.1$ . (a)  $a = 1.4 \times 10^{-6} \text{cm}$ , (b)  $a = 2.0 \times 10^{-6} \text{cm}$ , (c)  $a = 4.0 \times 10^{-6} \text{cm}$ .

FIG. 3.6. The Contour of integration used in Eq.(3.52).

FIG. 4.1. (a-e).The class of diagrams which contribute the high-frequency conductivity of electron-LO phonon system (f). Effective interaction for electron LO phonon system.

FIG. 4.2. Plot of  $\text{Re}(\sigma)$  (a) and  $\tau^{-1}$  (b) as a function of normalized frequency  $\Omega$  for GaAs-GaAlAs, where  $n_s = 3.6 \times 10^{11} \text{cm}^{-2}$ ,  $\delta = 0.004 E_F$  and  $a = 0.5 \times 10^{-6} \text{cm}$ . a, bare phonon scattering, b, coupled mode scattering.

FIG. 4.3. Plot of  $\text{Re}(\sigma)$  (a) and  $\tau^{-1}$  (b) as a function of normalized frequency  $\Omega$  for PbTe-PbEuTeSe, where  $n_s = 3.6 \times 10^{11} \text{cm}^{-2}$ ,  $\delta = 0.01 E_F$  and  $a = 0.5 \times 10^{-6} \text{cm}$ . a, bare phonon scattering, b, coupled mode scattering.

FIG. 4.4. Plot of  $\text{Re}(\sigma)$  (a) and  $\tau^{-1}$  (b) as a function of normalized frequency  $\Omega$  for PbTe-PbEuTeSe, a,  $n_s = 3.6 \times 10^{11} \text{cm}^{-2}$ ,  $\delta = 0.01 E_F$  and  $a = 0.5 \times 10^{-6} \text{cm}$ . b,  $n_s = 7.6 \times 10^{11} \text{cm}^{-2}$ ,  $\delta = 0.01 E_F$  and  $a = 1.0 \times 10^{-6} \text{cm}$ . The x-coordinate is  $\frac{\omega}{4E_F}$  where  $E_F$  is the value calculated by using  $n_s = 3.6 \times 10^{11} \text{cm}^{-2}$ .

FIG. 4.5. Plot of  $\text{Re}(\sigma)$  (a) and  $\tau^{-1}$  (b) as a function of normalized frequency  $\Omega$  for PbTe-PbEuTeSe for three different temperatures, where  $n_s = 3.6 \times 10^{11} \text{cm}^{-2}$ ,  $\delta = 0.01 E_F$  and  $a = 0.5 \times 10^{-6} \text{cm}$ .

FIG. 5.1. Dispersion curves for two high-frequency modes  $\omega_+$  and  $\omega_-$ . Here  $k_z = 0.45 \times 10^6 \text{cm}^{-1}$ ,  $n = 3.77 \times 10^{11} \text{cm}^{-2}$ ,  $\alpha = 0.87$ ,  $a = 2b$ . The region below the upper dotted line is the region for single particle excitation of light mass particle, and the region below the lower dotted line is the region for single particle excitation of heavy mass particle. The number above the vertical bar is the value of  $I(q, k_z, w_r)$ . (a),  $b = 300 \text{A}$ , (b),  $b = 350 \text{A}$ , (c),  $b = 400 \text{A}$ , (d),  $b = 450 \text{A}$ .

FIG. 5.2. Dispersion curves for high-frequency and low-frequency modes  $\omega_+$  and  $\omega_A$ . Here  $k_z = 0.45 \times 10^6 \text{cm}^{-1}$ ,  $n = 3.77 \times 10^{11} \text{cm}^{-2}$ ,  $\alpha = 0.2$ ,  $a = 2b$ . The region below the upper dotted line is the region for single particle excitation of light mass particle, and the region below the lower dotted line is the region for single particle excitation of heavy mass particle. The number above the vertical bar is the value of  $I(q, k_z, w_r)$ . (a),  $b = 80 \text{A}$ , (b),  $b = 120 \text{A}$ .

FIG. 5.3. Plot of  $\text{Im} F(q, k_z, \omega)$  as a function of incoming photon energy, here  $q = 0.2k_{Fe}$ ,  $k_z = 0.45 \times 10^6 \text{cm}^{-1}$ ,  $n = 3.77 \times 10^{11} \text{cm}^{-2}$ ,  $\alpha = 0.87$ ,  $\nu = 0.025E_{Fe}$  and  $a = 2b$ .  $b = 350\text{\AA}$ .

FIG. 5.4. Plot of  $\text{Im} F(q, k_z, \omega)$  as a function of incoming photon energy, here  $q = 0.1k_{Fe}$ ,  $k_z = 0.45 \times 10^6 \text{cm}^{-1}$ ,  $n = 3.77 \times 10^{11} \text{cm}^{-2}$ ,  $\alpha = 0.2$ ,  $\nu = 0.025E_{Fe}$  and  $a = 2b$ .  $b = 80\text{\AA}$ .

FIG. 5.5. Plot of  $\text{Im} F(q, k_z, \omega)$  as a function of incoming photon energy, here  $q = 0.2k_{Fe}$ ,  $k_z = 0.45 \times 10^6 \text{cm}^{-1}$ ,  $r_s = 0.1$ ,  $\alpha = 0.87$ ,  $\nu = 0.025E_{Fe}$  and  $a = 2b$ .  $b = 350\text{\AA}$ . From right to left  $d_e = 0.0, 1.0, 2.0 \times 10^{-6} \text{cm}$   $d_h = 0.8 * d_e$

FIG. 5.6. Plot of  $\text{Im} F(q, k_z, \omega)$  as a function of incoming photon energy, here  $q = 0.2k_{Fe}$ ,  $k_z = 0.45 \times 10^6 \text{cm}^{-1}$ ,  $r_s = 0.314$ ,  $\alpha = 0.87$ ,  $\nu = 0.025E_{Fe}$  and  $a = 2b$ .  $b = 350\text{\AA}$ . From right to left  $d_e = 0.0, 1.0, 2.0 \times 10^{-6} \text{cm}$   $d_h = 0.8 * d_e$

FIG. 5.7. Plot of  $\text{Im} F(q, k_z, \omega)$  as a function of incoming photon energy, here  $q = 0.2k_{Fe}$ ,  $k_z = 0.45 \times 10^6 \text{cm}^{-1}$ ,  $r_s = 0.314$ ,  $\alpha = 0.87$ ,  $\nu = 0.025E_{Fe}$  and  $a = 2b$ .  $b = 350\text{\AA}$ . From right to left  $d_e = 0.0, 0.5, 1.0 \times 10^{-6} \text{cm}$   $d_h = 0.8 * d_e$

FIG. 5.8. Plot of  $\text{Im} F(q, k_z, \omega)$  as a function of incoming photon energy, here  $q = 0.1k_{Fe}$ ,  $k_z = 0.45 \times 10^6 \text{cm}^{-1}$ ,  $n = 3.77 \times 10^{11} \text{cm}^{-2}$ ,  $\alpha = 0.2$ ,  $\nu = 0.025E_{Fe}$  and  $a = 2b$ .  $b = 80\text{\AA}$ . Three peaks from left to right corresponding to the case in which  $d_e = 0.0, 30\text{\AA}, 60\text{\AA}$  and  $d_h$  is chosen to be  $0.3d_e$ .

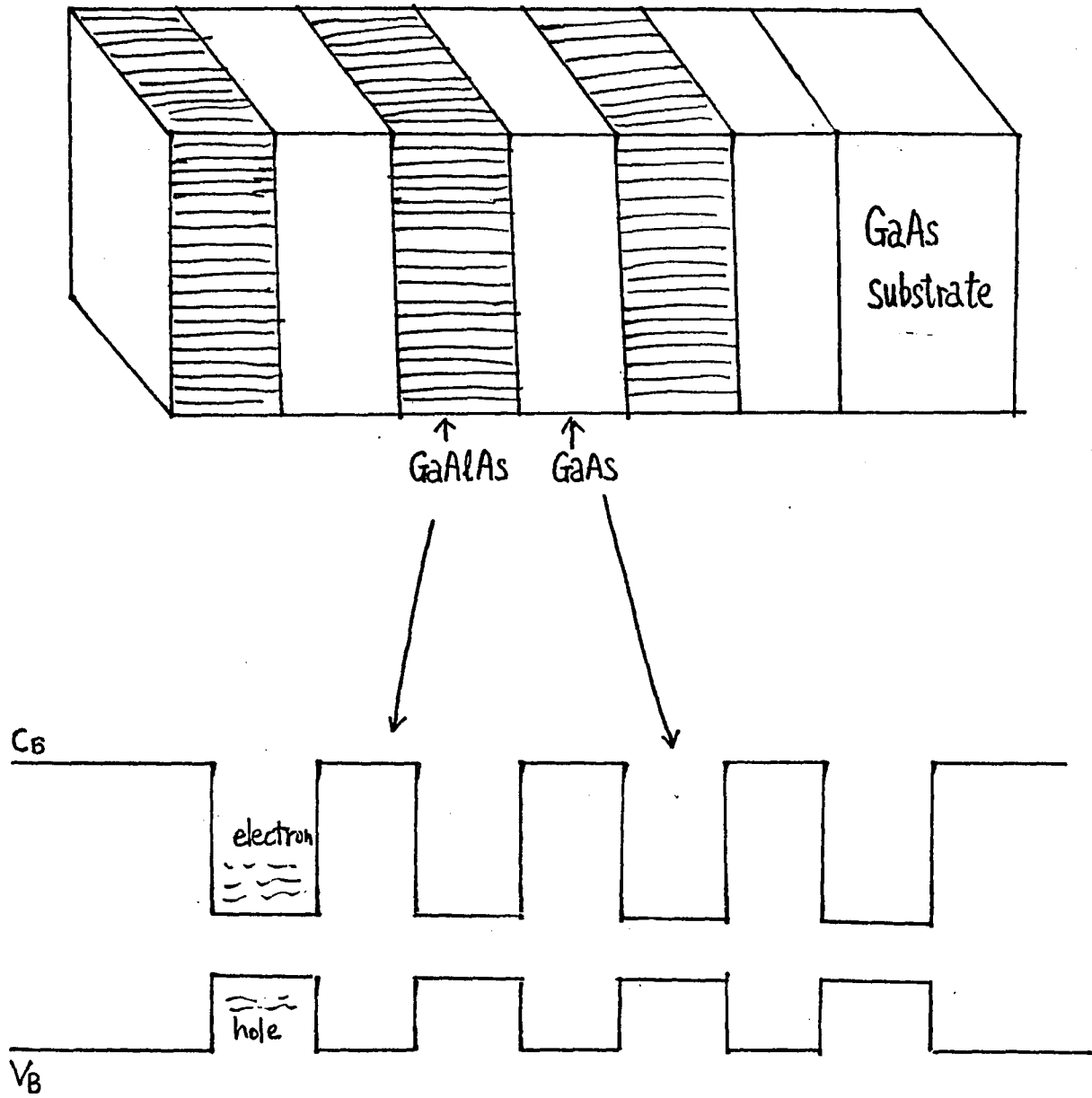


FIG. 1.1.

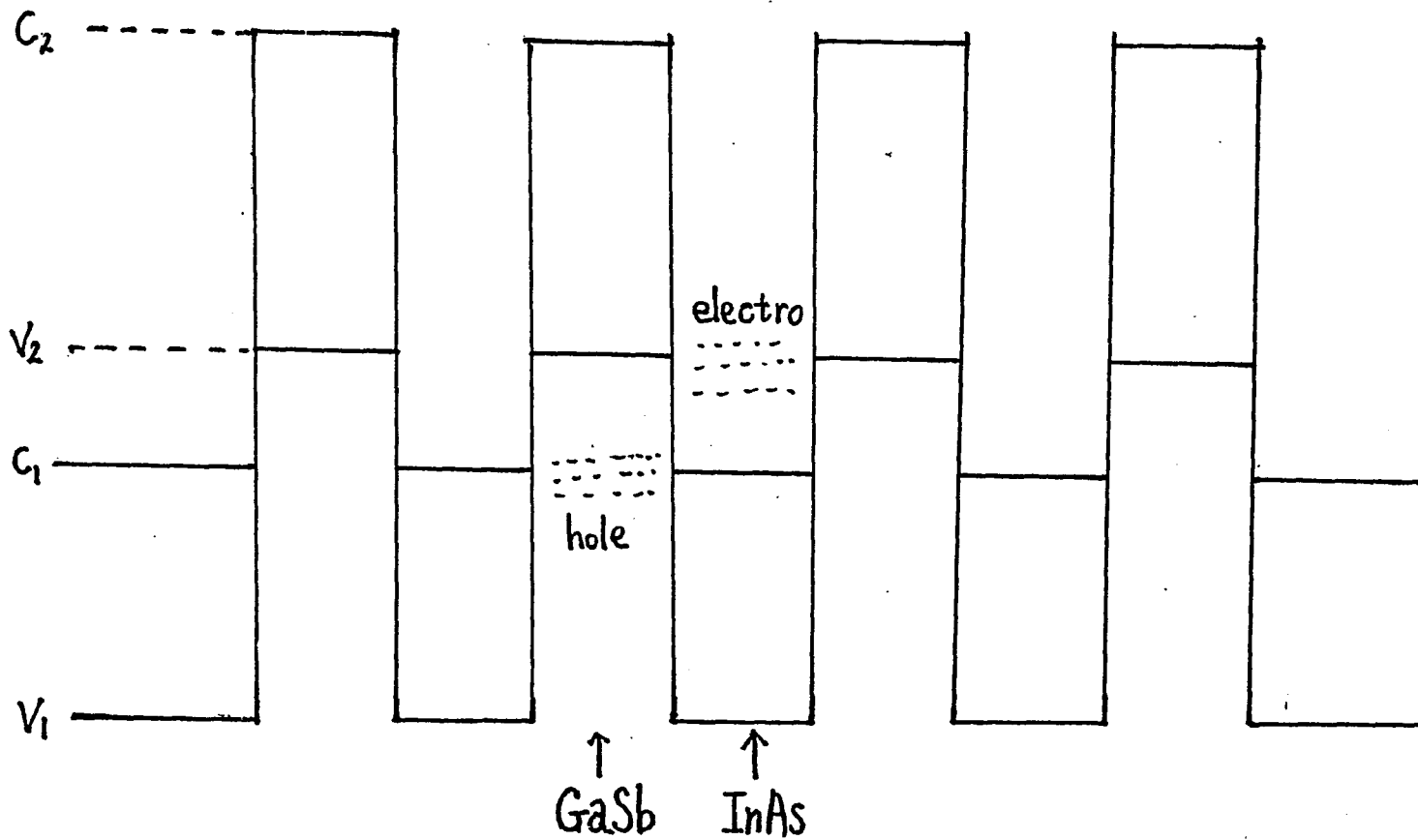


FIG. 1.2.

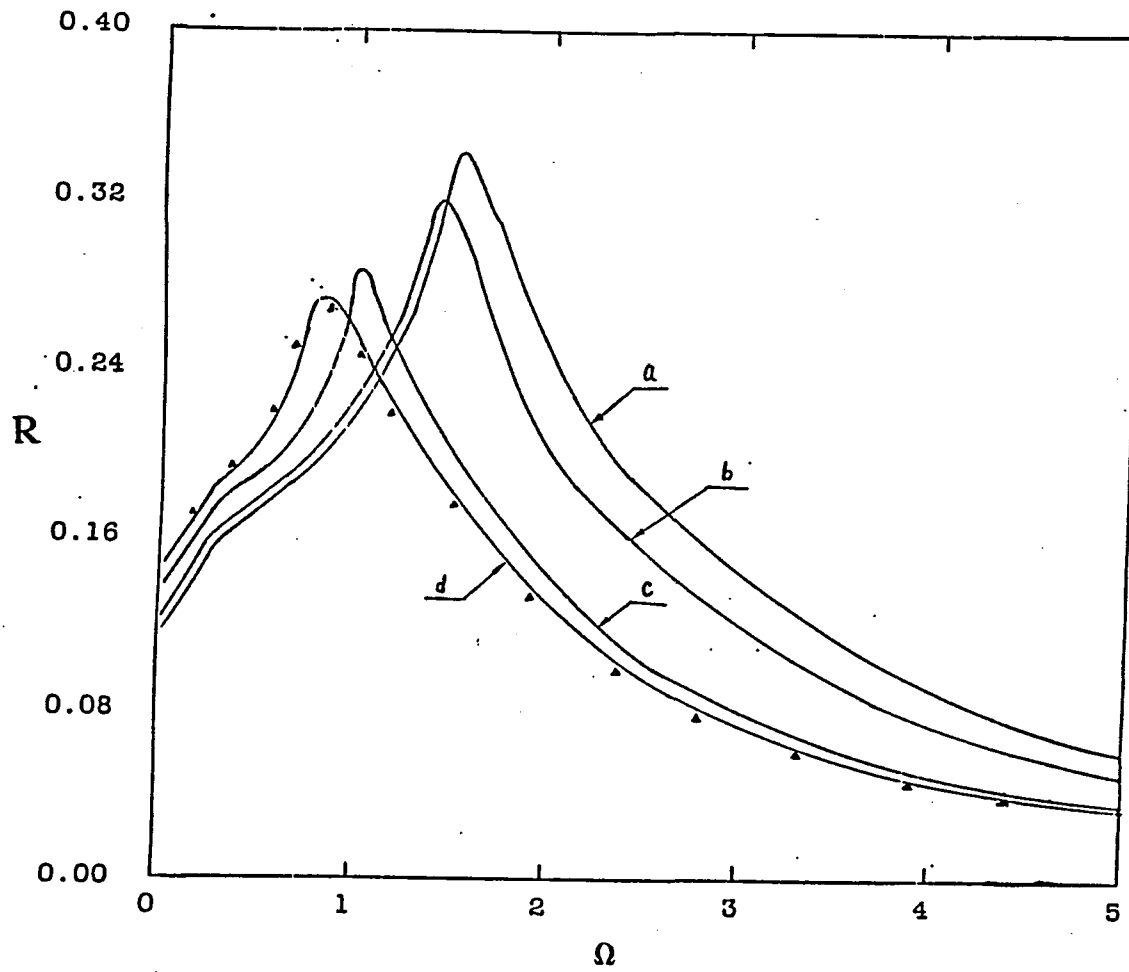


FIG. 21.

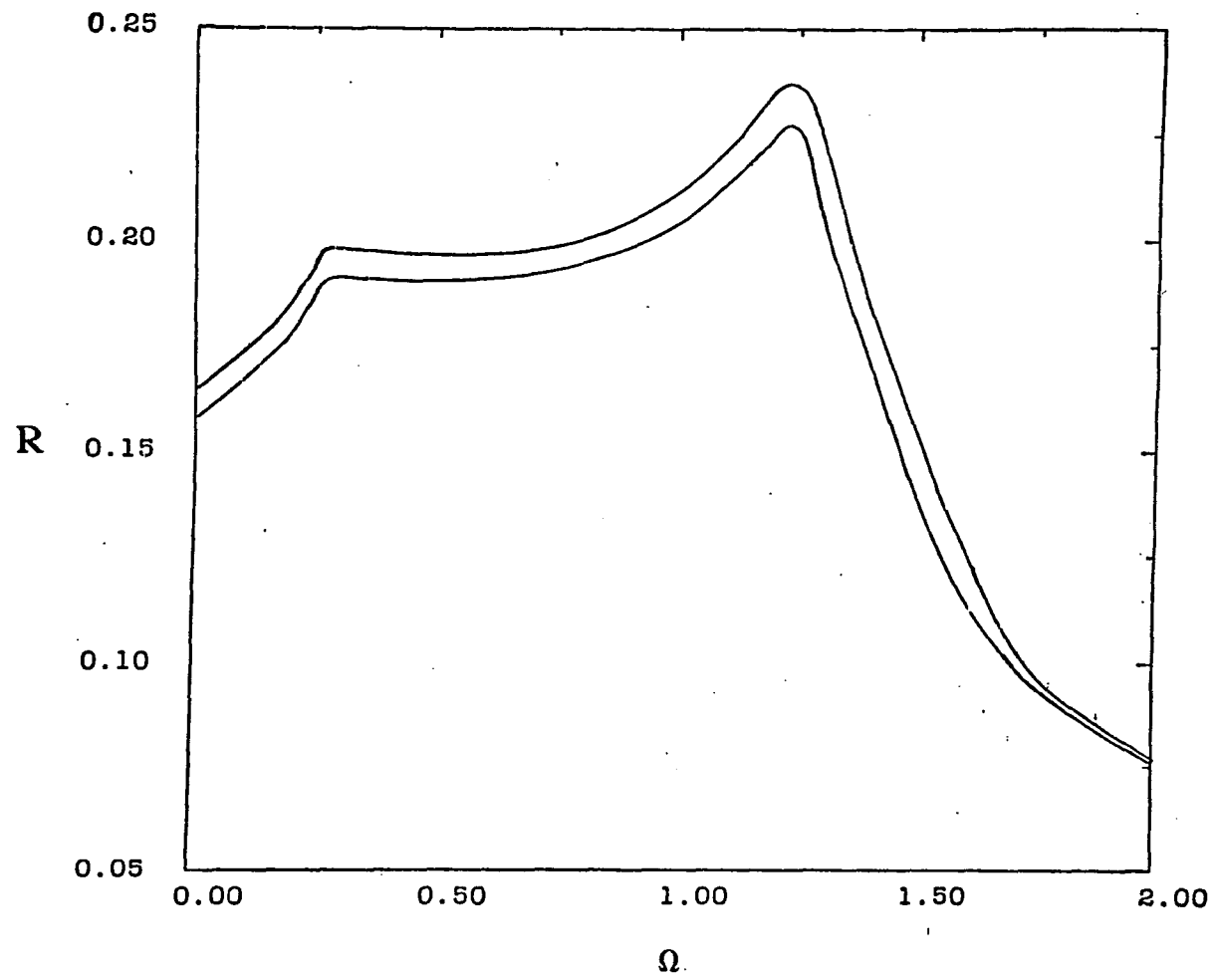


FIG. 22

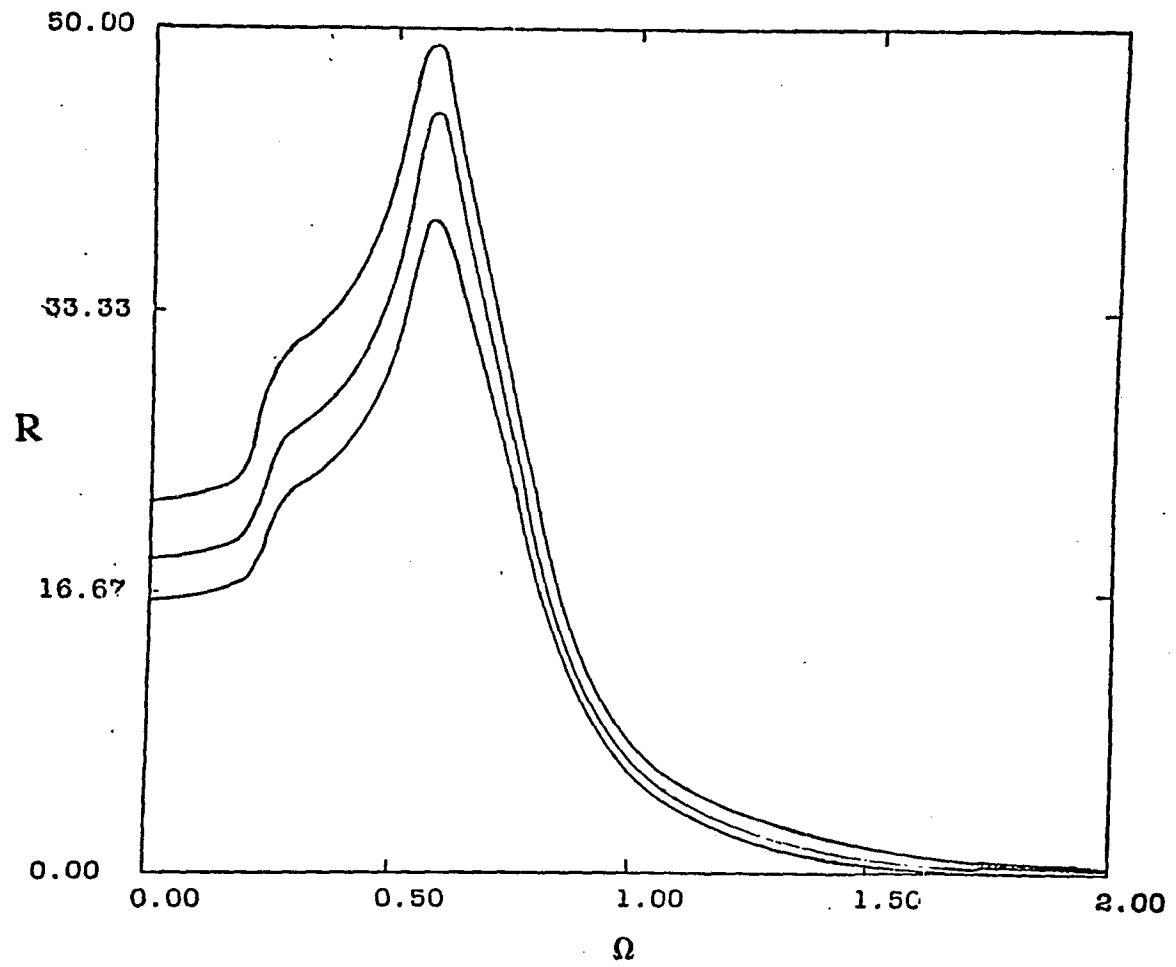


FIG. 23.

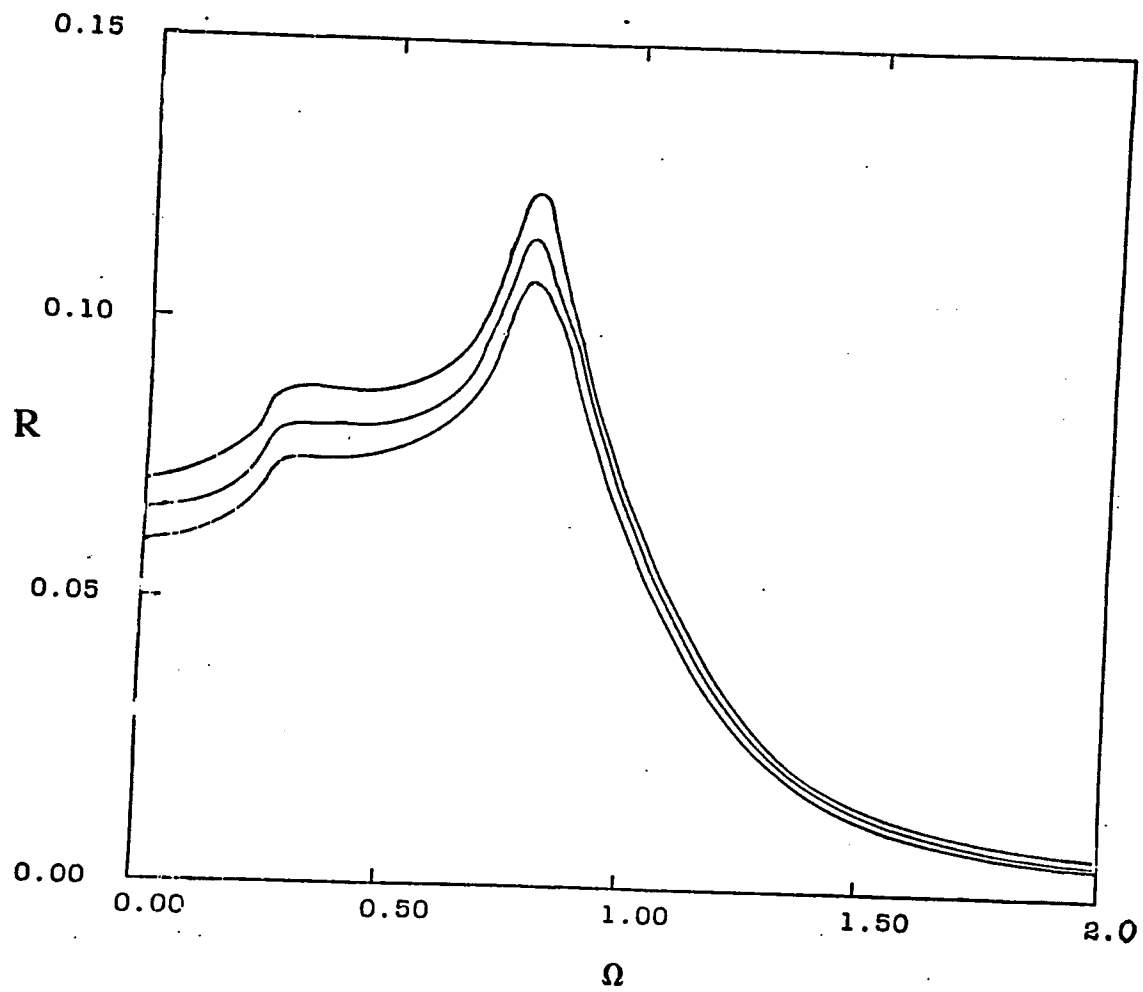


FIG. 24.

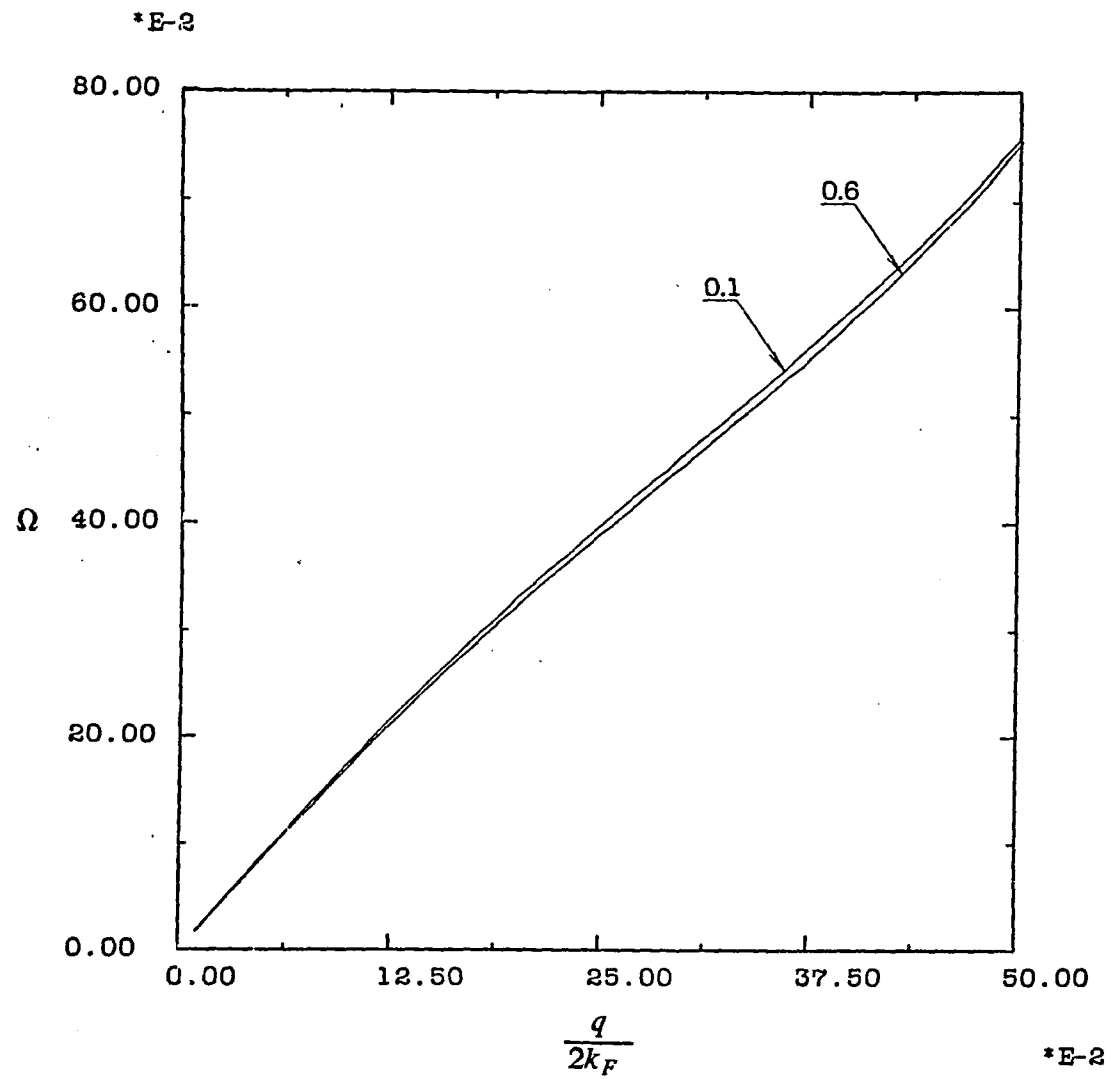


FIG. 25.

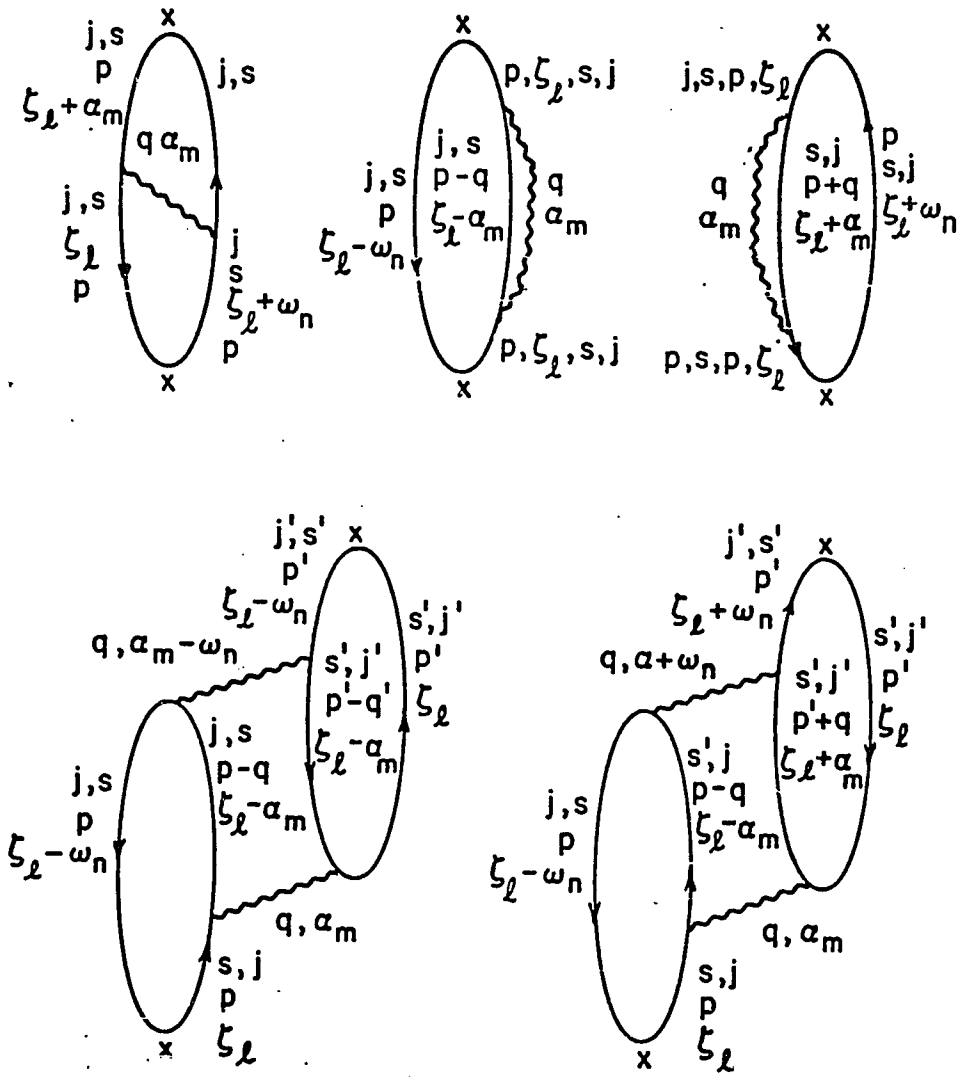


FIG. 3.1.

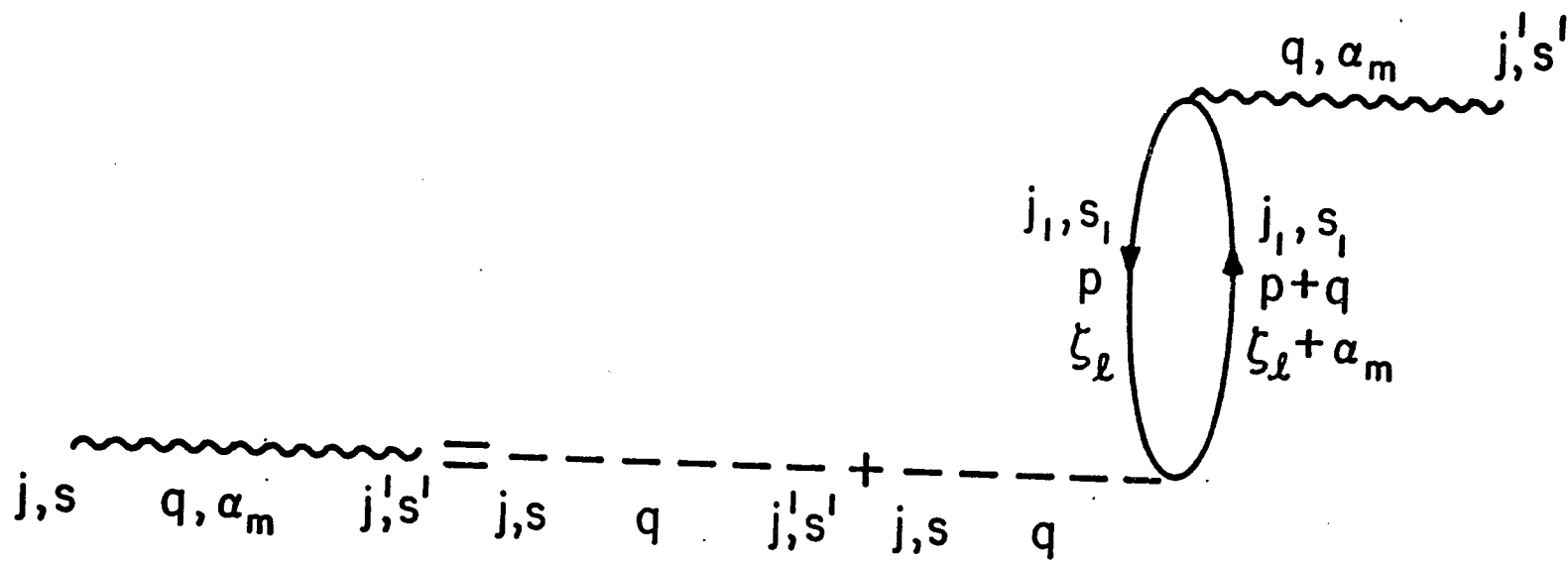


FIG. 3.2.

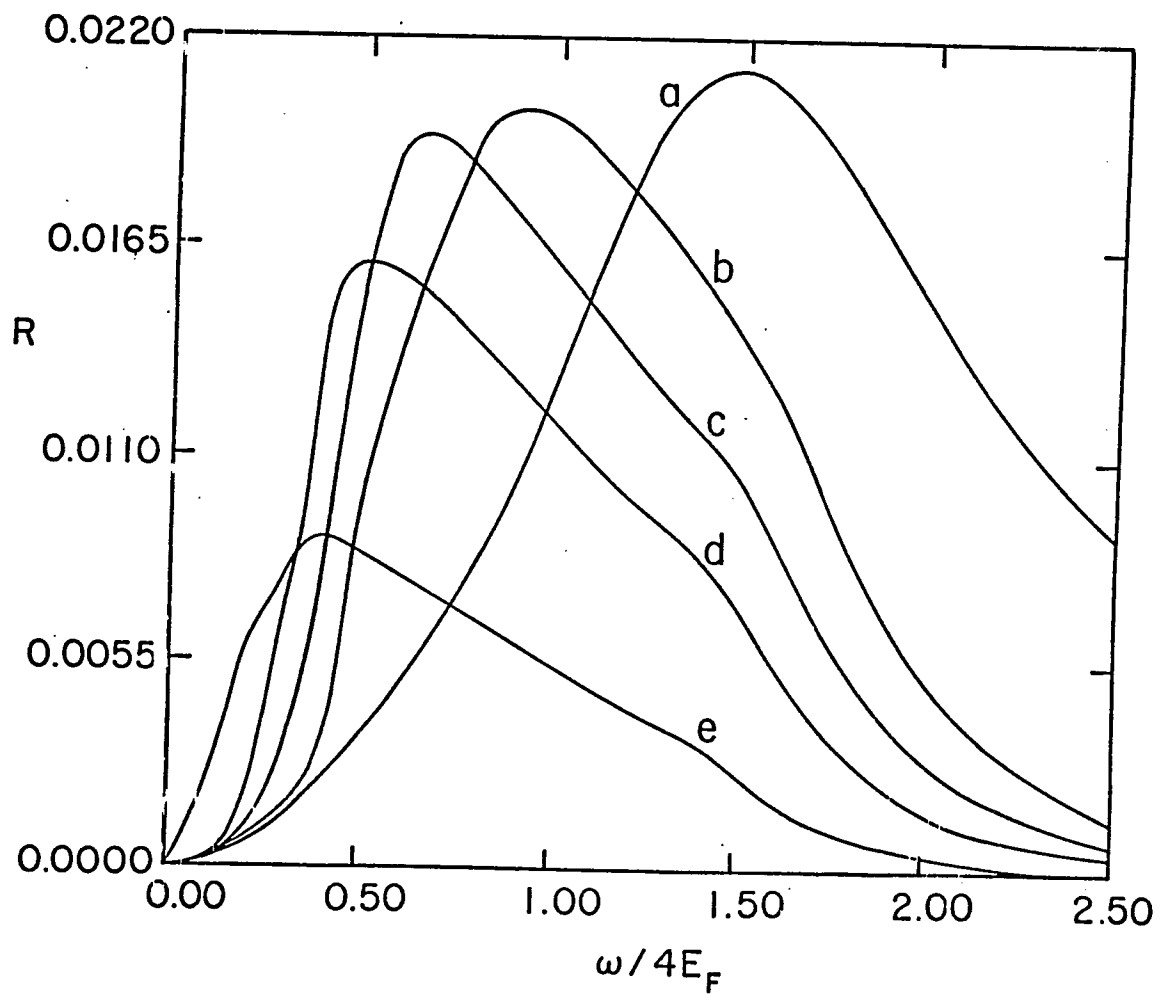


FIG. 3.3.

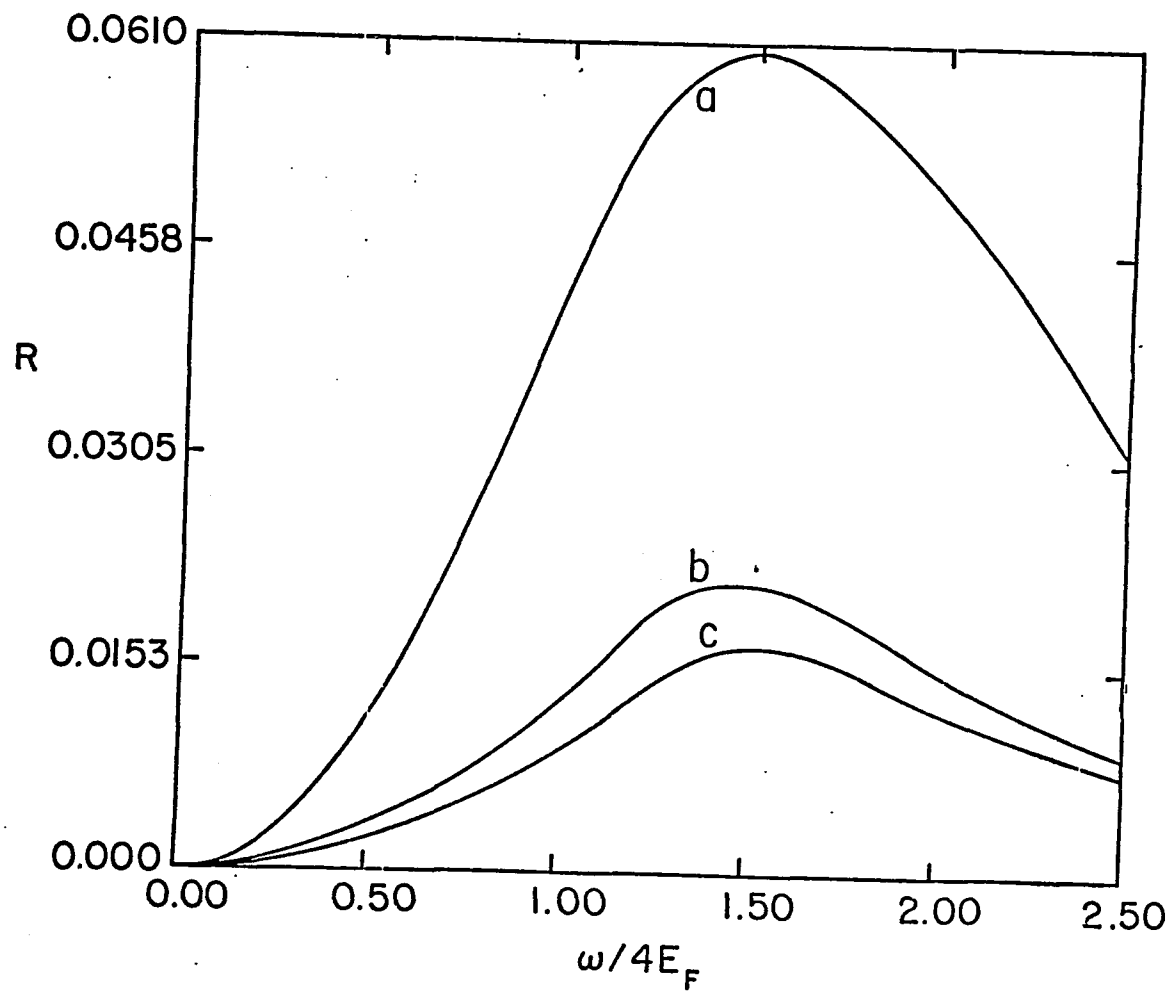


FIG. 3.4.

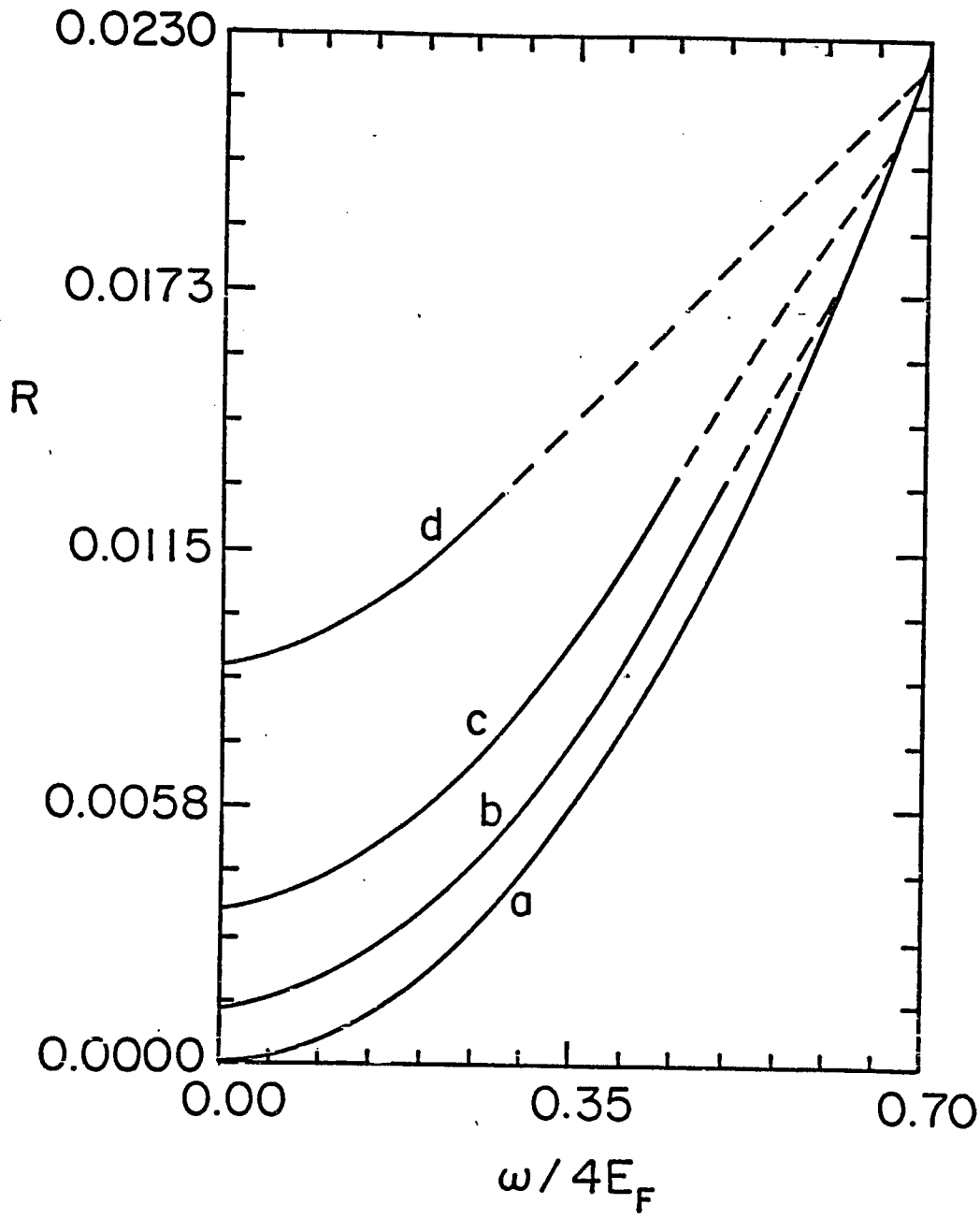


FIG. 3.5.

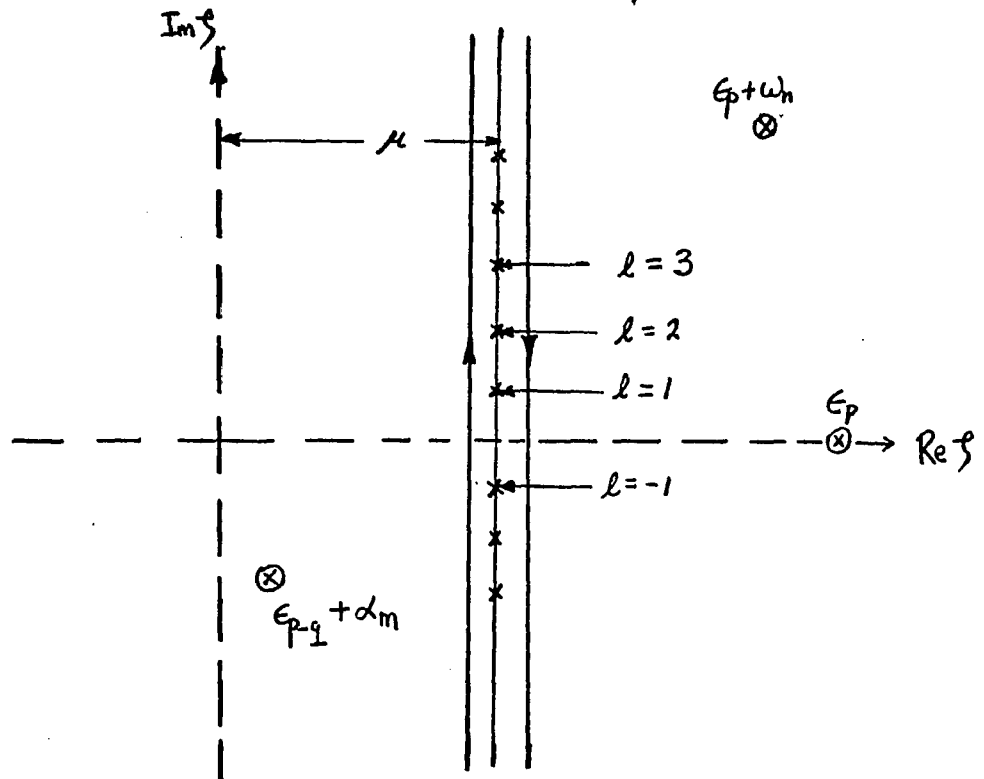


FIG. 3.6.



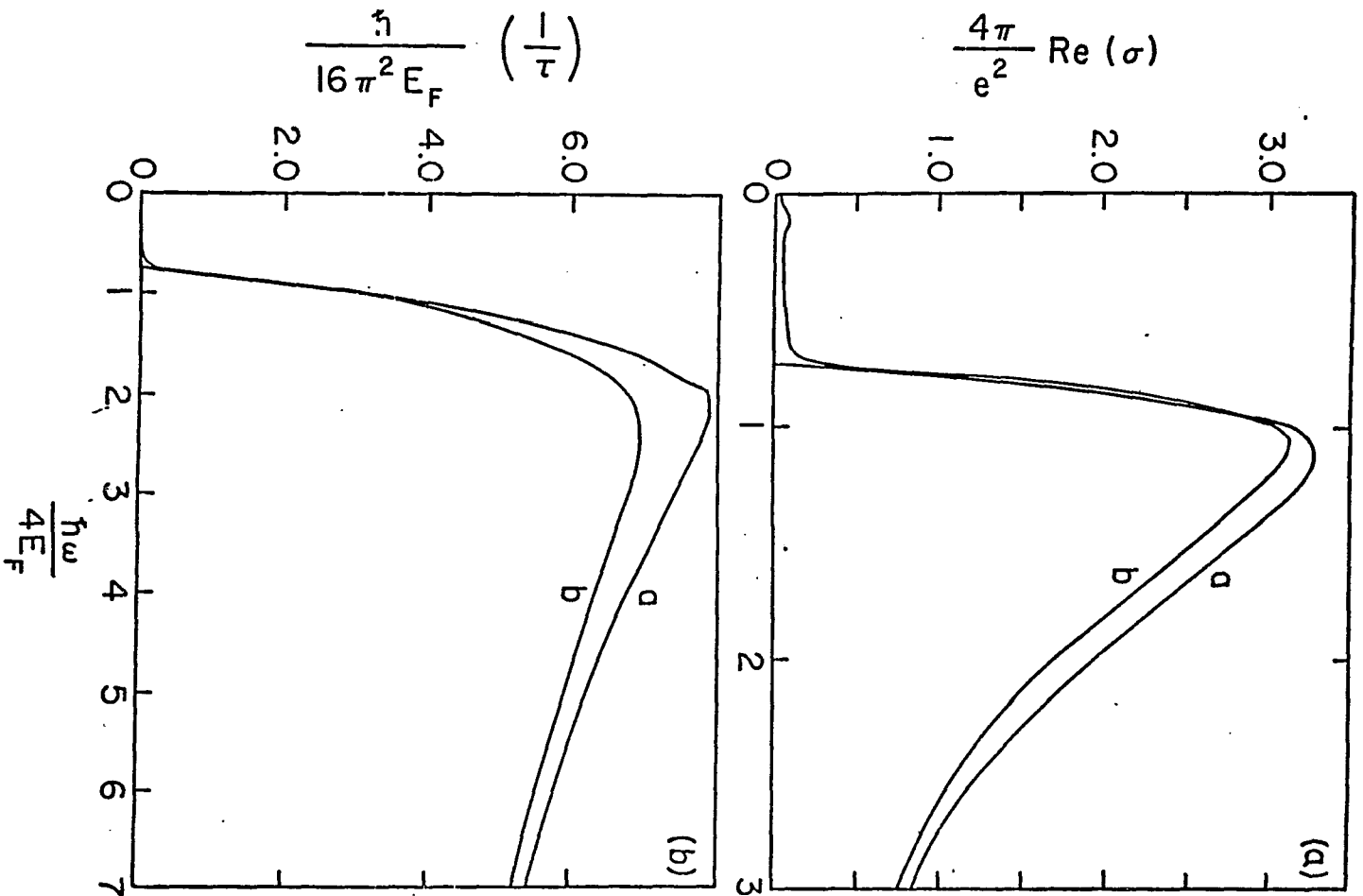


FIG. 4.2

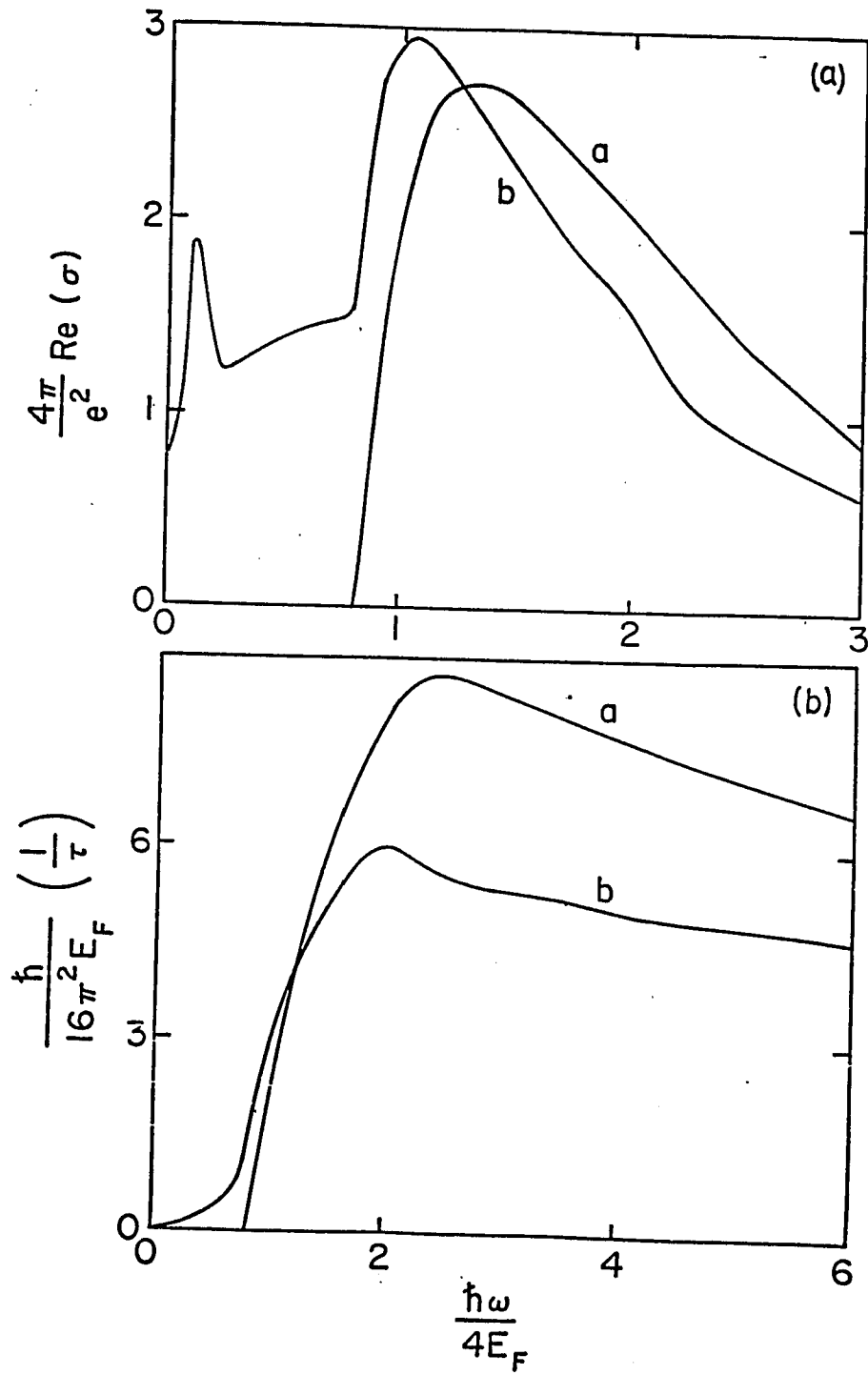


FIG. 4.3.

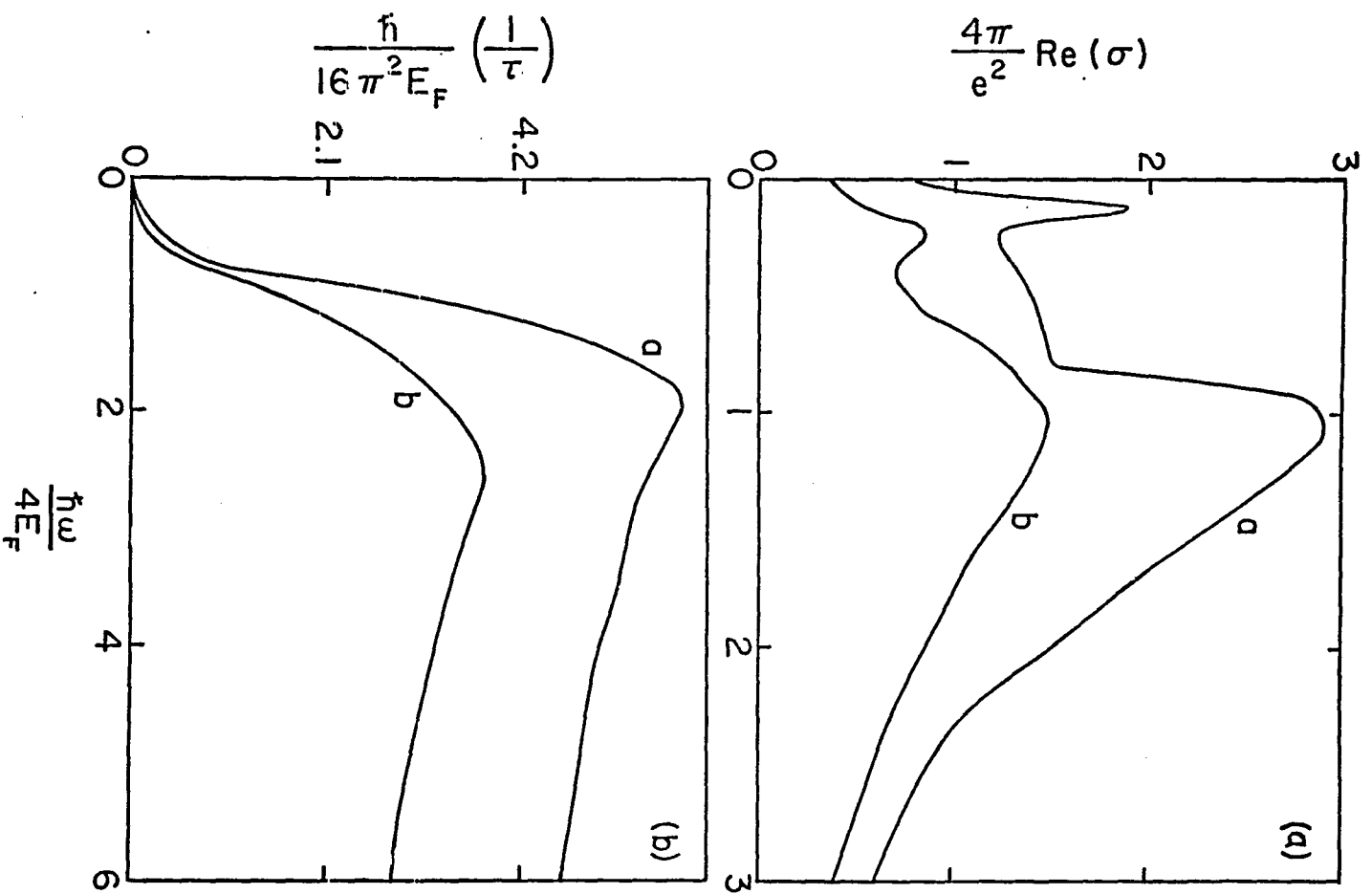


FIG. 4.4.

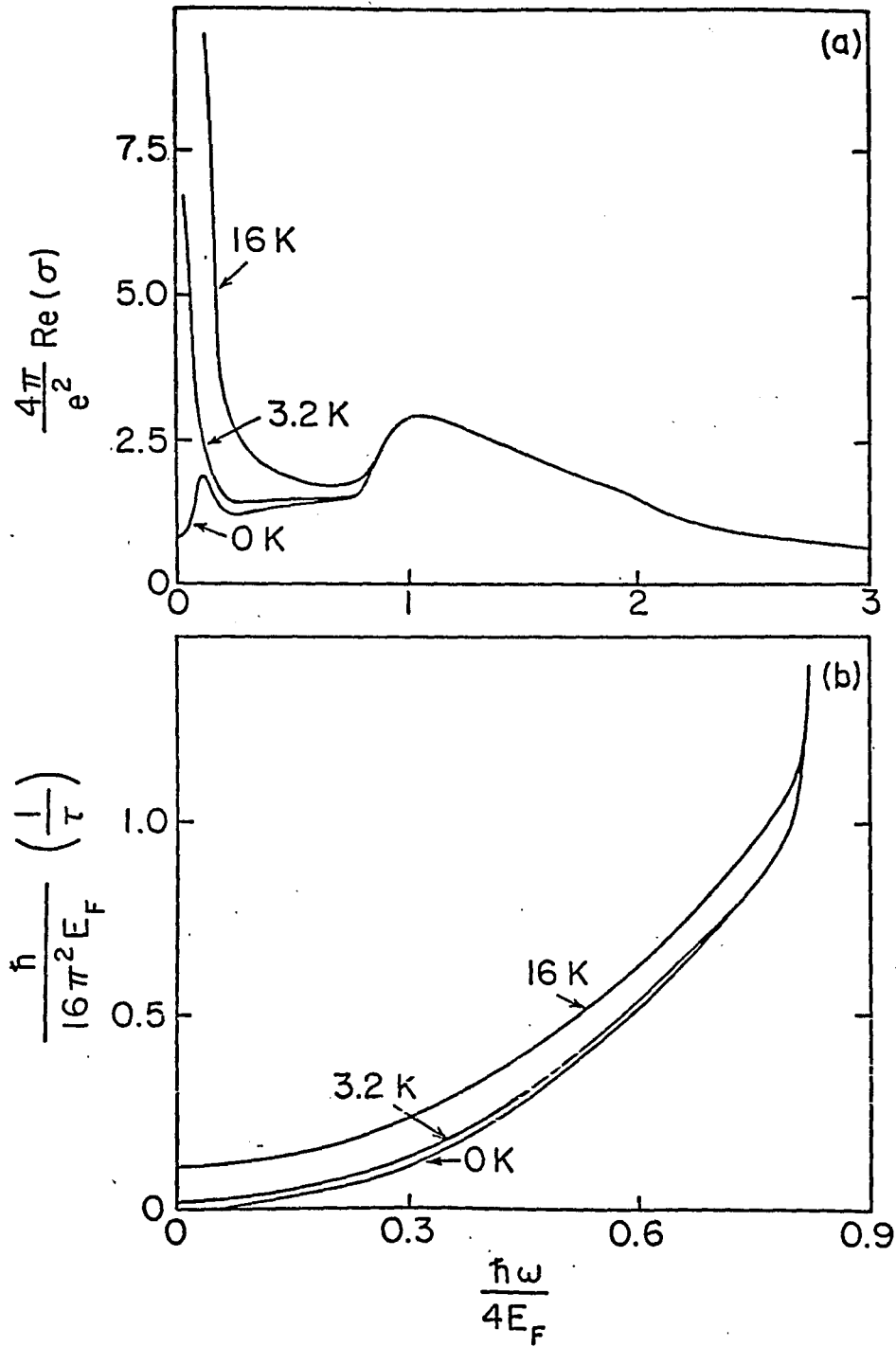


FIG. 4.5.

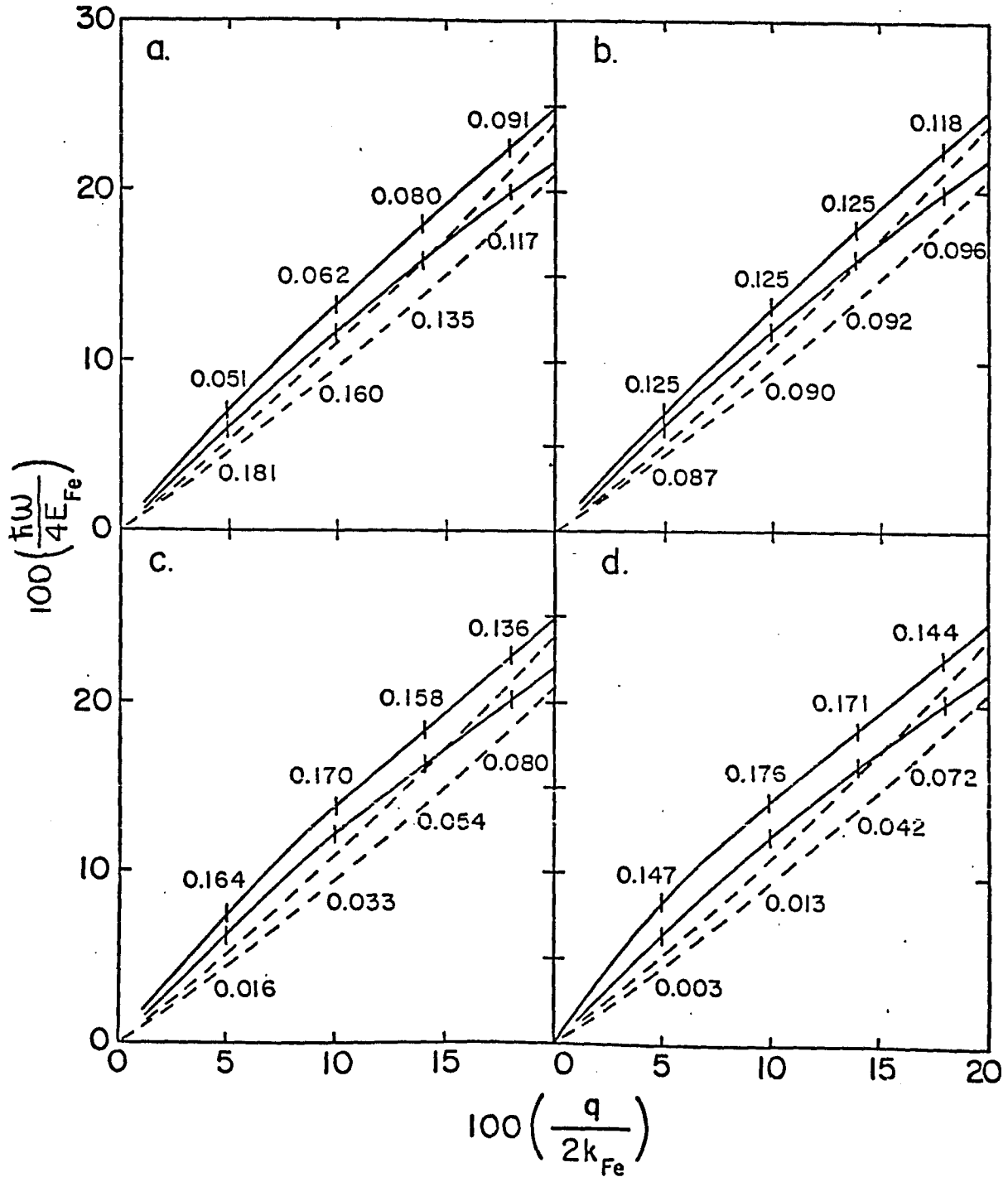


FIG. 5.1.

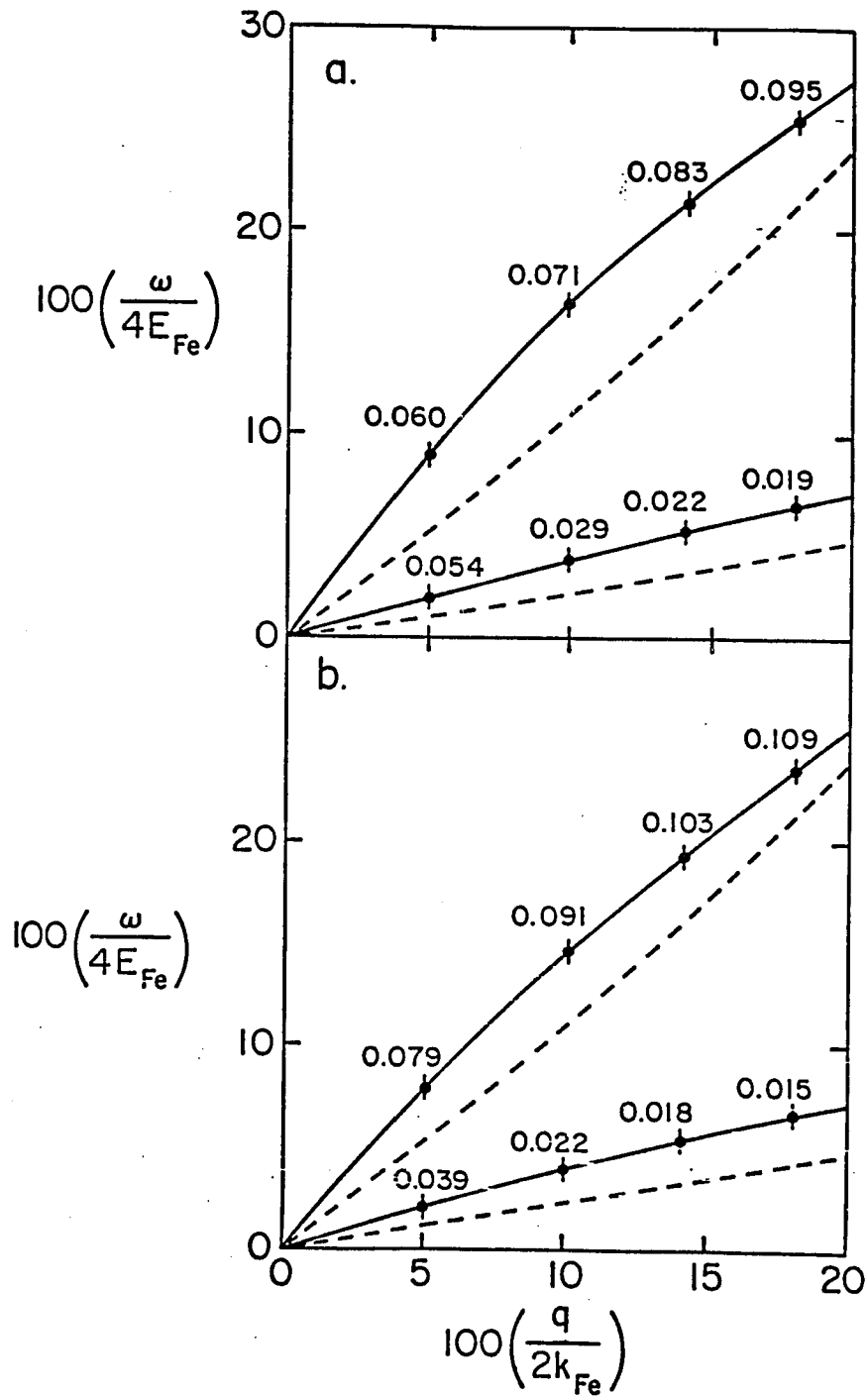


FIG. 5.2.

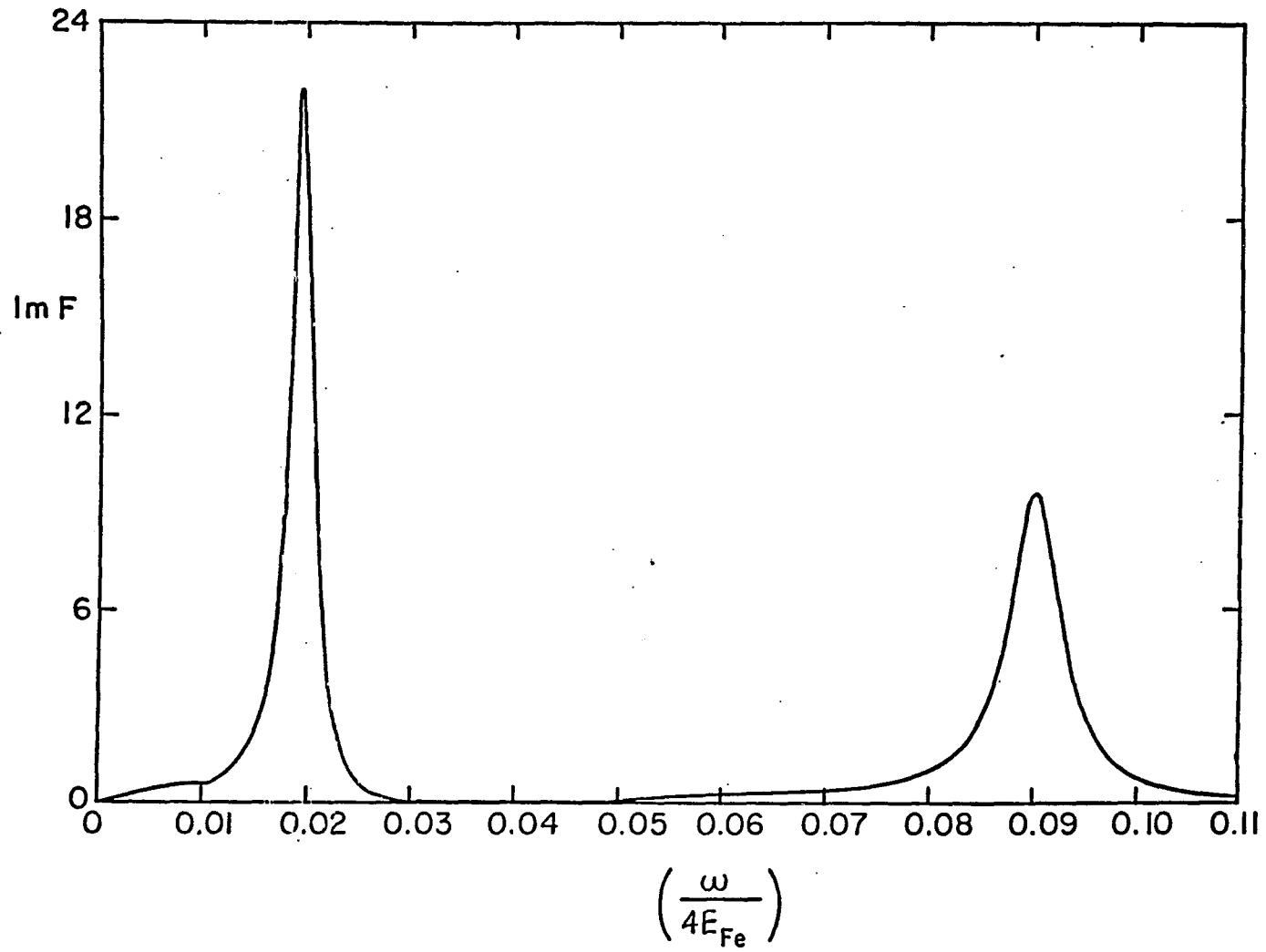


FIG. 5.3.

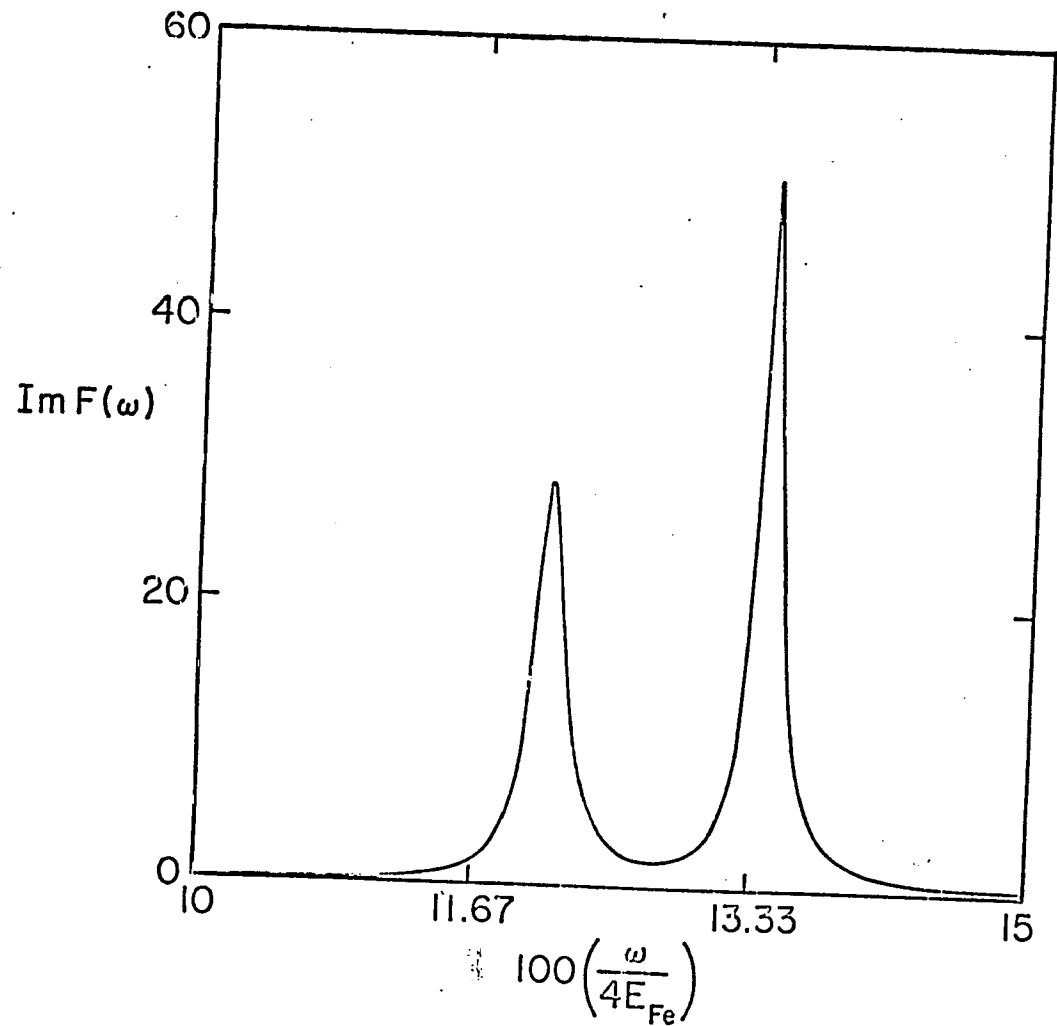


FIG. 5.4.

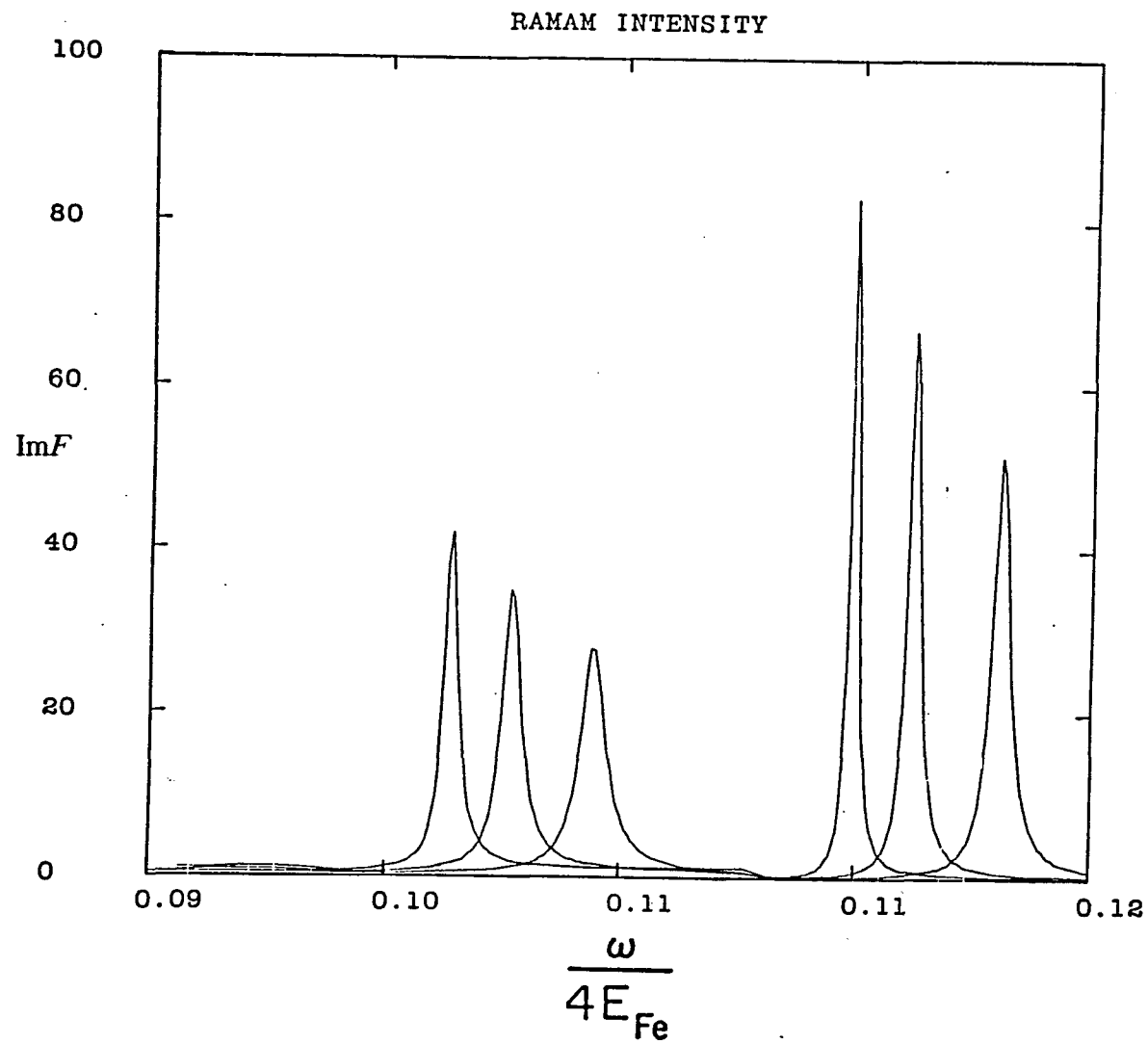


FIG. 5.5.

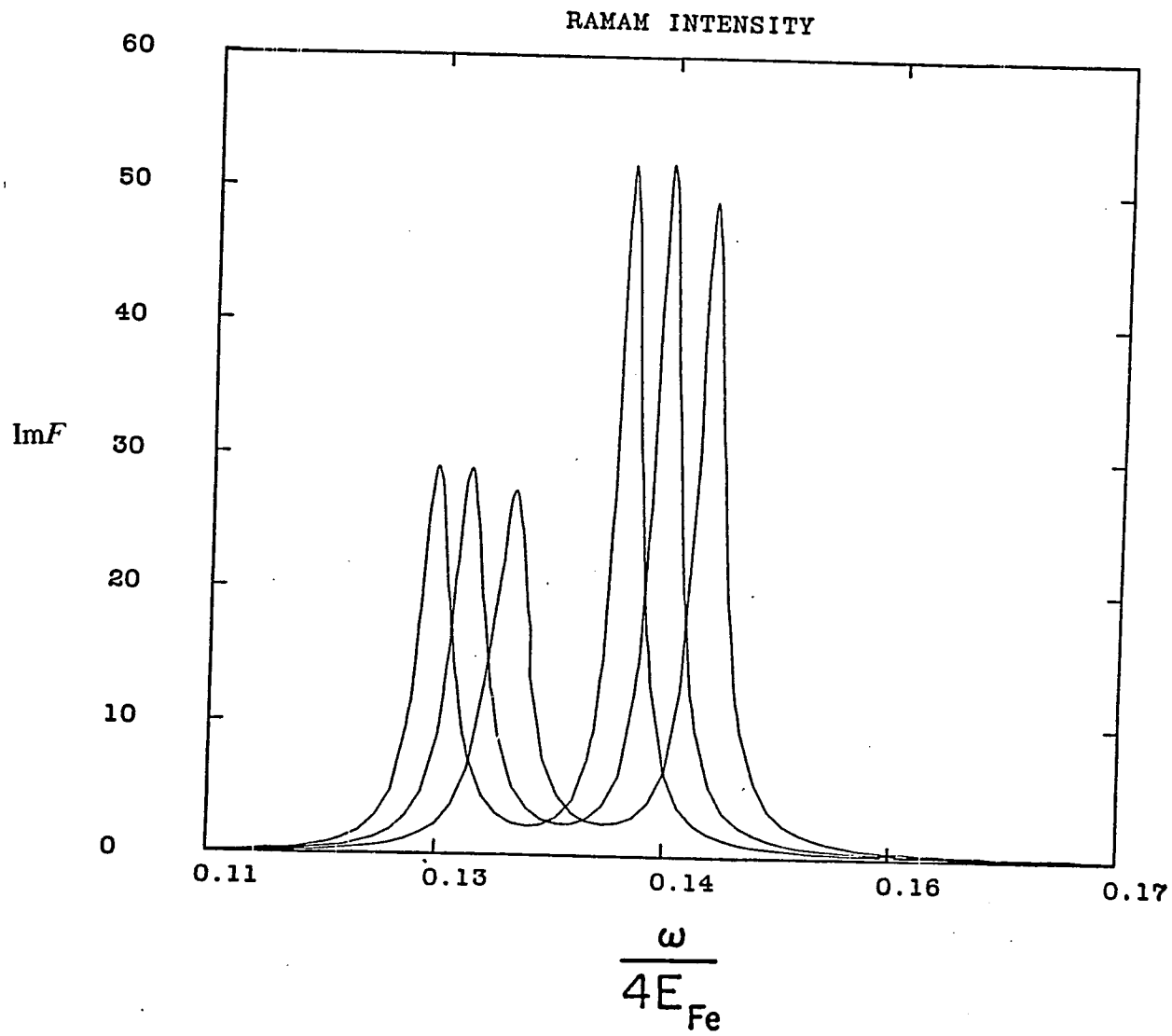


FIG. 5.6.

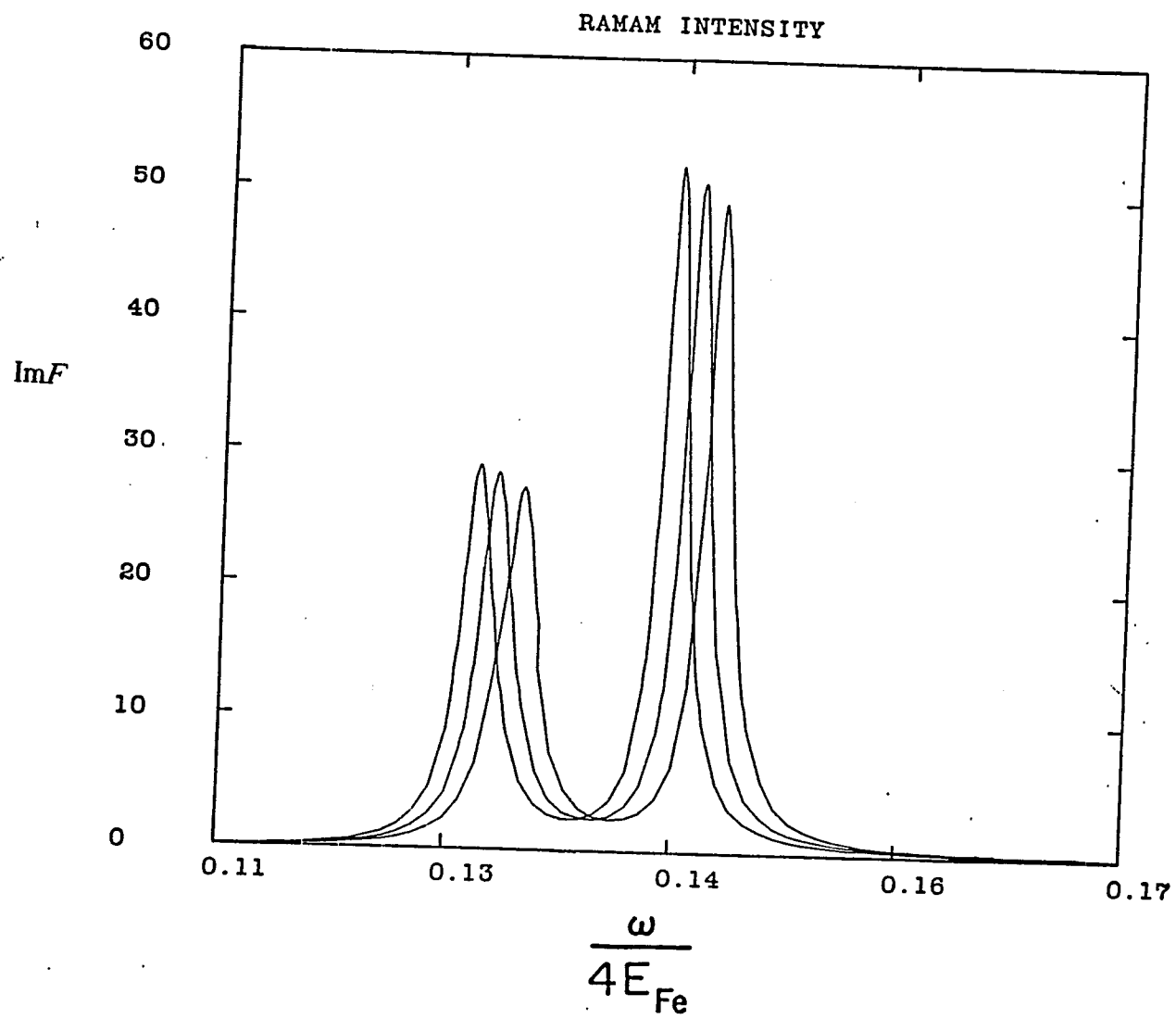


FIG. 5.7.

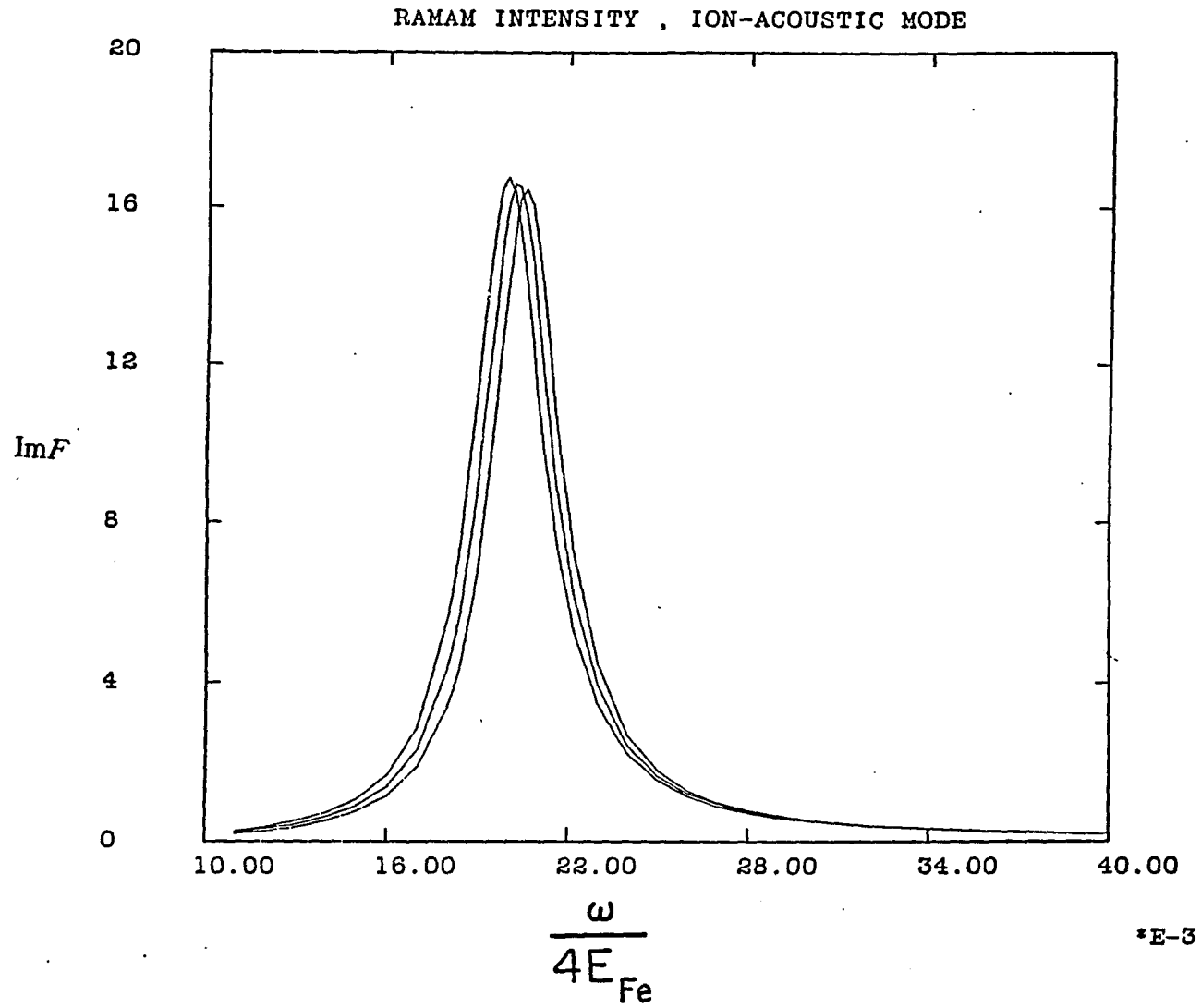


FIG. 5.8.

## REFERENCES

- [1] P. B. Visscher and L. M. Falicov, Phys. Rev. B3, 2541 (1971)
- [2] A. L. Fetter, Ann. Phys. NY. 88, 1 (1974)
- [3] S. Das. Sarma and J. J. Quinn, Phys. Rev. B25, 7603 (1982)
- [4] N Tzoar and C. Zhang, Phys. Rev. B32, 1149 (1985)
- [5] N Tzoar and C. Zhang, Phys. Rev. B33, 2624 (1986)
- [6] N Tzoar and C. Zhang, Phys. Rev. B34, May 15 (1987)
- [7] N Tzoar and C. Zhang, Phys. Rev. B34, 1050 (1986)
- [8] J. M. Ziman, "Principles of the Theory of Solids" Chapter 5, ( Cambridge University Press, Cambridge, England 1964 )
- [9] A. L. Fetter and J. D. Walecka, "Quantum Theory of Many-Particle System" section 3,14,15,33,and 34, ( McGraw-Hill, New York, 1971 )
- [10] L. Tonks and I. Langmuir, Phys. Rev. 33, 195 (1929)
- [11] D. Bohm and D. Pines, Phys. Rev. 92, 609 (1953)
- [12] L. H. Thomas, Proc. Cambridge Philos. Soc., 23, 542 (1927)
- [13] E. Fermi, Z. Physik, 48, 73 (1937)
- [14] F. Stern, Phys. Rev. Lett. 30, 278 (1973)
- [15] T. R. Brown and C. C. Crimes., Phys. Rev. Lett. 29, 1233 (1972)
- [16] J. Dawson and C. Oberman, Phys. Fluid, 5, 517 (1962)
- [17] C. Oberman, A. Ron and J. Dawson, Phys. Fluid, 5, 1914 (1962)
- [18] V. I. Perel and G. M. Eliashberg, Soviet Phys.-JETP 14, 633 (1962)
- [19] A. Ron and N Tzoar, Phys. Rev. 131, 12 (1963)

- [20] N. Q. Dong, Phys. Rev. 148, 151 (1966)
- [21] L. D. Landau, J. Physics (USSR) 10, 25 (1946)
- [22] P. A. Wolff, Phys. Rev. 132, 2017 (1963)
- [23] W. Gotze and P. Wolfle, Phys. Rev. B6, 1226 (1972)
- [24] J. S. Li, S. Y. Zhang and S. J. Zhang, Acta Phys. Sinica, 21, 1638 (1965)
- [25] Y. C. Lee and N. Tzoar, Phys. Rev. 135, 1326 (1965)
- [26] E-Ni Foo and N. Tzoar, Phys. Rev. 187, 1000 (1969)
- [27] See, "Proc. of the Intern. Conf. of Electronic properties of Quasi-two-dimensional system" Surface Sci., 58, (1976)
- [28] S. J. Allen Jr., D. C. Tsui and F. Derosa, Phys. Rev. Lett. 35, 1359 (1975)
- [29] See, "Proc. of the Fourth Intern. Conf. of Electronic properties of Quasi-Two-Dimensional System" Surface Sci., 98, (1981)
- [30] F. Stern, Phys. Rev. Lett. 18, 546 (1967)
- [31] P. M. Platzman and N. Tzoar, Phys. Rev. B13, 3197 (1976)
- [32] A. L. Fetter, Ann. Phys. NY. 81, 367 (1973)
- [33] N. Tzoar, P. M. Platzman and A. L. Simmons, Phys. Rev. Lett. 36, 1200 (1976)
- [34] P. M. Platzman, A. L. Simmons and N. Tzoar, Phys. Rev. B16, 2023 (1976)
- [35] A. Gold and W. Gotze, J. Phys. C14, 4049 (1981)
- [36] T. A. Kennedy, R. J. Wagner, B. D. McCombe and D. C. Tsui, Phys. Rev. Lett. 35, 1031 (1975)
- [37] For the recent work on superlattices, see the proceedings of Fifth International Conference on Electronic Properties of Two-dimensional System, Oxford, 1983 [ Surf. Sci. 142 (1984) ]
- [38] For an excellent review of the subject, see the review article by T. Ando, A. B. Fowler and F. Stern, Rev. Mod. Phys. 54, 437 (1982)
- [39] R. Dingle, H. L. Stormer, A. C. Gossard and W. Wiegmann, Surf. Sci. 98, 90 (1980)

- [40] L. L. Chang, and L. Esaki, Surf. Sci. 98, 70 (1980)
- [41] A. C. Tselis and J. J. Quinn, Phys. Rev. B29, 3318 (1984)
- [42] L. L. Chang, Surf. Sci. 73, 226 (1978)
- [43] R. Dingle, Surf. Sci. 73, 229 (1978)
- [44] A. Pinczuk, J. M. Worlock, H. L. Stormer, R. Dingle, W. Wiegmann and A. C. Gossard, Solid State Commun. 36, 43 (1980)
- [45] G. Abstreiter, Ch. Zeller and K. Plong, in Gallium Arsenide and Related Compounds, edited by H. W. Thim (Inst. of Phys. Bristol, 1980), p.741
- [46] P. Manuel, G. A. Sai-Halasz, L. L. Chang, C. A. Chang and L. Esaki, Phys. Rev. Lett., 37, 1701 (1976)
- [47] Jainendra K. Jain and Philip B. Allen, Phys. Rev. Lett. 54, 947 (1984)
- [48] W. A. Harrison, J. Vacuum Sci. Technol. 14, 1016 (1977)
- [49] G. A. Sai-Halasz, R. Tsu and L. Esaki, Appl. Phys. Lett. 30, 651 (1977)
- [50] G. A. Sai-Halasz, L. Esaki and W. A. Harrison, Phys. Rev. B18, 2812 (1978)
- [51] A. Madhukar, N. V. Dandekar and R. N. Nucho, J. Vacuum Sci. Technol. 16, 1507 (1979)
- [52] G. H. Dohler, Surf. Sci. 98, 108 (1980)
- [53] H. Bluysen, J. C. Maan, P. Wyder, L. L. Chang and L. Esaki, Solid State Commun. 31, 35 (1979)
- [54] G. A. Sai-Halasz, L. L. Cahng, J. M. Welter, C. A. Chang and L. Esaki, Solid State Commun. 27, 935 (1978)
- [55] H. Sakaki, L. L. Chang, G. A. Sai-Halasz, C. A. Chang and L. Esaki, Solid State Commun. 26, 589 (1978)
- [56] W. P. Chen, Y. J. Chen and E. Burstein, Surf. Sci. 58, 263 (1976)
- [57] D. Dahl and L. J. Sham, Phys. Rev. 16, 651 (1977)
- [58] A. Eguiluz and A. A. Maradudin, Ann. Phys., 113, 29 (1978)
- [59] B. Vinter, Phys. Rev. B15, 3947 (1977)

- [60] T. Ando, Z. Physik, B26, 263 (1977)
- [61] A. Tselis and J. J. Quinn, Surf. Sci., 113, 362 (1982)
- [62] K. W. Chui, J. J. Quinn, T. K. Lee and A. Eguiluz, Phys. Rev. B11, 4989 (1977)
- [63] S. Das Sarma and A. Madhukar, Phys. Rev. B23, 805 (1981)
- [64] M. Apostol, Z. Physik, B22, 13 (1975)
- [65] A. Caille, M. Banville and M. J. Zuckermann, Solid State Commun. 24, 805 (1977)
- [66] J. Mizuno, M. Kobayashi and I. Yokota, J. Phys. Soc. Japan, 39, 983 (1973)
- [67] L. Esaki, in Proceedings of the 17th International Conference on the Physics of Semiconductors, San Francisco, 1984, Edited by J. D. Chadi and W. A. Harrison (Springer, New York, 1985)
- [68] D. Olego, A. Pinczuk, A. Gossard and W. Wiegmann, Phys. Rev. B25, 7867 (1982)
- [69] R. Sooryakumar, A. Pinczuk, A. Gossard and W. Wiegmann, Phys. Rev. B31, 2578 (1985)
- [70] G. Fasol, N. Mestres, H. P. Hughes, A. Fischer and K. Ploog, Phys. Rev. Lett. 56, 2517 (1986)
- [71] A. Pinczuk, M. G. Lamont and A. Gossard, Phys. Rev. Lett. 56, 2092 (1986)
- [72] A. Pinczuk, D. Heiman, A. Gossard and J. H. English, in Proceeding of the 18th International Conference on the Physics of Semiconductors, Stockholm 1986 (World Scientific Press)
- [73] E. Burstein, A. Pinczuk and D. L. Mills, Surf. Sci. 98, 451 (1980)
- [74] S. Das Sarma, Phys. Rev. B29, 2334 (1984)
- [75] G. F. Giuliani and J. J. Quinn, Phys. Rev. Lett. 51, 919 (1983)
- [76] P. Hawrylak, J-W Wu and J. J. Quinn, Phys. Rev. B31, 7855 (1985)
- [77] P. Hawrylak, J-W Wu and J. J. Quinn, Phys. Rev. B32, 5169 (1985)
- [78] J. K. Jain and P. B. Allen, Phys. Rev. Lett. 54, 947 (1984),

- [79] J. K. Jain and P. B. Allen, Phys. Rev. B32, 997 (1985),
- [80] S. Katayama and T. Ando, J. Phys. Soc. Japan. 54, 1615 (1985)
- [81] R. D. King-Smith and J. C. Inkson, Phys. Rev. B33, 5489 (1986)
- [82] D. Pines, "The Many Body Problem" (W. A. Benjamin Company, New York, 1961)
- [83] D. C. Martin and J. Schwinger, Phys. Rev. 115, 1342 (1959)
- [84] W. Kohn, Phys. Rev. 123, 1242 (1961)
- [85] W. Kohn and J. M. Luttinger, Phys. Rev. 108, 590 (1957)
- [86] N. Tzoar and P. M. Platzman, Proceeding on the " Linear and Nonlinear Electron Transport in Solid " Edited by J. T. Devreese and V. E. Van Doren, Plenum Press (1976)
- [87] R. Balescu, Phys. Fluid. 4, 94 (1961)
- [88] J. M. Luttinger and J. C. Ward, Phys. Rev. 118, 1417 (1960)
- [89] J. Appel and A. W. Overhauser, Phys. Rev B10, 758 (1978)
- [90] N. Tzoar and P. M. Platzman, Phys. Rev. B20, 4189 (1979)
- [91] H. Ezawa, S. Kawaji and K. Nakamura, Japan. J. Appl. Phys. 13, 126 (1974)
- [92] F. Stern and W. E. Howard, Phys. Rev. Lett. 45, 1203 (1980)
- [93] S. Das Sarma and B. A. Mason, Ann. Phys. 163, 78 (1985)
- [94] S. Das Sarma and A. Madhukar, Phys. Rev. B22, 2823 (1980).
- [95] G. Kawamoto, J. J. Quinn and W. L. Bloss, Phys. Rev. B23, 1875 (1981); and T. S. Rahman, D. L. Mills and P. S. Riseborough, Phys. Rev. B23, 4081 (1981).
- [96] P. J. Price, Ann. Phys. 133, 217 (1981), and Surf. Sci. 113, 199 (1982).
- [97] D. K. Ferry, Surf. Sci. 75, 86 (1978); K. Hess, App. Phys. Lett. 35, 484 (1979)
- [98] P.K. Basu and B. R. Nag, Phys. Rev. B22, 4849 (1980).

- [99] S. Das Sarma, Phys. Rev. B27, 2590 (1983).
  - [100] S. Das Sarma, Phys. Rev. Lett. 52, 859 (1984).
  - [101] G. Lindemann, W. Seidebusch, R. Lassnig, J. Edlinger and E. Gornik, Physica 117B and 118B, 649 (1983).
  - [102] D. C. Tsui, Th. Englert, A. Y. Cho and A. C. Gossard, Phys. Rev. Lett. 44, 341 (1980); G. Kido, N. Miura, H. Ohno and H. Sakaki, J. Phys. Soc. Japan 51, 2168 (1982).
  - [103] J. Scholz, F. Koch, J. Zeigler and H. Maier, Solid State Commun. 46, 665 (1983).
  - [104] Th. Englert, J. C. Maan, Ch. Uihlein, D. C. Tsui and A. C. Gossard, Solid State Commun. 46, 545 (1983).
  - [105] M. A. Brummel, R. J. Nicholas, J. C. Portal, M. Razeghi and M. A. Poisson, Physica 117B and 118B, 753 (1983).
  - [106] M. Horst, U. Merkt and J. P. Kotthaus, Phys. Rev. Lett. 50, 754 (1983).
  - [107] A. Ron and N. Tzoar, Phys. Rev. 133, A1378 (1963)
  - [108] S. Katayama, D. L. Mills and R. Sirko, Phys. Rev. B28, 6079 (1983); and S. Katayama and D. L. Mills, Phys. Rev. B19, 6513 (1979)
  - [109] J. J. Quinn, Phys. Rev. ( to be published )
  - [110] D. Grecu, Phys. Rev. B8, 1958 (1973).
  - [111] D. Pines, Can. J. Phys. 34, 1379 (1956)
  - [112] I. Alexeff and R. Neidigh, Phys. Rev. Lett. 7, 223 (1961); Phys. Rev. 129, 516 (1963)
  - [113] A. Y. Wong, N. D'Angelo and R. W. Motley, Phys. Rev. Lett. 9, 415 (1962)
  - [114] P. M. Platzman and P. A. Wolff, "Waves and Interactions in the Solid state Plasmas" ( Academic, New York 1973 )
  - [115] E-Ni. Foo and N. Tzoar, Phys. rev. B6, 4553 (1971); N. Tzoar and E-Ni. Foo, in "Proceedings of the Second International Conference on Light Scattering in Solids" (Flammarion, Paris, 1971).
  - [116] S. Das Sarma and A. Madhukar, Phys. Rev. B23, 805 (1981)
-

- [117] Diego Olego, A Pinczuk, A. G. Gossord and W. Wiegmann, Phys. Rev. B26, 7876 (1982)